Master of Science Thesis

FLAx REinforced Aluminium (FLARE)

A bio-based Fibre Metal Laminate alternative combining impact resistance and vibration damping

Mathilde Alcaraz

Faculty of Aerospace Engineering Delft University of Technology

TU Delft Delft University of Technology

FLAx REinforced Aluminium (FLARE)

A bio-based Fibre Metal Laminate alternative combining impact resistance and vibration damping

Master of Science Thesis

For obtaining the degree of Master of Science in Aerospace Engineering
at Delft University of Technology

Mathilde Alcaraz

September 21st 2023

Faculty of Aerospace Engineering · Delft University of Technology

Delft University of Technology
Faculty of Aerospace Engineering
Department of Aerospace Structures and Materials

GRADUATION COMMITTEE

Dated: September 21st 2023

Chair holder:

Supervisor: Dr.ir. R.C. Alderliesten

Committee members:

Supervisor: Dr. Y. Mosleh

Dr. J. Sodja

Dr.ir. O.K. Bergsma

Preface

The subsequent report outlines the outcomes of my master's thesis conducted within the Faculty of Aerospace Engineering at TU Delft. The focus of my research was on FLAx REinforced Aluminium (FLARE), a bio-based Fibre Metal Laminate alternative. This report marks the culmination of my academic journey, particularly the challenging final two years devoted to my studies at TU Delft.

This master's thesis report would not have come to fruition without the contribution of several people. In this regard, I wish to express my gratitude to all those who have played a role in ensuring the accomplishment of this endeavour.

First and foremost, I would like to thank my supervisors Dr. ir. René Alderliesten and Dr. Yasmine Mosleh for entrusting me with an ambitious thesis project that challenged me from every angle. Their support and guidance throughout the year have made this project not only a rewarding academic experience, but also an enjoyable one. Our interactions were marked by numerous enriching discussions, and their feedback have always pointed me in the right direction without telling me what to do.

I also wish to acknowledge and express my gratitude to the DASML technicians, namely Victor, Johan, Roy, Chantal, Dave, and Alexander. Their invaluable assistance and practical insights greatly facilitated my experimental work. Furthermore, I extend my thanks to Dr. Jurij Sodja and Stefan de Boer for their assistance with the beam vibration tests, as well as to Valentin Perruchoud for the enlightening conversations regarding flax fibres.

Finally, I want to express my gratitude to my fellow master students, who have helped to create a friendly atmosphere over the last two years, and to my family for their unconditional support and trust.

Delft, University of Technology
September 21st 2023

Mathilde Alcaraz

Abstract

Fibre metal laminates (FML) were initially conceived as a hybrid material, aiming to create synergy between the impact resistance of metals and excellent fatigue resistance of fibre reinforced polymers. The purpose of this approach was to overcome the limitations of single-material structures. However, despite its considerable promise, the use of the FML concept has primarily been confined to aerospace applications and heavily relies on synthetic fibres that carry significant environmental implications. Hence, given the growing concerns about climate change and the challenges posed by recycling glass fibre composites, a new generation of FMLs with a reduced carbon footprint should be envisaged.

Research on flax fibre composites reveals convincing mechanical properties and remarkable damping capacities. However, the broader adoption of these composites remains restricted primarily due to issues related to low impact resistance, moisture absorption and flammability concerns. The FML concept presents a viable solution to surmount these constraints, consequently facilitating the integration of these materials into primary structures. Hence, the research endeavour aimed to attain comprehensive insights into FLAx REinforced aluminium (FLARE), particularly focusing on its impact resistance and vibration damping capabilities, which are believed to be the principal benefits of this hybrid material.

The research goal was divided into three distinct research tasks: conducting experimental analyses to characterise the damping behaviour of FLARE, evaluating the impact resistance through experimental means, and validating predictive tools to offer initial insights into the design principles governing such a FML. FLARE, along with flax fibre reinforced epoxy (FFRE) and GLARE specimens, were manufactured using wet layup combined with vacuum bagging techniques.

First, tensile tests were conducted to validate the applicability of the metal volume fraction (MVF) approach in predicting the mechanical properties of FLARE. Intriguingly, the well-known non-linear behaviour exhibited by flax was not observed in the case of FLARE. The results revealed that while the MVF method provided a satisfactory approximation, it was the "inelastic" modulus of FFRE that predominantly contributed to the stiffness of FLARE.

Dynamic mechanical analysis and vibration beam tests were carried out to assess the influence of incorporating metallic layers on the vibration damping characteristics of flax fibre composites. The investigation revealed that the metallic layer predominantly governs the

damping behaviour of the FML. Notably, an inverse rule of mixture emerged as the most effective means of approximating its loss factor.

Low-velocity impact tests were conducted to gain insights into the impact response of FLARE in comparison to conventional FMLs. The analysis indicated that the aluminium layers play a significant role in energy absorption, whereas the composite strength emerges as the critical factor influencing impact resistance. A quasi-static analytical model was also assessed, offering an initial estimation of the impact response, yet it warrants further refinement.

In conclusion, the FML concept holds promise for FLARE, but its application requires a novel approach compared to previous methods, to render FLARE viable for practical real-world applications.

Table of Contents

List of Figures

List of Tables

Nomenclature

Abbreviations

Abbreviation	Definition
CLT	Classical Laminate Theory
DMA	Dynamic Mechanical Analysis
DSC	Differential Scanning Calorimetry
EROM	Energy based Rule Of Mixture
FFRE	Flax Fibre Reinforced Epoxy
FLARE	FLAx REinforced aluminium
FML	Fibre Metal Laminate
FRC	Fibre Reinforced Composite
FRF	Frequency Response Function
FVF	Fibre Volume Fraction
GFRE	Glass Fibre Reinforced Epoxy
GLARE	GLAss REinforced aluminium
IROM	Inverse Rule Of Mixture
MEK	MEthyethyl Ketone
MVF	Metal Volume Fraction
ROM	Rule Of Mixture
UD	UniDirectional
VBT	Vibration Beam Test
VVF	Void Volume Fraction

Symbols

Symbol	Definition	Unit
a	Plate length	[mm]
b	Plate width	[mm]

Symbol	Definition	Unit
D	Displacement	[mm]
E	Young's modulus	[GPa]
E_{abs}	Total energy absorbed	[J]
F	Contact force	[N]
f_n	n^{th} resonance frequency	[Hz]
g	Gravitational acceleration	[m/s^2]
G_{IIc}	Mode II interlaminar fracture toughness	[N/mm]
m	Impactor mass	[kg]
R_t	Tangency radius	[mm]
t	Laminate thickness	[mm]
T_g	Glass transition temperature	[$^\circ C$]
V	Impact velocity	[m/s]
V_0	Initial impact velocity	[m/s]
V_f	Fibre volume fraction	[-]
α	Coefficient of thermal expansion	[$^\circ C^{-1}$]
Δ	Maximum displacement	[mm]
$tan(\delta)$	Loss factor	[-]
ϵ_{ult}	Ultimate tensile strain	[%]
ξ	Loss factor	[-]
ν	Poisson ratio	[-]
σ_{yield}, σ_0	Tensile yield strength	[MPa]
σ_{ult}	Ultimate tensile strength	[MPa]
ρ	Density at 23$^\circ C$	[g/cm^3]
ρ_A	Areal density	[g/cm^2]
τ_{ult}	Ultimate shear strength	[MPa]

Chapter 1

Introduction

After several airliner accidents in the early 20^{th} century, durability requirements, especially with regard to fatigue, led to the so-called damage tolerant design concept. Finding a material that has inherent resistance to crack growth then becomes paramount. It was in this context that fibre metal laminates (FMLs) were developed in the 1970's at the Faculty of Aerospace Engineering of the Delft University of Technology. Indeed, this combination of thin metal layers with a fibre-reinforced composite offers the advantage of excellent fatigue and corrosion resistance and good mechanical properties while remaining a lightweight material. One of the most successful FML is GLARE, which is notably used for the upper fuselage skin of the Airbus A380. It consists of aluminium layers bonded to glass fibre reinforced epoxy. Yet, despite its great potential, the scope of the FML concept is predominantly limited to aerospace applications and relies mainly on synthetic fibres with high environmental impact.

These synthetic fibres give the FML excellent specific properties, but their environmental impact is a major drawback. On the one hand, the production of glass fibre is energy-intensive and produces greenhouse gases, and on the other hand, at the end of its life, it is difficult to recycle the FML by separating its constituents. Therefore, with growing concerns about climate change, it is rational to envisage a new generation of FMLs with lower embodied energy by using bio-based fibre reinforced composite layers.

Currently, the focus is on the development of bio-based composites to reduce the carbon footprint of transport in particular. Natural fibres are thus gaining importance due to their low density, promising mechanical properties and cost effectiveness. Flax fibres have excellent tensile stiffness, and bending stiffness and strength, making them good candidates for transport and construction applications. But their use as reinforcement in composites is still limited to non-structural parts such as interior panels, as they do not yet meet the requirements of high-performance applications. However, by combining these composites with metal layers, their properties could benefit from a synergistic effect and their use as FML could then be extended to structural parts. Furthermore, the remarkable damping characteristics of flax fibre composites, when combined with the robust impact resistance commonly found in metals, have the potential to expand the scope of applications for Fibre Metal Laminates to applications which have not yet been considered.

In the end, the fundamental question revolves around whether the use of the Fibre Metal Laminate (FML) concept in conjunction with bio-based composites results in a synergistic material that optimally integrates its individual constituents. Guided by this consideration, the project aimed to investigate the benefits offered by FLAx REinforced aluminium laminate (FLARE), focusing specifically on its vibration damping and impact resistance capabilities.

Hence, in this report, the initial section will centre on a comprehensive review of existing literature, thereby refining the project's scope, and identifying its inherent challenges. This phase will lead to the formulation of the research questions. The subsequent part of the report will outline the undertaken endeavours to address these questions, starting with an overview of the methodology used to manufacture the samples. Subsequently, the investigation into vibration damping behaviour will be detailed, followed by an analysis of the low-velocity impact resistance. In Chapter 9, the amassed knowledge is discussed, and potential applications of FLARE are presented. Concluding the report, a succinct summary of findings and recommendations for prospective research directions are provided.

Part I

State of the art and Research scope definition

Chapter 2

Fibre Metal Laminates

Fibre metal laminates (FMLs) were first developed as a replacement for metal which suffer from poor fatigue resistance. Indeed, the insertion of fibre reinforced epoxy layers between the metal layers makes it possible to limit the crack opening through the so-called fibre bridging effect. This effect has been extensively described in the literature, which agrees that it is one of the main benefits of FMLs. However, other advantages of such a combination were also reported to demonstrate its potential for different structural applications.

In the following, the concept of FML is introduced through the example of GLARE which is the main FML on the market. Then, the methods developed to predict the properties of new FMLs from the properties of their components are presented. Finally, recent developments towards environmental concerns are discussed in order to determine what has been studied in the literature on this subject so far.

2.1 A conventional fibre metal laminate: GLARE

GLARE is one of the most studied FML in the literature, notably because of its success in the industrial world and in particular in aeronautics. It consists of thin aluminium sheets interleaved with a unidirectional S-glass reinforced epoxy prepreg arranged in different orientations. The number of metal layers can vary depending on the desired application of the FML, but generally there are two or three as shown in Figure 2.1.

It is important to note that GLAREs on the market are by definition made from unidirectional S-glass fibres, which are high strength glass fibres. However, this trade name can normally refer to any combination of aluminium and glass fibre reinforced composite, but this should be clarified. Indeed, some articles refer to GLAREs as FMLs made from E-glass fibres or woven fabrics, which can be misleading, especially if a comparison is to be made with other types of FMLs for a specific application [23,24]. For example, it is incorrect to compare the properties of flax fibres with those of E-glass fibres and conclude that the natural fibre metal laminate can be used for the fuselage skin, as is the case with GLARE. In other words, it is necessary to compare similar materials for the conclusions drawn to be valid. Special attention was therefore paid to this point in the literature review.

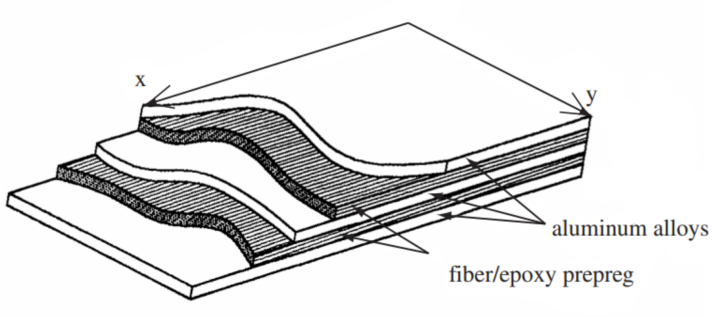

Figure 2.1: GLARE configuration 3/2 (3 layers of metal for 2 of prepreg). Adapted from [1].

Extensive research has concluded that the main advantages of GLARE are excellent fatigue resistance, high stiffness and strength, and improved impact resistance compared to pure aluminium [25–28]. In addition, this FML suffers fewer corrosion problems than thick aluminium while maintaining relatively good formability. But improvements over bare glass fibre reinforced composite can also be emphasised as Alderliesten et al. point out [29, 30]. GLARE has higher bearing strength and better impact resistance than composite. It is also much easier to repair a FML panel using patches. Finally, the metal layers create a protective barrier against environmental aggression, especially moisture, which limits the performance of a composite. All these characteristics highlighted in the literature already suggest the potential of combining the world of metals with that of bio-based composites.

All the studies carried out since the first design of GLARE have led to the development of six different standard grades of GLARE used in industry to meet different requirements. Indeed, each GLARE variant has its own advantages as can be seen in Table 2.1, which makes this type of FML suitable for multiple applications.

Grade	Alloy	Metal layer thickness	Fibre orientation	Main benefits
Glare 1	7475-T761	0.3-0.4 mm	0/0	Fatigue, strength, yield stress
Glare 2A	2024-T3	0.2-0.5 mm	0/0	Fatigue, strength
Glare 2B	2024-T3	0.2-0.5 mm	90/90	Fatigue, strength
Glare 3	2024-T3	0.2-0.5 mm	0/90	Fatigue, impact
Glare 4A	2024-T3	0.2-0.5 mm	0/90/0	Fatigue, strength in 0° direction
Glare 4B	2024-T3	0.2-0.5 mm	90/0/90	Fatigue, strength in 90° direction
Glare 5	2024-T3	0.2-0.5 mm	0/90/90/0	Impact
Glare 6A	2024-T3	0.2-0.5 mm	+45/-45	Shear, off-axis properties
Glare 6B	2024-T3	0.2-0.5 mm	-45/+45	Shear, off-axis properties

Table 2.1: Commercialised GLARE grades [2].

This diversity reflects the work already done in the scientific literature to optimise the properties of this FML. By varying the fibre orientation, thickness and number of layers, it has been shown that FMLs offer great versatility [28, 30]. It is noteworthy that the design principles already experimented with GLARE by different authors can certainly be reused to optimise new types of FMLs.

However, one area that is lacking in the literature is the evaluation and design of conventional fibre metal laminates for non-aerospace applications. In fact, most of the applications pointed

out are related to aircraft. But FMLs can be attractive for military, automotive or other applications [2,27,31]. This can be explained by the fact that the manufacturing process is quite long and expensive, and therefore mainly concerns parts for high performance applications. Indeed, most publications refer to an autoclave manufacturing process, which guarantees a good quality of the final part. Nevertheless, out-of-autoclave processes have also been mentioned in the literature, such as resin transfer moulding (RTM) or compression moulding, which allow for lower production costs [32]. However, the success of the RTM process hinges significantly on factors such as reinforcement permeability and matrix viscosity, mishandling these aspects can result in defects like dry spots, porosity, and distortion of fibres. Similarly, in the compression moulding process, the absence of vacuum can contribute to heightened porosity. Nonetheless, it is possible to attain a fibre volume fraction similar to what can be achieved through the autoclave method. In addition, the influence of defects on mechanical performance is mitigated in the case of fibre-metal laminates [33]. A comparison of the quality of the FMLs obtained by these different processes would be useful, but these studies already give a good overview of the manufacturing techniques that could be used to produce natural FMLs, knowing that they have specific limitations (especially in temperature).

2.2 Methods to predict the behaviour of a FML

While studying FMLs, different tools for estimating their properties have been developed in order to save time, particularly in the design of the variants discussed above. All the tools that exist to predict the behaviour of this hybrid material are based on knowledge of the behaviour of its constituents. They can therefore be used to predict the performance of the flax FML. For this reason, they will be detailed in the following.

2.2.1 Metal Volume Fraction method

The simplest prediction tool to use is based on the same concept as the rule of mixtures for composites. Indeed, in the literature everyone agrees that the properties of a FML are in fact a combination of those of the metal and the composite that constitute it. Thus, it has been assumed that certain mechanical properties can be predicted by using a rule of mixtures. It is from this assumption that the metal volume fraction (MVF) method was developed [28, 30].

Each component is then seen as a homogeneous and orthotropic material, without distinguishing between the matrix and the fibres for the composite layers. The relative contribution of the metal or metal volume fraction is evaluated by,

$$MVF = \frac{\sum_{1}^{n} t_{al}}{t_{lam}} \tag{2.1}$$

where t_{lam} is the total thickness of the FML, n the number of metal layers and t_{al} their thickness. Then, the properties of the laminate (P_{lam}) can be roughly estimated by a linear relationship:

$$P_{lam} = MVF \times P_{metal} + (1 - MVF) \times P_{FRC} \tag{2.2}$$

This approach has been shown to be valid for tensile modulus and strength, compressive modulus, or shear modulus. In addition, some authors specify a range of validity such as $0.45 < MVF < 0.85$ [2]. This range actually corresponds to the value for the different types of GLAREs currently used and tested. Hardly any literature reports the use of this method for lower MVF values. It is therefore relevant to check if this approach is valid for FML with a lower content of metal and with natural fibres instead of synthetic ones as this method has been developed specifically for conventional FMLs.

Moreover, this method has some limitations. Firstly, it cannot predict the entire behaviour of the FML but only discrete values corresponding to precise properties. Secondly, the properties of cured composites must be known even if sometimes they have no physical reality. For example, to assess the yield strength of GLARE, the "yield strength" of glass fibre reinforced epoxy must be determined. But this composite has a linear elastic behaviour until failure. Therefore, a virtual yield strength must be calculated using a reverse engineering method. That means that at least one variant of GLARE has to be tested to extrapolate this value as indicated in Figure 2.2.

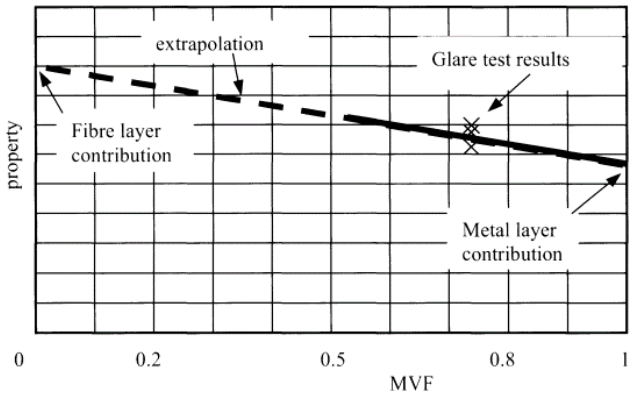

Figure 2.2: Linear evolution of the FML property [2].

Thus, assuming that the behaviour of a new FML can be predicted only using the MVF method is misleading. However, this tool is still good enough for preliminary design purposes and will therefore be used to evaluate the potential of flax fibre metal laminate as there is almost no values in the literature.

2.2.2 Classical Laminate Theory

Another possibility for modelling the behaviour of a FML is to use the Classical Laminate Theory (CLT). This theory, derived from composite mechanics, allows to describe the relationship between strains and stresses within a laminated material. Thus, many models dedicated to FMLs have been developed in the literature based on this theory [30, 34]. However, the CLT must be adapted to take into account the elements detailed below and thus

more accurately reflect the behaviour of a FML. Furthermore, it should be noted that the theory presented assumes plane stress condition which is verified for thin FMLs.

Firstly, the CLT does not take into account the internal stresses due to the manufacturing process of the FMLs, which are even more important as it is a hybrid material. Indeed, there is a significant mismatch between the coefficients of thermal expansion of the metal layers and those of the composite. This leads to residual stresses in the laminate. The coefficients of thermal expansion that can be found in the literature for GLARE components are given in Table 2.2.

	Al 7074-T6	UD S2-glass/FM94	
		0°	90°
α [10^{-6}/°C]	22	6.1	26.5

Table 2.2: Coefficient of thermal expansion of GLARE constituents ($V_f = 60\%$ for the composite) [13, 15].

In this sense, Homan [15] proposed a formulation based on the CLT to evaluate these internal stresses. For each lamina, in the principal coordinate system of the laminate, the curing stress vector can be calculated as follows:

$$\sigma_{ck} = Q_k \Delta T (\alpha_{lam} - \alpha_k) \tag{2.3}$$

where,

$$\alpha_{lam} = \frac{1}{t_{lam}} Q_{lam}^{-1} \sum_{k=1}^{n} Q_k t_k \alpha_k \tag{2.4}$$

with: α_k, α_{lam}= coefficient of thermal expansion of the k^{th} layer, or laminate,

Q_k, Q_{lam} = stiffness matrix of the k^{th} layer and the laminate,

t_k, t_{lam} = thickness of the k^{th} layer and the laminate,

ΔT = difference in temperature ($T_{envi} - T_{curing}$)

The residual curing stresses in each layer are then added to that calculated with the CLT from a strain state due to external loading. Another way of including thermal extension has been proposed by Honselaar and implemented in the Alderliesten model [30]. This time, the strain induced by the manufacturing process is included directly in the linear elastic relationship of the material, which is the basis of the CLT. This approach will in any case make it possible to predict the residual stresses of the flax FML as a function of the curing temperature and thus to adjust the manufacturing process.

Secondly, the CLT has been developed for linear elastic materials. But, as it can be seen in Figure 2.3, aluminium has an elasto-plastic behaviour, i.e., it behaves linearly up to its yield point, which indicates the beginning of strain hardening. To overcome this limitation, the CLT is adapted to take into account the plasticity of the metal constituent. For example, a plastic deformation component can be added in the same way as for thermal strains [30]. Another

possibility is to use the Ramberg-Osgood equation to describes the hardening behaviour of the metal:

$$\epsilon = \frac{\sigma}{E} + \alpha \frac{\sigma_0}{E} \left(\frac{\sigma}{\sigma_0} \right)^n \tag{2.5}$$

In particular, this equation can be used to adapt the Young's modulus of metal layers which decreases after yielding [13]. The stress-strain relationship is then better predicted with the modified CLT.

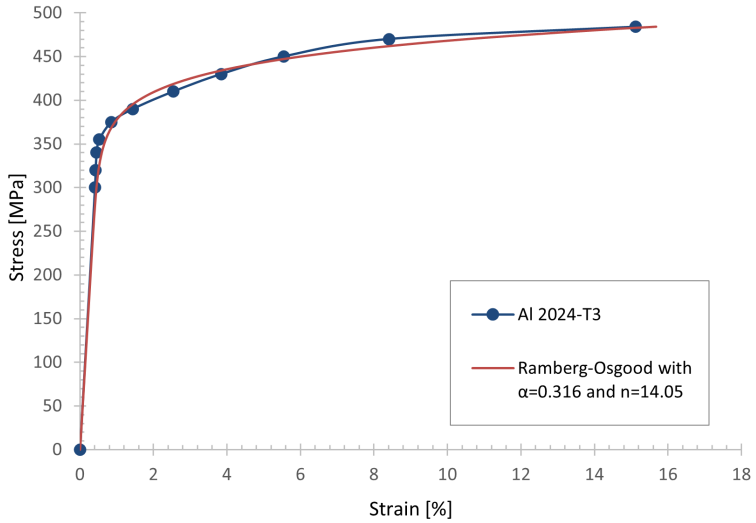

Figure 2.3: Stress-strain curve of Al 2024-T3 [3] and its approximation using the Ramberg-Osgood equation.

In the literature, only conventional FMLs have been considered to assess the accuracy of the laminate theory. Despite this, the modified classical laminate theory will also be used to predict the properties of natural fibre metal laminates. However, it can be expected that the non-linear behaviour of the composite will also have to be taken into account in order to obtain an accurate analytical model.

2.2.3 Impact modelling

FMLs are also known to have excellent impact resistance due to the metal layers, which is particularly important for aircraft structures that are subjected to low and high velocity impacts (hail, bird strikes, collisions...). The impact properties of conventional FMLs have been extensively evaluated experimentally in the literature. It has been reported that there are two main types of behaviour, namely fibre-dominated and metal-dominated. For example, GLARE dissipates impact energy through plastic deformation and delamination (metal-dominated behaviour), whereas carbon fibre metal laminate dissipates this energy through fracture and penetration (fibre-dominated behaviour) [35]. This distinction is relative to the type of fibre used. FMLs made from high-strain-to-failure fibres appear to have better impact resistance.

It is therefore necessary to understand how this material behaves under impact loading and to be able to predict the performance of a new type of FML.

In this sense, theoretical models have been developed to simulate the impact behaviour of the structures using a quasi-static approach [35]. A simple analytical model is the mass-spring system which supposes a constant stiffness of the FML when impacted by a mass and assumes a certain bending profile of the plate [36]. However, this model does not take into account the non-linear behaviour of the material and does not allow the influence of metallic and composite layers to be distinguished.

Thus, Morinière et al. [13] have developed a model able to predict the perforation behaviour of GLARE under a low velocity impact and to evaluate the contribution of each component in the energy absorption process. Firstly, the influence of the impactor contact on the FML is described by a by-directional deflection profile of the neutral line of the FML plate. This flexural profile depends on the impactor shape, plate dimensions and metal volume fraction. It evolves throughout the duration of the impact. Using the First-order Shear Deformation Theory with the Von Kármán equations it is then possible to deduce the membrane and bending strains that occur in the plate. Subsequently, the stress state in each layer can be calculated using the Classical Laminate theory. Once again, the CLT is adapted to take into account the curing stresses, strain hardening behaviour of the metal and the strain-rate effect on the composite layers. A sequential failure analysis is finally performed to quantify the energy absorbed at each failure event and to assess the impact response. For the energy calculation, Morinière et al. assumed that of the experimentally observed failure mechanisms, the plate deformation and delamination are the ones contributing the most to the total absorbed energy.

Through this energy partitioning approach, Morinière et al. proved that the metal layers absorbed substantial energy. Indeed, due to the high stiffness and strength of the glass fibre composite layers, the stresses are effectively redistributed in the plate, allowing the aluminium to undergo large deformation. This mechanism is responsible for the greater impact resistance of GLARE compared to monolithic aluminium. Furthermore, this method can be adapted to the case of ballistic and high velocity impact. It has also been used to describe the behaviour of a FML subjected to blast loading [37].

Finally, it may be valuable to investigate to what extent the use of a composite with a non-linear elastic behaviour, lower strength and strain-to-failure influences the results obtained for GLARE. Indeed, previous comparative studies on FMLs have underscored the significance of fibre type in determining failure modes and, consequently, the primary mechanisms for energy absorption [35, 36]. Given that flax fibres possess an intermediate strain-to-failure range between carbon and glass fibres, predicting the impact behaviour of FLARE is not straightforward. And as Morinière's model mainly considers the energy absorption mechanisms associated with metal-dominated behaviour, it can lead to incorrect results for FLARE if the latter leans towards fibre-dominated behaviour. Furthermore, the model relies on the CLT, assuming linear elastic behaviour of the composite to derive stresses from strains, which fails to capture the stiffness reduction characteristic of flax fibre composites. Therefore, it might be useful to adapt the model of Morinière to the case of natural FMLs, similar to how the plasticity of aluminium is considered.

2.3 Natural fibre metal laminates

Following the success of GLARE, new types of FMLs have been developed using mostly other metals (titanium, magnesium) or other types of synthetic fibres (carbon, polymer fibres). But with the increasing pressure on environmental impact concerns some authors have recently looked at the use of bio-based fibres within the FMLs. Indeed, natural fibres are biodegradable, energy efficient and cheaper than man-made fibres. They possess good specific properties but their mechanical strength remains lower than synthetic fibres commonly used in FMLs [38]. In addition, knowledge of these fibres is still incomplete and shortcomings such as poor adhesion to polymer matrices retard their use for primary structural applications.

In this sense, the literature mainly focuses on the replacement of only part of the synthetic fibres by natural fibres, leading to the so-called hybridisation concept. Hybrid composites can reduce environmental impact and costs while maintaining mechanical properties comparable to those of conventional FMLs [39]. Most publications deal with the hybridisation of carbon fibres with natural fibres such as flax [40, 41], sugar palm [38], jute [42] or kenaf fibres [41]. In comparison, few of them combine glass fibres with natural fibres [43–45]. One explanation may be that carbon fibres are more expensive than glass fibres but have greater rigidity, which is advantageous in limiting the opening of cracks thanks to the bridging effect of the fibres. They therefore seem to be the first candidates to be replaced by natural fibres and thus allow the commercialisation of their FML.

However, as only part of the fibres is biodegradable, the problem of recyclability of FMLs is not solved. For this reason, over the last decade, research has been carried out on natural FMLs. For example, Kuan et al. [4] studied the tensile and impact properties of various environmentally friendly FMLs and compared them to the composites concerned. As was found for conventional FMLs, they concluded that bonding aluminium layers to bio-based composites improves their overall mechanical performance. The same conclusion were drawn for FML made of sisal fibre woven fabrics [46, 47]. Ishak et al. [48] went a step further by comparing the moisture absorption, thickness swelling and formability of a kenaf fibre reinforced composite and its FML. As expected, the aluminium layers protect the composite from moisture penetration except on the edges, but several solutions were proposed to overcome this issue. They also concluded that natural FMLs have better formability than aluminium sheet. However, it should be borne in mind that this conclusion was drawn for a particular type of FML using a thermoplastic matrix and that little information is available on the fibre volume fraction or thickness of the aluminium sheets used for comparison.

Thus, the combination of natural fibres with metallic sheets can help to accelerate the use of natural fibres for engineering applications. Unfortunately, natural FMLs do not seem to be ready to replace components made of aluminium. Indeed, it was found that the performance of FMLs made of oil palm fibres [49] or hemp fibres [5] is much lower than that of the metal alone. This was excepted as the mechanical properties of the natural fibre reinforced composite used are lower than that of aluminium. However, the values and conclusions reported in the literature should be treated with caution.

For example, Santulli et al. [5] found a significant difference between the tensile properties

predicted by the MVF method and those obtained experimentally. On the contrary, Kuan et al. [4] found in a previous study a good agreement between the predictions of the MVF method and the measured values for the same FML. Their results for tensile modulus and strength are reported in Figure 2.4 as well as the prediction using the rule of mixtures (ROM).

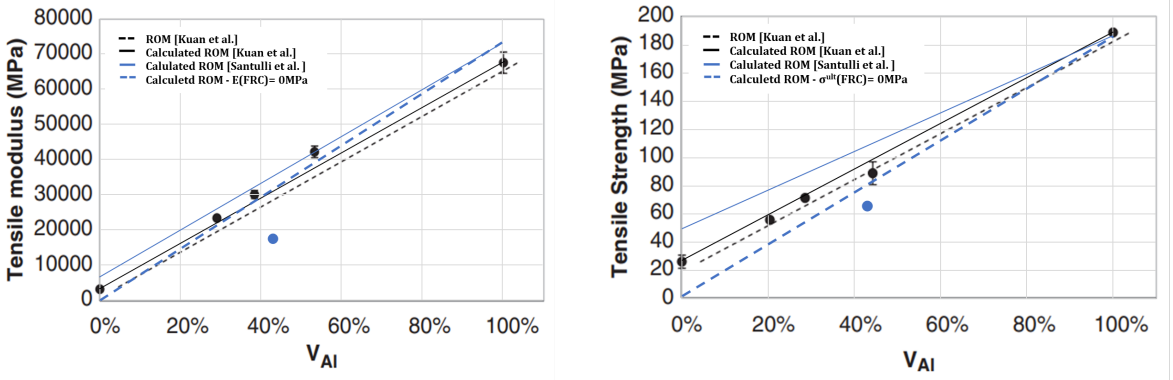

(a) Tensile modulus measured and estimated using different rule of mixtures.

(b) Tensile strength measured and estimated using different rule of mixtures.

Figure 2.4: Comparison of the tensile properties measured by Kuan et al [4] (black dots) or Santulli et al [5] (blue dots) and estimated via the rule of mixtures.

It can be seen from these two graphs that the values measured by Kuan et al are consistent while those found by Santulli et al. are very suspicious. Indeed, the ROM is plotted in dashed blue if we consider that the composite has no stiffness and no strength. This represents an extreme case that is never encountered. By definition, the properties of the FML are therefore necessarily superior to this limit case since the composite contributes to its stiffness (or strength). However, the values measured by Santulli et al are found to be lower than this limit case. It cannot be only due to a poor adhesion between the constituents as the author suggested, the measurement procedure is wrong.

Furthermore, it should be borne in mind that the properties assessed depend on the quality of the material being manufactured, which is not often discussed in the literature. In other words, by improving in particular the adhesion between the constituents of the FML, its performance can be enhanced. In fact, it has already been proven in the literature that pre-treatment of natural fibres to strengthen the adhesion to the polymer matrix improves the tensile and flexural properties of FMLs [43, 50]. Meanwhile, Qu et al. [51] investigated different surface treatments for aluminium layers used in a flax fibre metal laminate, which is the material of interest in the rest of this report. The best static properties were obtained by etching and applying a coupling agent to the aluminium. This demonstrates that by playing with the parameters related to the manufacturing process, it will be possible to optimise the performance of a natural FML.

Besides that, Ramakrishnan et al. [52] have experimentally evaluated the influence of adding a metal foil to flax and glass fibre composites. It is not exactly a FML that is being studied, but it does provide some interesting information about their behaviour. They concluded that this combination does indeed greatly improve the impact resistance of the flax fibre composite but does not perform as well as that of glass fibres. It can therefore be expected that FLARE is less resistant to impact than GLARE.

In the end, what emerges from the literature is that the properties of natural FMLs can outperform composites but do not appear to be competitive with metal or conventional FMLs. The reasons that limit their commercialisation are the low strength of the natural fibres, insufficient reproducibility of their properties and poor adhesion with the matrix [23, 38, 41]. However, in recent years, manufacturers of natural fibres, and in particular of flax fibres, have developed processes that enable them to achieve a uniform quality of their fabrics. Moreover, as regards fibre/matrix adhesion, it is possible to improve it by surface treatments and by choosing a matrix that is as compatible as possible with the fibres. Indeed, in many studies on natural FMLs, the resin used is a thermoplastic (e.g. polypropylene), which does not offer optimal adhesion with the fibres. This choice may be due to the willingness to have a fully recyclable material but leads to too low mechanical properties for structural application [24]. Finally, the rather pessimistic conclusions found in the literature must be taken with hindsight as the design of the proposed FMLs is not always optimised for specific applications.

Conclusion

FMLs have received much attention due to their excellent mechanical properties. Unfortunately, there is still a limited amount of work evaluating the mechanical properties of natural FMLs, especially flax fibre metal laminates. Furthermore, those hybrid materials are most often considered for very demanding aeronautical applications, but they may be of interest for other uses such as land transport. There is therefore a gap in the literature that deserves to be filled to some extent by an experimental and/or predictive study of the performance of flax fibre metal laminates.

Chapter 3

Flax fibre reinforced composites

In order to understand the behaviour of a natural fibre metal laminate and to be able to predict its performance, the mechanical properties of the natural fibre reinforced composite must first be known. Natural fibres, and in particular plant-based fibres, have gained in importance in recent years, as can be seen from the increasing number of publications [53]. However, research is far from having reached the maturity enjoyed by synthetic fibres. Indeed, as will be seen, there is not always a consensus on the mechanisms explaining the behaviour of natural fibre reinforced composite or on their actual performance.

In this report, the focus is on flax fibres, which are predominantly used in the bio-based composites industry. This is due to their relatively higher strength and stiffness compared to other plant fibres. They are already widely used in the automotive industry and can also be employed in other sectors such as the marine sector, sports and leisure, or household sector. In addition, research and development activities are underway to use flax fibre reinforcements in other applications such as wind turbine blades or for aerospace components. However, flax fibres also have disadvantages that slow down their commercialisation.

In the following, a critical review of the literature on the properties of flax fibre reinforced composites is presented. It will allow to deduce the properties of flax fibre metal laminates and to target the most relevant applications for this kind of materials.

3.1 Flax fibres

First of all, in order to understand the behaviour of flax fibre reinforced composites, it is necessary to know the main characteristics of the flax fibre, starting with its anatomy.

Flax fibres, like most of the bast fibre plant, are composed of amorphous hemicellulose reinforced by semi-crystalline cellulose microfibrils which ensure a good mechanical resistance. Lignin and pectin, other amorphous polymers, act as a binder between the cellulose fibres and give them a certain rigidity. The fibres also contain wax, which is mainly found on their

surface. Finally, flax fibre contains 60 to 80% cellulose, which makes it one of the most resistant natural fibres [6, 7, 16].

In addition to this chemical composition, flax fibres have a multi-scale hierarchical structure. Each fibre consists of a bundle of elementary fibres whose diameter is about $20\mu m$. At a microscale, an elementary fibre is made of a central channel called lumen and concentric cell walls. The inner walls, or secondary walls (S1, S2 and S3), have a specific angular orientation of the cellulose fibrils while the primary wall (P) is a disordered arrangement, as it can be seen in Figure 3.1. It is on the surface of the latter, i.e. at the level of the middle lamella, that most of the waxy substance is found, which plays an important role in the hydrophilic character of the fibre, as will be seen later [6, 16, 54].

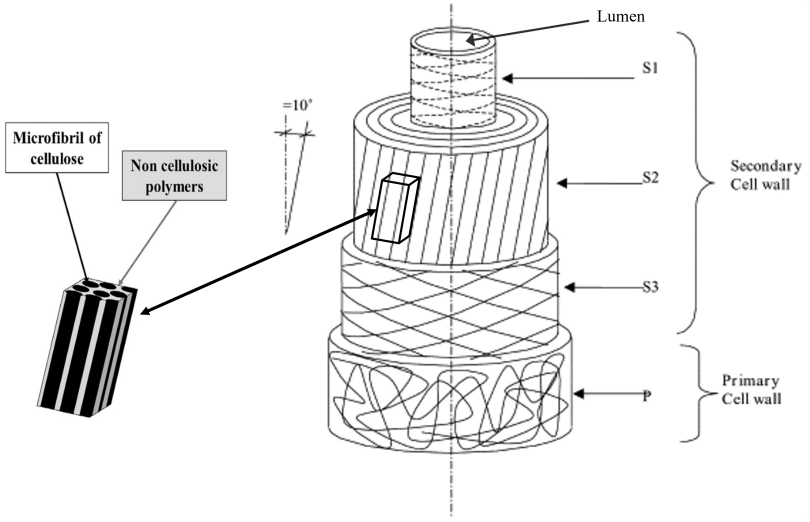

Figure 3.1: Hierarchical structure of an elementary fibre. Adapted from [6, 7].

This specific structure leads to a complex anisotropic behaviour. Indeed, the secondary wall S2 represents 80% of the cross section, meaning that this element is mainly responsible for the mechanical properties of the fibre. And, as the microfibril angle is small in this wall (around 10°), flax fibres have good mechanical properties along the fibre direction but poor in the radial one.

However, to compare the mechanical properties of flax fibres with those of synthetic fibres, it is more appropriate to use so-called technical fibres. A technical fibre is a bundle of 10 to 40 elementary fibres (up to $100\mu m$ in diameter) bound together by pectin and hemicellulose. The use of a technical fibre allows the properties to be averaged and thus to be closer to the reality. Indeed, they are not identical from one fibre to another, as these are natural fibres. It is therefore necessary to pay attention in the literature to the type of fibre used for the reported values. The properties of technical flax fibres are compared with the one of glass fibres in Table 3.1.

It can be seen that the properties of flax fibres are almost similar to those of E-glass fibres, but their density is lower. This explains why in the literature materials made of these two

Fibre	Tensile modulus [GPa]	Ultimate tensile stress [MPa]	Elongation at break [%]	Density [g/cm^3]
Flax	30-75	500-1500	1.2-3	1.2-1.5
E-Glass	60-80	1400-3500	1.8-4.8	2.5-2.6
S-Glass	86-88	4300-4900	4-5.7	2-2.5

Table 3.1: Properties of glass and technical flax fibres [7, 16–18].

types of fibres are often compared [23,24,55,56]. In addition, some variation in the properties of flax fibres can be observed. This can be explained by a different origin of the fibres and a different manufacturing process.

To isolate the flax fibres from the plant several steps can be followed [16, 57]. Some fibres undergo a retting stage during which the pectin that binds the fibres to the bast and the flax stem is damaged by water, fungi or dew. This stage is followed by a decortication process, either manual or automated. Finally, to obtain the technical fibres, the fibre bundles are separated by a hackling comb. Throughout this process, structural defects can be introduced, leading to different fibre qualities. These defects, which may also occur naturally in the elementary fibres, are called kink bands and can be seen in Figure 3.2. They are weak points where tensile fracture often initiates. The more defect there are (linked to the fibre length), the lower the fibre tensile strength is. Kink bands are also probably responsible for the compressive failure as it will be seen later [6, 16, 58].

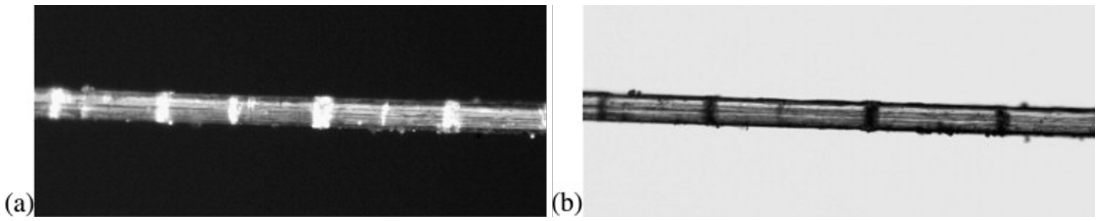

Figure 3.2: Kink bands at the surface of an elementary fibre, revealed by optical microscopy in transmitted polarised (a) and non-polarised (b) light [6].

At the end of the manufacturing process, technical fibres are often spun to produce a continuous yarn. During this step, the fibre may be twisted to improve its strength. But, as will be discussed, this does not have a positive impact on the properties of the composite. Finally, the quality of the fibre manufacturing process is important to obtain good mechanical properties and therefore the choice of fibre (i.e. manufacturer) is crucial to obtain a high performance composite.

In addition to the manufacturing process of the fibres, their high moisture absorption capacity can limit their mechanical properties. Indeed, compared to synthetic fibres, flax fibres contain hydroxyl and polar groups (hydrophilic chemical groups) which react with water molecules by forming hydrogen bonds. This causes the fibres to swell. For the composite, this can affect the curing reaction, weaken the fibre/matrix interface or cause hygro-thermal ageing [6, 9]. Thus, the moisture content during processing of the composite should be controlled to ensure identical properties. Apart from the problem of low moisture resistance, they have low thermal stability, which limits the temperature at which they can be processed. And they

are therefore flammable, but this issue can be mitigated for the composite by including a fire retardant in the resin.

Nevertheless, flax fibres have the advantage of having a reduced environmental impact compared to synthetic fibres. Le Duigou et al. [8] proposed a comparison of multiple environmental indicators[1] for the production of one kilogram of flax fibre and glass fibre, illustrated in Figure 3.3. Besides being less toxic for workers, flax fibres have a negative impact on global warming. This can be explained by the fact that plants are absorbing part of the CO_2 by photosynthesis during their life. In addition, the production process for flax fibres is less energy-intensive and less harmful to the environment than for glass fibres. Furthermore, if flax fibres are used instead of glass fibres for transport applications, the reduction in weight will reduce fuel consumption and thus limit the carbon footprint of the vehicle. Finally, concerning the end of life, as for synthetic fibres, it is difficult to preserve the properties of flax fibres for re-use. However, some energy can be recovered through incineration, especially as flax fibres do not need to reach a high temperature to burn.

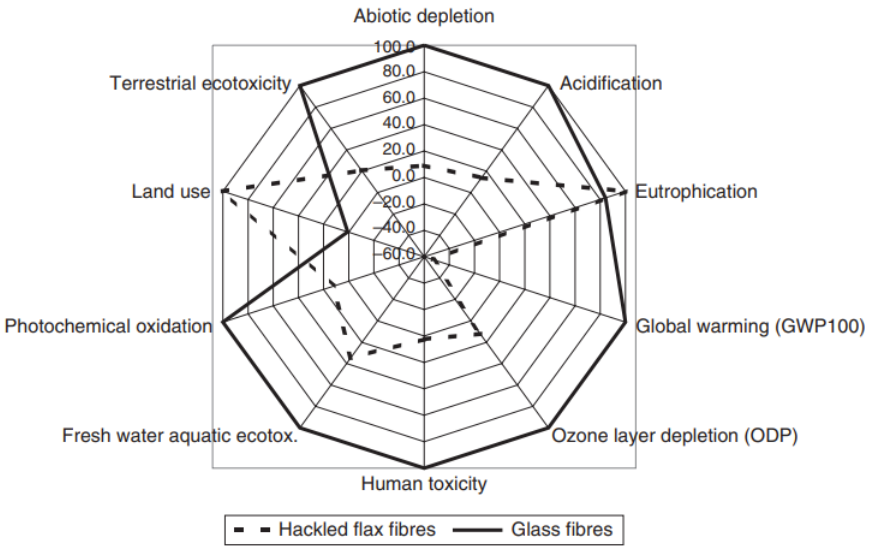

Figure 3.3: Comparison of the impact of producing $1kg$ of flax fibres and glass fibres [8].

Flax fibres therefore have a strong potential due to their low environmental impact, although it should be kept in mind that the results presented in Figure 3.3 are relative to the system and assumptions considered in the life cycle assessment. Moreover, Bos [16] states that the advantage of flax fibres over glass fibres from an environmental point of view depends on the application. Indeed, for highly loaded parts, the use of flax fibre reinforced composites can be counterproductive in view of the amount of material required and its life span. Flax fibre reinforced composites are therefore particularly interesting for transport applications.

[1] **Abiotic depletion**: Depletion of non-living resources (minerals, metals, fossil fuels...).
Eutrophication: Excessive accumulation of nutrients (nitrogen and phosphorus) in an aquatic or terrestrial environment.

3.2 Mechanical properties of the composite

Once the characteristics of the flax fibre are known, it is necessary to evaluate the properties of the composite since it is these properties that are needed to predict the FML behaviour. The following section will focus on the main mechanical properties of unidirectional flax fibre reinforced epoxy. The choice of an epoxy matrix is explained by the fact that this is the matrix type used in GLARE, so a comparison of FMLs can be made, but also because it ensures a good adhesion with the flax fibres [16]. Thermoset polymers also outperform thermoplastics in terms of mechanical properties, thermal stability, and durability, but most importantly, they can be cured over a reasonable temperature range given the low thermal stability of flax fibres.

3.2.1 Tensile properties

By far the most evaluated properties in the literature for flax reinforced epoxy are tensile properties. Some values for the Young's modulus, ultimate tensile strength and elongation at break are reported in Table 3.2. It can already be noticed that the results are quite fluctuating. To assess the reliability of the properties reported, a back calculation of the fibre Young's modulus has been done using the rule of mixtures. Only the values for Young's modulus are provided for clarity, and they are calculated using the Young's modulus of the epoxy given in the study or 3GPa when nothing is specified.

Study	Fibre specification	Manufacturing process	V_f [%]	Density [g/cm]	Modulus E [GPa]	Strength σ^{ult} [MPa]	Fail strain ϵ^{ult} [%]	Fibre modulus [GPa]
[9]		Compres. moulding	51	1.27	35	380	1.7	65.3
[59]	Hackled fibres	Autoclave, hot melt	42		28.2	378		63
	Roving	Autoclave, drumwinder	48		26.2	377		51.4
[60]	Hermes fibres	Compres. moulding	22		13	208	1.2	48.5
			42		22	362	1.3	48.2
			51		26	408	1.3	48.1
	Andrea fibres	Compres. moulding	23		11	165	1.1	37.8
			36		20	207	1.2	50.2
			51		28	290	1.1	52
	Marylin fibres	Compres. moulding	36		24	271	1.3	61.3
			48		31	348	1.2	61.3
			54		34	364	1.3	60.4
[61]	Hackled	RTM	40		28	340	1.6	64.8
[2]	FlaxDry© LINEO		60	1.33	35	330	1.8	57.2
[3]	FlaxPreg© LINEO		51 (wt)	1.3	35	365	1.35	
[17]	FlaxPly© LINEO	Compres. moulding	50	1.31	31.4	287	1.53	60
[62]	ArticFlax	RTM	42	1.24	35	280	0.9	79
			47	1.32	39	279	0.8	79.4
	Retted fibres	RTM	32	1.23	15	132	1.2	40.2
[12]	FlaxTape© LINEO	Autoclave	53	1.26	35.6	300	1.8	64.7
[63]	UD380 LINEO	Compres. moulding	57	1.31	23.4	283	1.6	38.8
	UD200 LINEO	Compres. moulding	61	1.33	26.7	304	1.72	41.9
	'UD180' LINEO	Compres. moulding	59	1.31	32.7	351	1.77	53.3
[57]	Arianne fibres	Autoclave	40	1.3	28	133		65.5
[64]	Hackled fibres	Autoclave, film stack.	40	1.3	26	190		60.5
	Roving	Autoclave, drumwinder	48	1.32	32	268		63.4

Table 3.2: Reported tensile properties of flax fibre reinforced epoxy.

[2] Lineo-ecotechnilin, Technical Data Sheet - FlaxDry (2019)
[3] Lineo-ecotechnilin, Technical Data Sheet - FlaxPreg (2019)

Despite this spreading of the tensile properties, the literature agrees that flax fibre reinforced epoxy has a non-linear behaviour under tensile loading. In fact, the stress-strain curve shows two distinct parts as can be seen in Figure 3.4. The composite behaves as a purely elastic material up to about 0.2% of strain [55, 60, 63]. It then exhibits visco-elastoplastic behaviour which covers almost 70% of the total tensile curve [9, 63]. This is a major difference from the behaviour of synthetic fibres, which are linearly elastic until failure. A decrease in the stiffness of the flax fibre reinforced composite is therefore observed. This is slightly counter-intuitive as during loading an increase in the stiffness of the flax fibre is observed due to a reorientation of the microfibrils. Mechanisms at other scales must therefore be involved. For example, Baets et al. [59] initially thought that this degradation could be due to damage to the fibre bundles or the matrix, but it turned out that this reduction in stiffness is a reversible phenomenon. Unfortunately, this non-linear behaviour remains poorly explained in the literature. In addition, it is important to note that the way in which stiffness is measured can have a significant impact on the results. Indeed, the measurement of modulus via the stress-strain curve in the standards is based on a strain range that is not limited to the elastic part in the case of natural fibres [59, 63]. Unfortunately, most of the studies concerning flax fibre composites do not mention the method used to evaluate this stiffness.

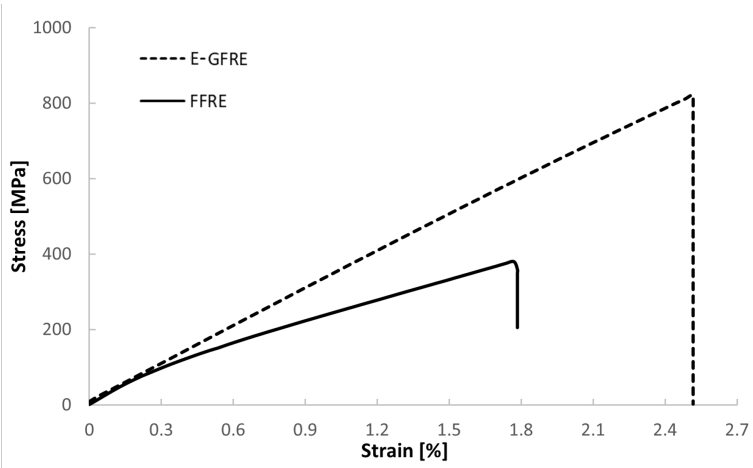

Figure 3.4: Example of stress-strain curve for FFRE ($[0°]$ and $V_f = 0.51$) and E-GFRE ($[0°]$ and $V_f = 0.4$). Adapted from [9].

As explained, the choice of the variety of flax fibres to be incorporated into the polymer resin is crucial. Coroller et al. [60] evaluated the properties of similar composites made of different variants of flax fibres. The climatic conditions in which they were produced, but also the decortication process, differentiated them. In particular, they concluded that the hackling step results in better performing composites. Duc et al. [61] also compared the properties of composites made from flax fibres of different qualities (with more or less defects). Indeed, kink band defects not only weaken the fibres but also create a stress concentration in the composite, which leads to cracking. Thus, they concluded that high quality fibres are those that can compete with E-glass fibres as reinforcements. Therefore, different type of fax fibres can explain the variation in the tensile properties observed in the literature.

However, it is not the only explanation. The pre-treatment applied to the fibres influence the mechanical properties of the composite. Indeed, even if it is often assumed that epoxy adhere well to flax fibres some improvement can be made by applying different surface treatment to the fibres. In particular, removing the wax helps to enhance the interfacial bonding with the matrix which is by nature hydrophobic. A better adherence leads to a more efficient load transfer within the composite and less pores, increasing thus the tensile properties. Bos [16] has notably proved that dewaxed flax fibres are sufficiently reactive towards the epoxy resin and that no compatibilizer, such as maleic anhydride is required. Georges et al. [65] found that an alkaline treatment that removes the wax but also part of the pectin is the best compromise for mechanical properties. Weyenberg et al [64] go a step further by pre-impregnated the fibres with dilute resin to fill the micropores inside fibre bundles. Therefore, different surface treatments can be considered to solve this problem but also to limit moisture absorption.

In addition to the surface treatments, the twist angle of the fibre can affect the properties of the composite. The literature agrees that twisting should be avoided to obtain good mechanical properties [6, 60, 61]. For example, Baets et al. [59] compared composites made from hackled fibres, rovings with little twist and yarns containing more twist. They concluded that hackled fibres gave the best performance because of their good orientation in the composite. Untwisted yarns are also better impregnated by the matrix due to good individualisation of the fibres. However, it is more difficult to manufacture a composite from hackled fibres as they tend to become misaligned during impregnation and their distribution is not uniform.

It is therefore necessary to check the quality of the impregnation of the fibres during the process to be sure of obtaining a high-performance composite. Unfortunately, only a few papers provide information on the structural quality of their composite, whether it be impregnation via microscope images [17, 61, 63] or adhesion via interfacial shear strength tests [60]. For example, Panzera et al. [12] observed the presence of resin-rich regions and porosities in SEM images of the cross section of a unidirectional composite. They were then able to assess the pore volume fraction in the composite. These data allow an informed comparison of the mechanical properties of different composites, but also to determine the most appropriate manufacturing process.

Concerning the transverse tensile properties, as expected they are lower than the longitudinal ones because of the architecture of the fibres. In the literature [12, 17, 64], a modulus around 4.5 GPa and an ultimate strength of about 20 MPa are reported for a composite containing 60% of fibre in volume. Flax fibre reinforced epoxy is thus very similar to its glass fibre counterpart regarding the transverse properties.

Finally, various parameters affect the tensile properties of the flax fibre composite and by optimising them, it is possible to obtain higher performances than those sometimes reported in the literature. This also means that care must be taken with the values that will be used for the prediction of the FML properties.

3.2.2 Impact properties

Another important characteristic to assess in order to understand the behaviour of a FML is the impact resistance of the composite. Different types of tests for low velocity, high velocity or ballistic impacts are described in the literature. The focus will be on the low velocity impacts described by a drop weight test as it is the more representative of a real impact situation.

The literature generally reports a low resistance of natural fibre reinforced composites under low velocity impact loading, which is mainly ascribed to the low fibre strength. Indeed, when flax fibre reinforced epoxy is compared against its glass fibre counterpart, a significant difference in behaviour and damage mechanism is observed. Flax fibre reinforced epoxy fails because of fibre breakage [10,52,66]. As shown in Figure 3.5, flax fibre composites experience almost no delamination as the crack develops through the thickness. In contrast, delamination dominates the damage mechanism of glass fibre reinforced epoxy until major fibre failure is reached. In fact, the glass fibres resist the load while cracks in the matrix form and lead to these large delamination damages, especially between plies with different fibre orientations. Panciroli et al. [66] have found that despite an identical flexural stiffness, flax fibres break at an impact force much lower than that required to attain fibre breakage in the glass fibre composite.

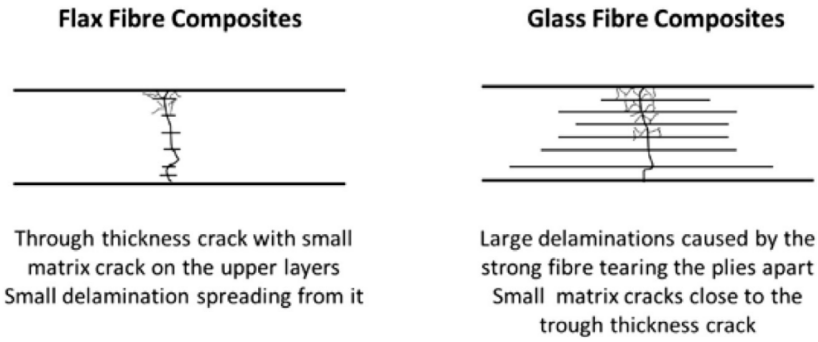

Figure 3.5: Low velocity impact damage for flax and glass fibre reinforced epoxy [10].

However, the flax fibre-based composite absorbs more energy during impact than the glass fibre composite. Wambua et al. [67] have also shown that among natural fibres, flax fibres allow the best energy absorption during ballistic impact thanks to their higher strain to failure.

To improve the impact resistance of flax fibre composites it is possible to work on the choice of the matrix or on the architecture of the layup sequence. Indeed, the ductility of the polymer matrix affects the energy absorbed at perforation, the damage resistance and tolerance. Thermoplastics allow for example to limit the propagation of matrix cracks by forming a plastic zone at their tip. Moreover, limited fibre/matrix adhesion is beneficial for impact resistance. Unfortunately, by making these choices, the tensile and compressive properties are greatly reduced. Another possibility is to use a cross-ply layup instead of a unidirectional composite, with a high fibre volume fraction because the impact behaviour is fibre dominated [10]. The use of a metal sheet bonded to the surface to improve the impact resistance of the flax fibre

composite is also reported in the literature. This is similar to the concept of FML. It has therefore been proven that by adding a layer of steel, the material suffers less damage but absorbs more energy than a monolithic metal [52, 67].

Finally, it appears that composites perform badly under impact, particularly natural fibre composites. But these performances remain poorly evaluated in the literature, hindering the adoption of natural fibres in structural applications.

3.3 Additional functionalities

Apart from the mechanical properties described above, flax fibre composites have functionalities that may be of interest when a structural application requires a multifunctional material. Thanks to their particular microstructure, flax fibres have good thermal insulation properties and can be used as electromagnetic transmitters (for aircraft radome) due to their low dielectric dissipation. But even more interestingly, flax fibre composites have excellent vibration or noise damping properties compared to conventional composites, as will be shown.

3.3.1 Vibration damping properties

Damping properties refer to the ability to eliminate mechanical energy by converting it into another form of energy. This energy dissipation is particularly effective in flax fibres because it involves multi-scale friction mechanisms [6]. Indeed, the multi-layer structure of the fibre allows a high damping by friction of the microfibrils contained inside the cell walls (intra-cell wall friction) and by inter-cell wall friction. At the composite scale, friction between the elementary fibres (intra-bundle friction) and inter-bundle friction are also involved. It is therefore known that composites based on natural fibres have much better damping properties than those based on synthetic fibres, regardless of the type of matrix used.

To characterise the damping performance of a composite multiple variables exist such as the loss factor ξ or damping ratio ζ. They are linked by a simple relationship at low damping levels [11]:

$$\xi = tan\delta = \frac{E''}{E'} = \frac{\lambda}{\pi} = 2\zeta \tag{3.1}$$

where, E'' and E' are the loss and storage modulus measurable via a Dynamic Mechanical Analysis (DMA). The damping ratio is measured using a vibration beam test (VBT) which provides free vibration decay curve in which the logarithmic decrement λ can be assess [68].

Duc et al. [11, 69] compared the damping properties of a conventional composite and a flax fibre reinforced epoxy. They proved by DMA that the flax fibre composite has a better damping at room temperature compared to carbon or glass fibre composites. The influence of fibre twist, fibre pre-treatment, fibre quality and composite architecture on the damping

properties was also evaluated. This comparison is shown in the two graphs in Figure 3.6 which represent the loss factor, measured by DMA or VBT at room temperature, against the specific Young's modulus of the composite.

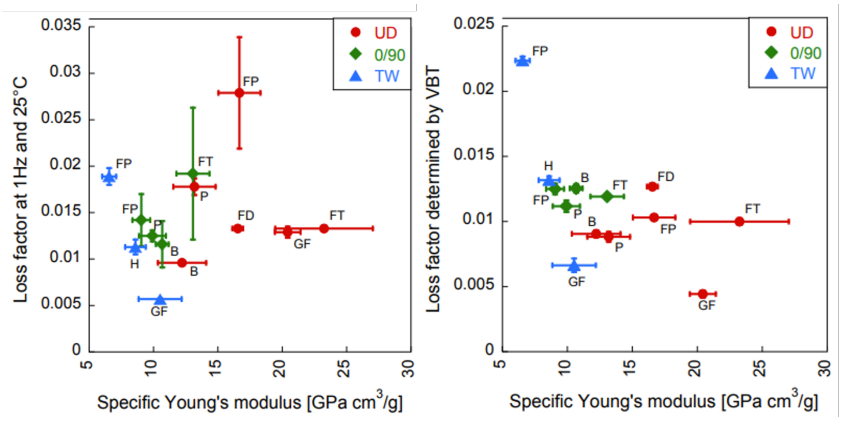

	Fibre type	Twist angle	Sizing
GF	Glass	0°	None
FP	Flax, High quality	13°	Epoxy
FD	Flax, High quality	13°	None
FT	Flax, High quality	0°	None
P	Flax	0°	Epoxy
B / H	Flax	13°	None

Figure 3.6: Loss factor determined by DMA or VBT against the specific Young's modulus of different composites [11].

It can be noticed that the distribution of the tested specimens is not the same from one graph to another. This is because the two tests are not performed at the same vibration frequency. During DMA, the vibration frequency was 1 Hz, which is lower than that at which the VBT measurements were carried out. At low frequencies, the friction mechanisms have more time to occur, which increases the amount of energy dissipated. But beyond that, the influence of parameters such as the architecture of the composite or the torsion of the fibres is not identical. In the case of the VBT measurement, weaving and twisting of the fibres is beneficial for good damping. Indeed, at large deformations, inter- and intra-bundle friction are the dominant friction mechanisms. However, for small deformations, the main dissipation mechanisms are inter- and intra-cell wall friction, which is enhanced by the improved adhesion between the fibres and the matrix. Finally, in both cases the quality of the fibres is important to improve the damping properties which are always better than for conventional composites.

Conclusion

Finally, flax fibre reinforced epoxy shows promising properties but is not competitive in all respects with conventional composites. Panzera et al. [12] compared the specific properties of flax and glass fibre composites. It can be seen from Figure 3.7 that the stiffness is very similar but the strength of the flax fibre composites is unfortunately lower. This difference is even more pronounced for S-glass fibre composite.

However, flax fibres have the advantage of having diverse properties and being bio-based, which makes them very attractive, especially in the field of transport. It therefore makes sense to combine them with a metal in a FML for use in structural applications requiring multiple functionalities.

Load direction	Specific properties ($MPa/g.cm^{-3}$)	Glass fibre composite	Flax fibre composite	Percent variation (%)
Longitudinal	Tensile strength	**521.6**	238.5	↓118%
	Tensile modulus	21.2	**28.3**	↑33%
	Flexural strength	**621.6**	263.6	↓136%
	Flexural modulus	**20.9**	19.5	↓7%
Transverse	Tensile strength	10.8	**15.1**	↑39%
	Tensile modulus	**5.2**	3.4	↓118%
	Flexural strength	**40.9**	11.5	↓255%
	Flexural modulus	**5.9**	2.6	↓129%
45°	Shear strength	13.0	**29.9**	↑39%
	Shear modulus	**40.9**	3.4	↓1100%

Figure 3.7: Comparison of the specific properties of flax and E-glass fibre composites [12]. *Modulus values are given in* $GPa/g.cm^{-3}$.

Chapter 4

Research Definition

In view of the very limited literature on flax fibre metal laminates, it appears both pertinent and justifiable to conduct research on their performance, particularly regarding their impact resistance and damping capacity. The preliminary assessment of the benefits of the flax fibre composite and the metal layer suggests that they may be particularly suitable for applications requiring this set of properties.

The principal aim of this thesis is to conduct a comprehensive experimental investigation to provide an initial evaluation of FLARE's impact resistance and damping characteristics. Another crucial goal of this study is to furnish analytical tools capable of predicting these material properties. This dual objective not only facilitates the comparative analysis between FLARE and traditional FMLs, but also significantly contributes to the design phase for forthcoming applications.

4.1 Research Questions

To ensure that the objectives described above are met the following main research question has been formulated:

To what extent the impact resistance and vibration damping properties of FLARE are suitable and predictable for designing feasible solutions where they are key to meet requirements?

To answer this question, the impact response and vibration damping capabilities of the material must be evaluated separately before concluding on how to optimise the design of the FML for specific applications. Thus, the following sub-questions will pave the way to answer the main research question:

1. To what degree does FLARE maintain the advantageous vibration damping properties inherent in flax fibre composites?

1.1. *What influence does the metal volume fraction have on the damping properties of FLARE?*

1.2. *What influence does the fibre orientation have on the damping properties of FLARE?*

2. How does FLARE behave under a low velocity impact?

2.1. *What influence does the metal volume fraction have on the impact properties of FLARE?*

2.2. *What influence does the fibre type have on the low velocity impact response?*

3. What predictive tools developed for conventional FMLs are applicable for natural fibre metal laminate?

3.1. *To what extent the metal volume fraction method can predict the main mechanical properties of FLARE?*

3.2. *To what extent the damping behaviour of FLARE can be predicted knowing the one of the metal and composite?*

3.3. *To what extent does the impact analytical model developed for conventional FML give similar results to the impact experiments?*

4.2 Research Framework

In order to provide conclusive answers to the above questions, it is imperative to establish a well-defined research framework and the basic hypotheses of the study. Given the wide range of possible sample configurations and methods for assessing parameters, it is necessary to make informed choices to ensure that the study is both meaningful and representative.

Firstly, the present work focuses solely on the 2/1 configuration of the fibre metal laminate. This decision was taken to streamline the study, as this straightforward configuration is frequently examined in existing literature, facilitating direct result comparisons. In addition, this sandwich arrangement is believed to address a multitude of issues, as it aligns with the objective of minimising structural weight – hence reducing the number of aluminium layers – while simultaneously providing protection to the composite against external factors.

Regarding the assessment of damping behaviour, as elucidated in the literature review, there exist several methods to evaluate it, each yielding varying outcomes. Hence, a decision was made to employ both Dynamic Mechanical Analysis and Vibration Beam Testing to measure the damping factor. This choice is grounded in the belief that these methods capture two distinct mechanisms of energy dissipation, and therefore lead to different conclusions with regard to the research questions posed.

With regard to impact resistance, as can be deduced from the research questions, the emphasis is on low velocity impact. Indeed, investigating high-speed impact or blast loading in the context of FLARE can be also of interest, yet establishing such experiments within the TU DELFT laboratory proves to be more intricate. Consequently, preliminary conclusions will be drawn based on the low-velocity impact response, providing an initial assessment of FLARE's performance in comparison to other well-established materials.

Lastly, for the purpose of comparing experimental findings with predictions, the selection of predictive tools becomes essential. For the main mechanical properties, the metal volume fraction approach is employed, as it is anticipated to offer a sufficiently accurate initial estimation. The intention here is to avoid complex methodologies such as Classical Laminate Theory (CLT) in order to facilitate the design process a posteriori. Regarding the assessment of damping behaviour, the literature suggests that a straightforward rule of mixture could provide a reasonable prediction. Nonetheless, given the intricate nature of damping mechanisms, the comparison will encompass various types of mixture rules. Both volume and weight fractions of the materials will be considered, given that material density substantially influences damping performance. Finally, when it comes to impact behaviour, a more complex analytical model is required. The model proposed by Morinière et al. [13] is considered a robust starting point for predicting FLARE's performance under low-velocity impact conditions. This model has been developed with insights from previous models and is both comprehensive and feasible for application to the present case.

It is important to note that all results presented in this study are limited to the defined research framework, in particular the FLARE configuration examined. It should be considered that different configurations may produce superior results, and it is essential to acknowledge that not all potential influential parameters have been explored in this research. For instance, the geometry of the samples, particularly their overall thickness, or the volume fraction of fibres in the composite, could influence vibration damping and energy absorption during impact.

Part II

Methodology, Results and Discussion

Chapter 5

Composite and Fibre Metal Laminate manufacturing

To address the research questions stated in previous chapter, a methodological framework based on experimental work was followed. This initial experimental phase entails the manufacturing of multiple samples necessary for subsequent testing.

Subsequently, the upcoming section elucidates the material selection and expounds upon the chosen manufacturing method, namely wet layup combine with vacuum bagging. To validate this manufacturing process, a sample quality assessment was also carried out, and is explained in the following.

5.1 Material Selection

In general, GLARE panels used in the aerospace industry consist of thin sheets of aluminium alloy 2024-T3 and layers of UD S2-glass/FM94-epoxy prepreg. In the case of FLARE, raw materials as close as possible to those used for GLARE were chosen while respecting availability constraints. This limits the sources of discrepancies in the comparison of the two FMLs. However, it should be borne in mind that when looking for specific characteristics and taking into account factors such as cost and mechanical performance, different choices of metals and resins can be considered.

Metallic material

The aluminium alloy 2024-T3 was chosen. This heat-treated alloy is already widely used in the aircraft industry and can be an optimal choice for other vehicle applications. Indeed, it has an excellent fracture toughness and high strength to weight ratio, which is favourable for impact properties. Its main properties are shown in Table 5.1.

Specifically, the Al 2024-T3 sheets used in the project have a thickness ranging from 0.3 to $0.5mm$. They are chromic acid anodised and coated with BR 127 primer to provide a protective layer against corrosion and to enhance the adhesion with the epoxy resin.

ρ $[g/cm^3]$	2.78	Density at $23°C$
α $[1/°C]$	23.2 10^{-6}	Coefficient of thermal expansion
E [GPa]	71 - 73	Tensile Young's modulus
σ_{yield} [MPa]	345	Yield tensile strength
σ_{ult} [MPa]	450 - 496	Ultimate tensile strength
ϵ_{ult} [%]	10 - 20	Elongation at break
μ [-]	0.33	Poisson ratio

Table 5.1: Aluminium alloy 2024-T3 properties [19–21].

Composite materials

In the case of FLARE, the S2-glass fibres are replaced by flax fibres. As mentioned in the literature review, the choice of flax fibres has a direct impact on the final mechanical properties of the product. Ideally, the choice of a high performance unidirectional prepreg would have provided characteristics close to those of GLARE, particularly in terms of the manufacturing process. But, for reasons of availability, the ampliTex™ UD 280 gsm technical fabric from Bcomp was chosen. It is a non-crimp unidirectional flax fabric, designed to maximise the performance of the composite (high quality of the fibres, optimal twist of the yarn). In addition, a treatment (not specified) is applied to the fibres to improve the fibre-matrix interface. The mechanical properties of the dry fibres are shown in Table 5.2.

In addition, according to the manufacturer's specifications, this fabric is non-toxic to humans and has a beneficial effect on limiting global warming through the sequestration of CO_2 by photosynthesis. This fabric is recommended for application ranging from sport to automotive, aerospace, and marine industries.

ρ $[g/cm^3]$	1.35	Density at $23°C$
α $[1/°C]$	~ 0	Coefficient of thermal expansion
E_1 [GPa]	61	Longitudinal tensile Young's modulus
E_2 [GPa]	6.4	Transverse tensile Young's modulus
σ_{ult} [MPa]	580	Ultimate tensile strength
ϵ_{ult} [%]	1	Elongation at break

Table 5.2: Flax fibre dry fabric properties.

In order to establish a comparison and in particular to benchmark the vibration damping properties of FMLs, glass fibre-based metal laminates are also manufactured. A quasi-unidirectional E-glass fabric similar to the flax fabric, especially in terms of thickness, was kindly provided by Suzlon Energy for this purpose. It is crucial to acknowledge that FMLs created using these fibres differ from GLARE, as GLARE employs S2-glass fibres instead of E-glass fibres. However, considering factors such as availability and cost, an E-glass fabric was selected. Although it may not precisely match the properties of GLARE's fibres, it still provides a reliable benchmark, particularly for intended applications that do not demand the same level of performance as aerospace applications. The aspect of the dry fabrics and composites manufactured from them are shown in Figure 5.1.

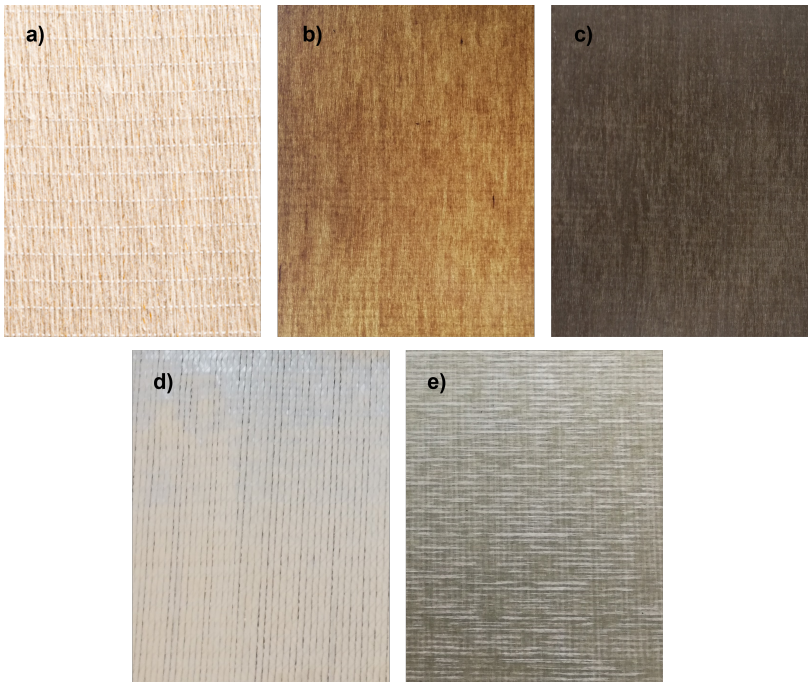

Figure 5.1: Aspect of the dry fibres and their composite. a) Flax fabric, b) Flax fibre composite observed against light, c) Flax fibre composite, d) Glass fabric, e) Glass fibre composite $[0/90]_s$.

In both cases a structural laminating epoxy is used to impregnate the dry fabrics. The epoxy resin Resoltech 1200/1204 has been selected because it is appropriate for hand lamination and possesses mechanical properties that are quite similar to FM® 94 epoxy, which is commonly employed in GLARE prepreg. Its main characteristics and properties are shown in Table 5.3.

Tg $[°C]$	71 - 86	Glass transition temperature
ρ $[g/cm^3]$	1.18	Density at $23°C$
E [GPa]	3.42	Tensile Young's modulus
σ_{ult} [MPa]	67.6	Ultimate tensile strength
ϵ_{ult} [%]	3.30	Elongation at break

Table 5.3: Resoltech 1200/1204 epoxy properties.

5.2 Manufacturing process

In the literature, the prevailing manufacturing method for fibre metal laminates is the autoclave process, known for ensuring a high-quality final product [32]. But for this project, as the raw materials are dry fabrics, this process is not suitable. Nonetheless, the literature is also mentioning out-of-autoclave processes [41, 70]. Due to the presence of aluminium plates, infusion-based fibre impregnation is not feasible, as it hampers resin flow throughout the material's thickness [71]. The remaining option, which will be employed to manufacture FLARE panels, is wet layup combined with vacuum bagging. In that process, described in Figure 5.2 and detailed in the following, the liquid resin is manually applied onto each dry fibre ply.

Figure 5.2: Fibre metal laminate production process.

Cutting: The materials are first cut to the appropriate size. The aluminium layers are cut using a Darley Shear guillotine, as shown in Figure 5.3, while the dry fabric is hand cut using scissors.

Figure 5.3: Darley Shear Guillotine.

Aluminium layer cleaning: Moving on to the pre-treated and primed sheets of aluminium 2024-T3, their surfaces undergo a cleaning process. A cloth containing MEK (2-butanone) is used to eliminate organic dirt, followed by a light sanding with Scotch Brite (3M). The surfaces are then cleaned again with a cloth containing MEK to remove any remaining dust and organic dirt. This cleaning process also helps activate the primer in preparation for the layup.

Wet layup: Subsequently, the hand layup process takes place. As it can be seen in Figure 5.4 a), it starts by placing the first aluminium layer on a flat mould that has been coated with a release agent. A first layer of pre-mixed resin is applied to the area where the composite will be bonded. Each fabric ply is then impregnated with the epoxy resin. Two different techniques were employed to apply the resin. The first method involves using a brush to ensure a uniform distribution of the resin. In the second method, the resin is first degassed before being poured into the centre of the ply as shown in Figure 5.4 b). The ply is then covered with a plastic sheet, and the resin is spread from the centre using a resin spreader (cf. Figure 5.4 c)). This technique removes some of the air bubbles while preserving the integrity of the fibres. This process is repeated for each layer until the metal layer is positioned on top (cf. Figure 5.4 d)).

Vacuum bagging: To provide consolidation pressure and remove trapped air and volatiles during curing, vacuum bagging is employed. This is particularly important when working with flax fibres, as they have a tendency to expand as they absorb resin. Additionally, the

manufacturer of the fibres acknowledges that flax fibres may appear dry despite absorbing a substantial amount of resin. Therefore, it is recommended to impregnate the fabrics with an excess of resin. Vacuum bagging assists in removing this excess resin by exerting pressure. In the present case, to obtain a fibre weight content of around 50%, twice as much resin was mixed as fibre in terms of weight.

The vacuum bagging process involves the use of a perforated release film, as shown in Figure 5.4 e) to minimise adhesion between the product and the consumable. In addition, the perforations allow excess resin to bleed out of the laminate during the curing process. On top of this, a bleeder/breather fabric is placed to collect any surplus resin, and provide a flow path to allow air and volatiles to escape (cf. Figure 5.4 f)). The vacuum bag is then sealed to the mould with sealant tape, and vacuum is drawn using a vacuum pump (cf. Figure 5.4 g)). Instead of achieving a full vacuum, which would remove an excessive amount of resin from the laminate, a moderately high vacuum level is used. This compromise, which corresponds to around 60% of full vacuum, still allows air bubbles to be extracted and the laminate to be compressed to a reasonable degree.

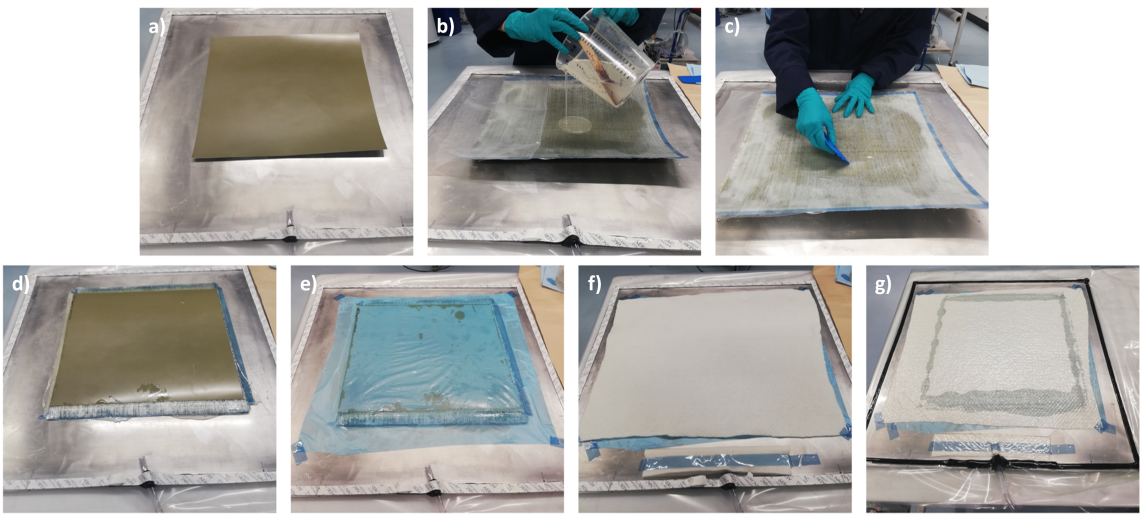

Figure 5.4: Wet layup and vacuum bagging process steps.

Curing: The resin is finally cured according to the manufacturer recommendations, i.e. at room temperature for 24 hours under 60% vacuum, and an oven post-cure for 16 hours at 60° to obtain a high quality product. The post-curing process increases the degree of cure of the resin and improves mechanical properties of the final product.

Unfortunately, this manufacturing process suffers from several drawbacks that have a significant influence on the mechanical properties of the final product. Indeed, problems related to fibre misalignment and potential damage to the reinforcement can occur during the layup process. Moreover, due to the limited pressure applied during the curing process, the resulting parts exhibit higher void content and lower consolidation compared to parts cured in an autoclave, for instance. However, for impact and damping properties, these defects are considered acceptable for a first study. In any case, the wet layup process is the one that is

feasible in the laboratory but will probably not be the one used on an industrial scale.

In addition to FLARE panels, composite panels are also manufactured as some of their properties are needed to validate the predictive tools used for conventional FMLs. To ensure that they are manufactured under the same conditions as the FMLs, the fibre plies are covered by a flat mould before vacuum bagging the laminate. Glass fibre reinforced epoxy and GLARE panels were also manufactured.

5.3 Specimen characterisation

To validate the manufacturing process and facilitate accurate interpretation of mechanical test results, the quality of the composite and FML plates was evaluated by analysing their porosity content, fibre volume content, and the degree of cure of the resin.

5.3.1 Differential Scanning Calorimetry (DSC)

To validate the recommended curing cycle of the epoxy manufacturer, a differential scanning calorimetry (DSC) analysis was conducted on the TA instruments DSC 250. Flax fibre reinforced epoxy and glass fibre reinforced epoxy samples were extracted from the composite plates manufactured. The DSC analysis involved subjecting the samples to a heat-cool-heat cycle ranging from 20°C to 120°C, with a heating rate of $20°C/\text{min}$. During the first heating cycle, water absorb by the fibres, or any residual solvent are removed. The variations in heat transfer between the sample under analysis and a reference are then quantified to identify and characterise endothermic and exothermic phase transitions.

Although direct measurement of the degree of cure is not feasible using this method, it is possible to get an idea of the cross-linking state of the polymer via the glass transition temperature (Tg), which can be measured by DSC. The Tg increases with the number of cross-links formed between the resin and the hardener. By comparing the Tg value with that indicated by the epoxy manufacturer, it is possible to assess whether the resin has reached a satisfactory level of cure leading to optimum mechanical properties.

The DSC curves obtained for the composite component of FLARE_5_0.5 are displayed in Figure 5.5. The first heating cycle differs from the second in that it contains the previous thermal history of the sample, which is subsequently erased by heating the material above a transition.

The glass transition temperatures measured are summarised in Table 5.4. Considering that the manufacturer specifies a glass transition temperature ranging from 71°C to a maximum of 86°C, it can be reasonably concluded that the manufacturing process is satisfactory, as the observed Tg values fall within the acceptable range.

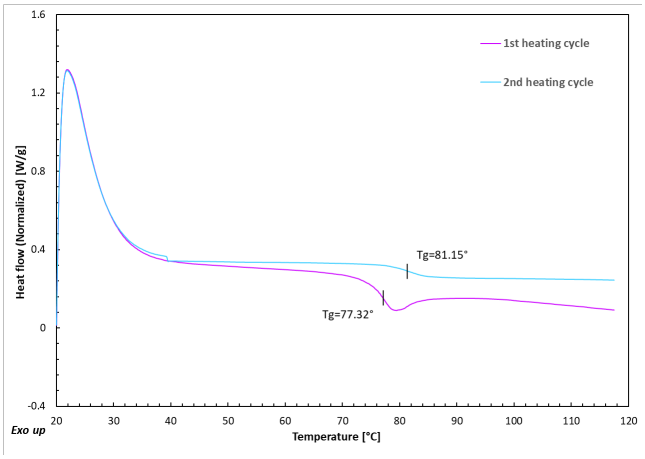

Figure 5.5: DSC curves for the composite component of FLARE_5_0.5 sample.

Specimen	T_g 1^{st} heating cycle [°C]	T_g 2^{nd} heating cycle [°C]
FFRE $[0°]_4$	73.9	81.5
FLARE_5_0.5	77.3	81.2
GFRE $[0°/90°]_s$	75.8	80.7

Table 5.4: Glass transition temperature measured using DSC.

5.3.2 Void content measured by Microscopy

To determine the void content of composite and FML plates, the burn off test cannot be used as it necessitates exposing the material to high temperatures to eliminate the resin through ignition. Indeed, this process would also lead to the decomposition of the flax fibres. As an alternative, microscopy observation was conducted on a Keyence Laser Scanning microscope, and subsequent image analysis was performed using the *voidContentMeasurement* plugin within the ImageJ software. Using this plugin, a threshold is determined which includes the pixels corresponding to a void and excludes pixels corresponding to fibre/matrix, as shown in Figure 5.6. In this way, it is possible to quantify the volume of void present in the image.

To do this, three small samples are cut from different location of the composite and FML plates using respectively a diamond blade and a silica carbide blade. Using samples from different locations gives a more complete picture of void content across the whole panel, avoiding over-generalisation of conclusions based on isolated cases. These samples are then embedded in a slow curing epoxy resin and polished before being observed under the microscope.

An example of void content measurement is shown in Figure 5.6. As it can be seen in the distribution of the pixel in the grey scale, there is no clear distinction between the voids (darker area) and the rest of the image. Indeed, if we are looking closer, the fibre outer walls are counted as void. So the value obtained using that method is most likely to be an overestimation of the real void volume fraction.

This discrimination issue is even more present for the cross-ply samples where the fibres running parallel to the cutting direction are dark. To help the void detection a manual selection has been performed. The void content results are shown in the summarising Table 5.5. The values observed are comparatively high compared with those achievable by manufacturing techniques involving the use of prepregs. However, it was determined that these values did not compromise the required quality of the fibre metal laminates in this study.

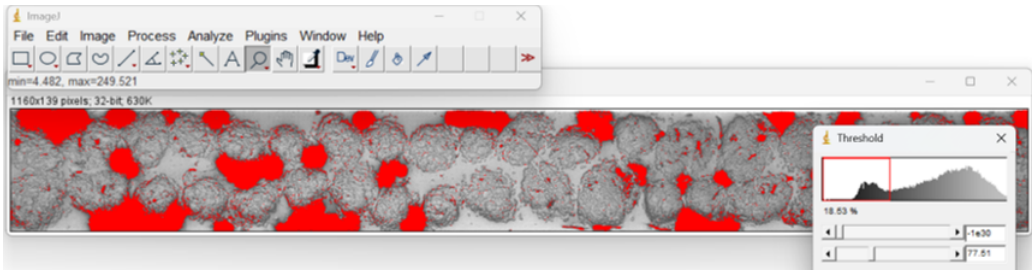

Figure 5.6: Void content measurement using ImageJ for UD composite sample.

Finally, these microscopic observations reveal the presence of distinct elements of natural fibre composites identified in the literature review, including fibre bundles, technical fibres, and elementary fibres with their lumens. These characteristic components of flax fibre composites are depicted in Figure 5.7. This differs significantly from glass fibre composites, which have perfectly circular individual fibres distributed almost homogeneously in the matrix.

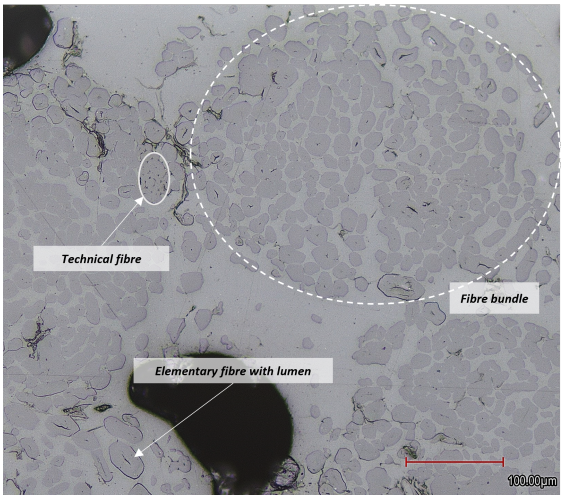

Figure 5.7: Microscopic observation of flax fibre reinforced epoxy with the characteristic features highlighted.

5.3.3 Fibre volume fraction measurement

To determine the fibre volume fraction, without using the burn-off test method, microscopy image analysis could be performed. However, as it can be seen in Figure 5.6, the colour on the gray scale of the matrix and the fibre is almost the same. Therefore, it is not possible to segregate the fibres from the resin using the software ImageJ. A manual cut out of the fibre bundles is possible, but it is a time consuming process and not completely reliable as some matrix penetrates the fibre bundles.

Thus, to determine the fibre volume fraction, a simple method based on weight and dimensions measurement have been followed. This gives first an estimation of the fibre weight fraction of the composite:

$$\mathrm{FWF}_c = \frac{n_f \rho_{A_f} A}{w - n_{Al} \rho_{A_{Al}} A} \tag{5.1}$$

where, n_f and n_{Al} are respectively the number of fibre and metal layers within the laminate, ρ_{A_f} and $\rho_{A_{Al}}$ the areal density of the fabric and aluminium sheets, A the area of the plate and w its weight. The dimensions of the panels were measured using a ruler and a caliper for the thickness, and the weight using a precise scale.

The volume fraction can also be deduced knowing the density of the fibres:

$$\mathrm{FVF}_c = \frac{n_f \rho_{A_f} A / \rho_f}{V - n_{Al} t_{Al} A} \tag{5.2}$$

where, ρ_f is the density of the fibres, V the volume of the plate and t_{Al} the thickness of the aluminium sheet.

This method gives a first estimation of the fibre volume fraction in the composite layers within a FML plate. The void volume fraction can be deduced using similar equation for the resin material.

Conclusion

In summary of this section, the manufacturing process involving wet layup combined with vacuum bagging successfully produced samples of both FFRE and FLARE. Nonetheless, it should be noted that this method is not without its drawbacks, as microscopy revealed a relatively significant presence of voids within the samples. But, as mentioned in the literature review, the effect of voids on mechanical properties is mitigated when considering a FML.

Furthermore, the determination of the fibre volume in the case of flax fibre reinforced epoxy was found to be more intricate compared to traditional composites. Enhancing this process could involve exploring alternative measurement techniques for improved accuracy.

Finally Table 5.5 summarises the manufacturing conditions and quality of each sample.

Type of layup	**Tlab** [°C]	**RHlab** [%]	**Thickness** [mm]	**MVF** [%]	**FVF** [%]	**Void content** [%]	**Density** [g/cm^3]
FFRE $[0°]_4$	20.6	36	1.79	/	44.7	9.71	1.18
FFRE $[0°/90°]_s$	21.6	43	1.86	/	43.0	6.76	1.21
GFRE $[0°/90°]_s$	21.6	35	1.92	/	52.4	7.99	1.81
FLARE_2_0.5	20.2	30	1.94	51.6	42.6	14.6	1.99
FLARE_2_0.4	20.2	30	1.65	48.5	47.1	11.4	1.96
FLARE_5_0.5	20.4	32	2.95	34.5	42.1	10.2	1.72
FLARE_5_0.5	21.4	39	2.89	34.6	42.4	13.5	1.72
FLARE_5_0.4	20.7	38	2.64	30.0	42.9	15.3	1.63
FLARE_5_0.3	21.2	37	2.54	23.6	41.2	5.89	1.57
GLARE_5_0.3	29	34	2.61	23.0	50.1	13.1	1.94

Table 5.5: Manufacturing condition and properties of manufactured plates.

Chapter 6

Mechanical properties of FFRE and FLARE

As mentioned earlier, in order to forecast the performance of a fibre metal laminate (FML), it is crucial to have knowledge about the mechanical properties of its individual components. Specifically, the elastic properties and strength of the materials are necessary for accurately modelling the impact behaviour of the FML. The properties of the aluminium alloy, presented in Table 5.1, are already extensively documented. However, in the case of the flax fibre reinforced epoxy, as discussed earlier, a significant degree of variability is observed. This scattering arises due to various factors such as the quality of the flax fibres, their pretreatment, or the manufacturing process of the composite material. Therefore, in order to address this variability, the tensile properties of flax fibre reinforced epoxy (FFRE) samples are assessed in the following.

In addition, a series of tensile tests were carried out on FLARE samples to evaluate the reliability of the metal volume fraction method to predict the FML behaviour in relatively straightforward cases such as Young's modulus and tensile ultimate strength. All the tensile tests performed are summarised in the test matrix Figure 6.1.

	Fibre	Metal thickness		Fibre orientation			
Tensile test	Flax	0.4	0.5	0°	90°	+/-45°	Nb of samples
Test 1	x			x			6
Test 2	x				x		6
Test 3	x					x	6
Test 4	x	x		x			6
Test 5	x		x	x			6
							30

Figure 6.1: Tensile test matrix.

Finally, this chapter presents the findings from the tensile tests and compares them to both the predictions made using the MVF method and to the behaviour of the reference material, GLARE.

6.1 Tensile tests: experimental set-up

All the tensile tests were conducted using a 20kN Zwick Universal quasi-static test machine. This particular tensile test machine was chosen as it allows to generate sufficiently high forces to reach failure of the strongest tested samples (in this case, the FLARE samples). Furthermore, it is equipped with an automatic extensometer, which is necessary for precise measurement of elongation at the gauge area. In the case of the weakest composite samples (FFRE $[90°]_4$), a 1kN load cell was installed on the machine to ensure accurate results when the ultimate load does not exceed 1kN.

The tensile tests conducted on the composite samples followed the ASTM Standard B3039-08. Rectangular specimens were cut from the composite plate using water jet cutting. To prevent compressive damage caused by the mechanical grips used to apply the tensile load, paper end tabs were bonded to the composite material. Specimen dimensions are shown in Figure 6.2. The extensometer gauge length was $100mm$.

The $[0°]_4$ and $[\pm 45°]_4$ samples were subjected to a testing speed (or displacement controlled rate) of $2mm/min$. However, for the $[90°]_4$ samples, the testing speed was reduced to $1mm/min$ due to their lower ultimate load compared to the other samples.

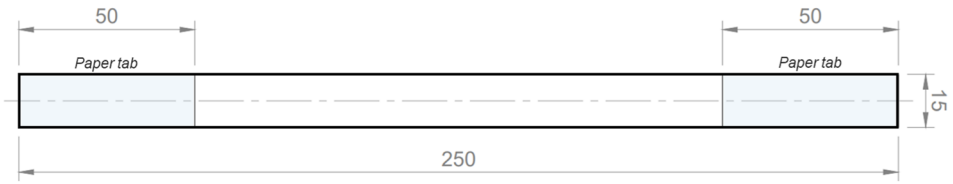

Figure 6.2: FFRE tensile test coupon. *All dimensions are in mm.*

Regarding the fibre metal laminate specimens, the test procedure was adjusted based on the recommendations provided by the Fibre Metal Laminates Centre of Competence [72]. The specimens were cut using water jet cutting into the dogbone geometry illustrated in Figure 6.3. Subsequently, the extensometer gauge length was set to $70mm$. The tests were carried out with the recommended loading rate of $6mm/min$.

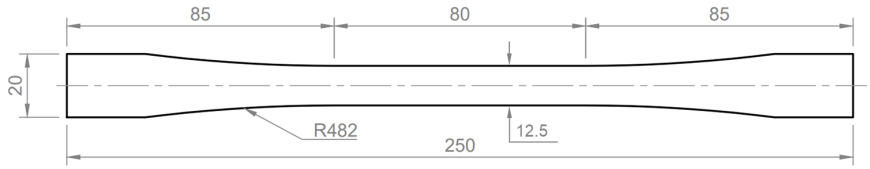

Figure 6.3: FLARE tensile test coupon. *All dimensions are in mm.*

Finally, in order to determine the Poisson ratio of the flax fibre reinforced epoxy, bi-axial strain gauges were employed in the case of the $[0°]_4$ specimens. These gauges enabled the measurement of both transverse and longitudinal strain at the centre of the specimen. The comprehensive configuration for the tensile test can be observed in Figure 6.4.

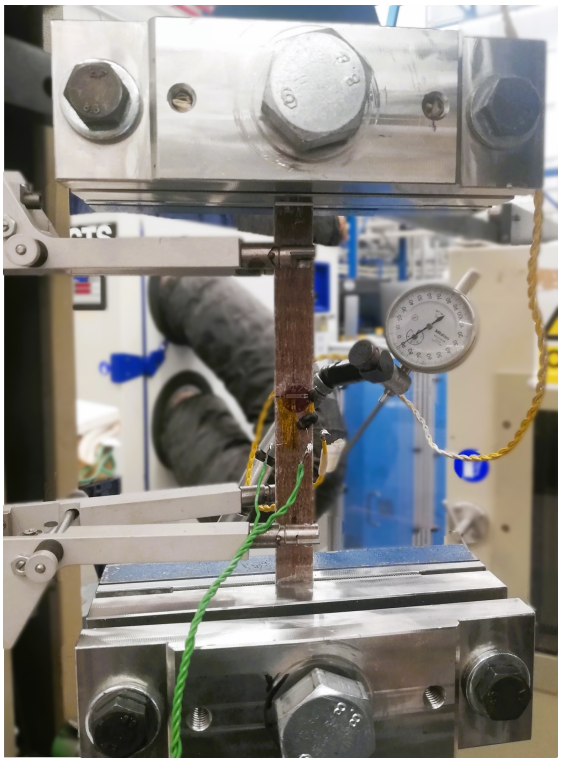

Figure 6.4: Tensile test set-up with installation of extensometer and strain gauge.

6.2 Tensile tests results

6.2.1 Flax fibre reinforced epoxy

First of all, the stress-strain curves displayed in Figure 6.5 for the longitudinal tensile behaviour of the composite, exhibit a nonlinear behaviour, as expected. Specifically, these curves are characterised by a bilinear shape, with an inflection point occurring at around 0.15% strain. Consequently, determining the Young's modulus for such a material is not as straightforward as it is for linear elastic materials. Indeed, according to the ASTM Standard D3039-08, the elastic modulus is typically defined as the slope of the stress-strain curve within the strain range of 0.1% to 0.3%. Hence, as FFRE presents a transition region within that strain range, the tensile chord modulus of elasticity is considered. Moreover, a second modulus, referred to as the "inelastic modulus", is evaluated to quantify the stiffness of the composite material beyond a deformation of approximately 0.2%. It is crucial to emphasise that the predominant stiffness describing the tensile behaviour of flax fibre reinforced epoxy is the inelastic modulus, rather than the initial stiffness. Consequently, care must be taken when asserting that flax fibre composites possess a stiffness equivalent to their glass fibre counterparts, as this statement holds true only for a small portion of their tensile response.

Regarding the transverse behaviour, the stress-strain curves are presented in Figure 6.6. It is observed that the ultimate strength in the transverse direction is comparatively lower than that in the longitudinal direction. This discrepancy can be attributed to the fact that the

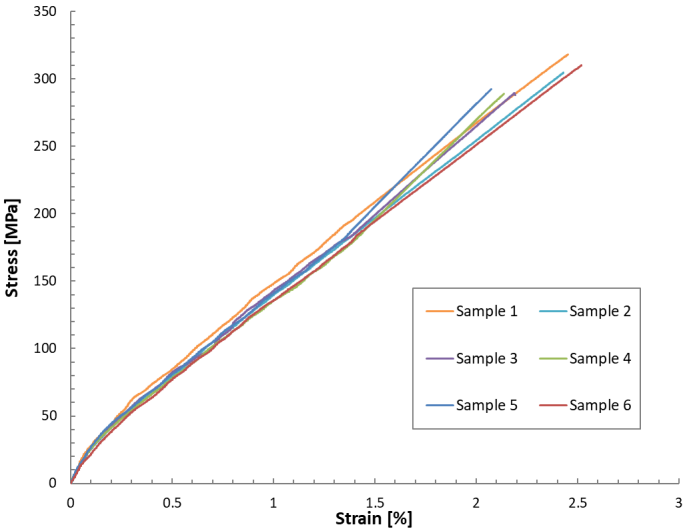

Figure 6.5: Tensile response of FFRE $[0°]_4$ specimens.

transverse behaviour of the composite is predominantly influenced by the matrix, whereas the longitudinal one is primarily governed by the fibres. Specifically, the matrix exhibits relatively low stiffness, and the transverse stiffness of flax fibres is also lower than their longitudinal stiffness, which means they do not contribute significantly in this regard. Furthermore, defects introduced during the manufacturing process have a detrimental impact on the transverse behaviour of the composite. The presence of a high level of porosity adversely affects the matrix dominated properties, particularly the strength. Consequently, there is a belief that by enhancing the manufacturing process, the current poor transverse properties can be improved.

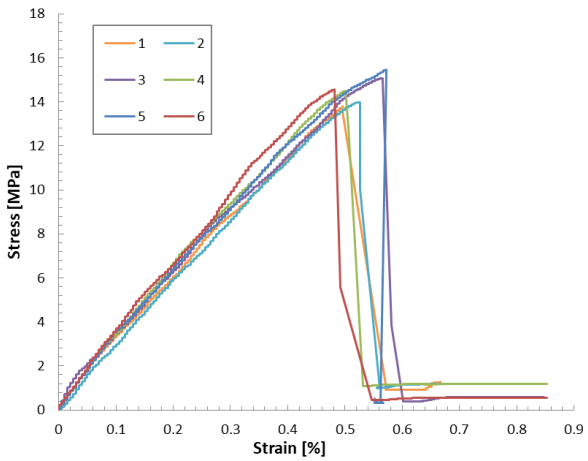

Figure 6.6: Tensile response of FFRE $[90°]_4$ specimens.

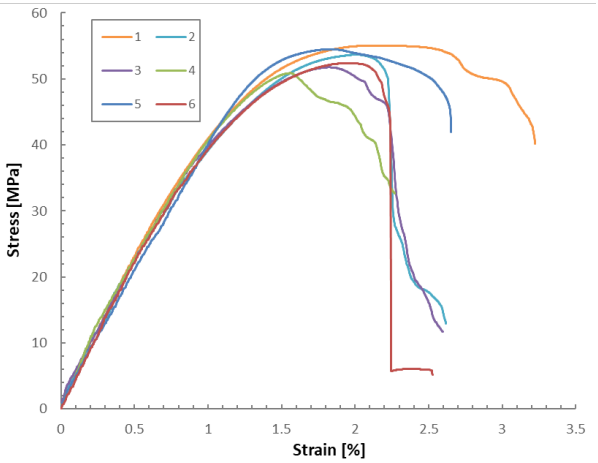

Figure 6.7: Tensile response of FFRE $[\pm 45°]_s$ specimens.

Lastly, the stress-strain curves for FFRE $[\pm 45°]$ are depicted in Figure 6.7. It is worth noting that despite the inherently brittle nature of flax fibre composites, all the tested specimens exhibit a characteristic pseudo-ductile behaviour prior to failure. This behaviour can be at-

tributed to the reorientation of fibres during the loading process and the occurrence of local plastic deformation within the matrix.

Therefore, in accordance with the findings from the literature, flax fibre composite demonstrates a tensile behaviour that is partially comparable to that of conventional composites like glass fibre composites. However, it is important to note that its longitudinal non-linear behaviour, attributed to the nature of flax fibres, sets it apart from synthetic fibre composites.

The tensile mode of failure in flax fibre reinforced epoxy also exhibits similarities to the observed failure modes for conventional composites. As it can be seen in Figure 6.8, for the longitudinal case, the main modes of failure are long splitting along the fibre direction due to debonding at the fibre/matrix interface and fibre breakage. They depict a fibre dominated type of failure, in agreement with the good mechanical properties in that loading direction. For the transverse case, the failure is dominated by the matrix, with a matrix crack in the gauge area leading to the failure of the composite. Finally, concerning the $[\pm 45°]_s$ samples, a combination of fibre breakage and inter-ply delamination is observed.

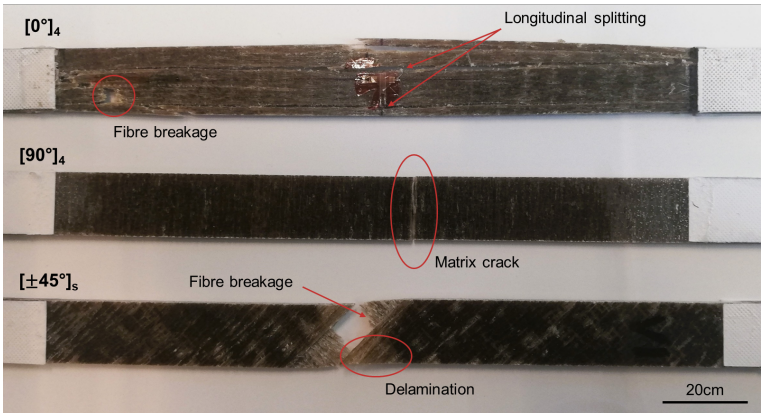

Figure 6.8: Failure mode of the different types of composite specimens tested.

In summary, the tensile properties of the composite are given in Table 6.1. The longitudinal properties align closely with those reported in the literature for a comparable fibre volume fraction. However, the other properties show lower values due to the limited quality of the samples, particularly with regard to void content, as discussed above. Despite these limitations, these obtained values will serve as the composite properties for further analysis. Moreover, based on the values obtained for the $[\pm 45°]_s$ specimens, the required shear strength for subsequent calculations can be derived, which is determined to be 26.5 MPa.

Laminate	Elastic modulus [GPa]	Inelastic modulus [GPa]	Ultimate strength [MPa]	Ultimate strain [%]	Poisson's ratio
$[0°]_4$	28.9 (1.90)	12.1 (0.42)	301 (12.1)	2.52 (0.02)	0.42 (0.03)
$[90°]_4$	2.88 (0.13)	-	14.6 (0.63)	0.80 (0.08)	-
$[\pm 45°]_s$	4.67 (0.24)	-	53.0 (1.63)	1.88 (0.20)	-

Table 6.1: Tensile properties of flax fibre reinforced epoxy. *Standard deviations in brackets.*

6.2.2 Flax fibre reinforced aluminium

Flax fibre reinforced aluminium laminates (FLARE) were also subjected to tensile testing to validate the use of the metal volume fraction method. To simplify result interpretation, a straightforward configuration was employed, involving two unidirectional plies of composites sandwiched between two aluminium layers (equivalent to grade 2 for GLARE).

The stress-strain curves of FLARE specimens, featuring both 0.4mm and 0.5mm thick aluminium layers, are depicted in Figure 6.9. These curves can be divided into three distinct phases. Initially, a linear elastic behaviour is observed until the yielding point is reached. Subsequently, a reduction in stiffness occurs, which can be attributed to the plasticity induced by the aluminium layers. The first stress drop is caused by the brittle failure of the composite plies within the fibre metal laminate. Following this, different scenarios can be distinguished. In the first case, one aluminium layer fails before the other, leading to a second stress drop after the first plateau at around 250MPa. In the second case, both aluminium layers fail simultaneously after the composite failure. Lastly, in the case of FLARE_2_0.4 sample 6, the composite failure coincides with the failure of one of the aluminium layers, directly leading to a plateau at around 125MPa.

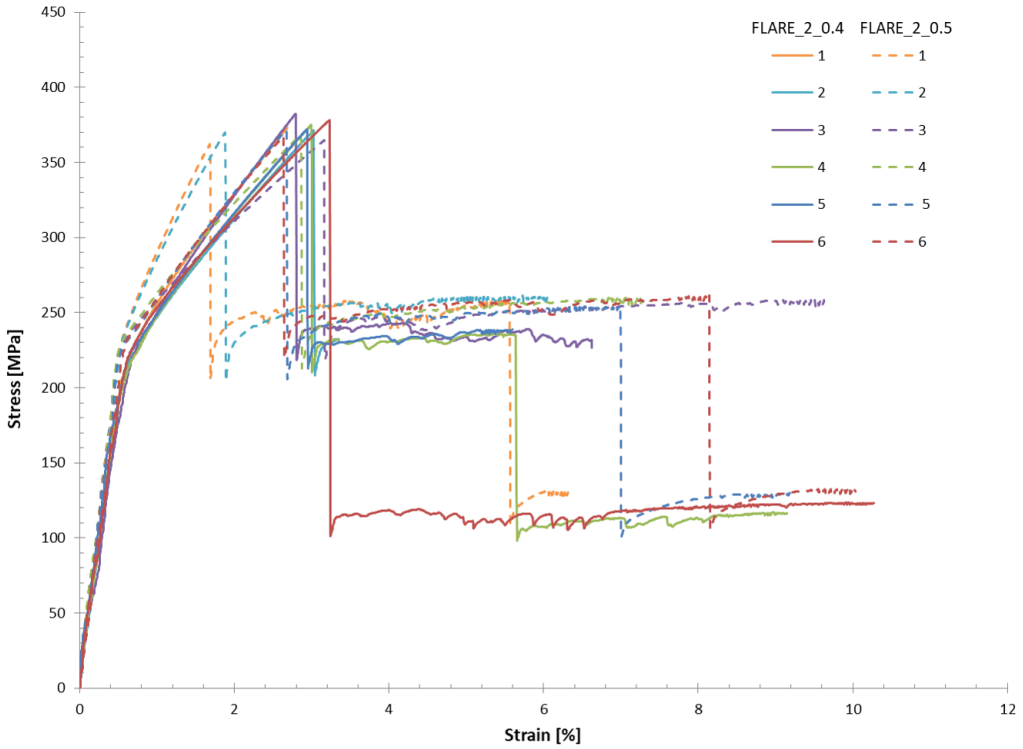

Figure 6.9: Tensile response for flax fibre metal laminate specimens with 0.4mm and 0.5mm thick aluminium layers.

These two plateaus, representing the presence of either one or two layers of aluminium without the composite material, offer a means of recovering the stress of Al 2024-T3 within this deformation range. This can be achieved by dividing the force associated with these plateaus

by the remaining cross-section, which corresponds to the thickness of either one or two layers of aluminium. When calculating the average stress of all the samples and taking into account the two plateaus, an average ultimate strength value of 486.6MPa (SD: 7.7MPa) is obtained. This value falls within the range specified for 2024-T3 aluminium in Table 5.1.

Observations from the graph reveal that for FLARE_2_0.5 samples 1 and 2, the slope of the second part of the curve deviates from the trend observed in the other samples. This discrepancy arises primarily due to a displacement measurement issue during the tensile test. During the test, there are two methods to measure displacement: using the extensometer or relying on the crosshead displacement. The displacement recorded by the crosshead is considered less reliable because it includes factors such as the internal movement and stiffness of the grips, joints, and attachment frame. Moreover, for a dogbone shape sample the elongation needs to be measured essentially in the gauge area. To address this concern, an extensometer is commonly employed as it provides more accurate measurements. However, to avoid potential damage to the automatic extensometer during failure events involving high-energy release, it is removed before reaching failure. Subsequently, after removing the extensometer, strain values are calculated using the crosshead displacement along with a correction factor derived from the two previous extensometer measurements. However, it's important to note that for the first two tensile tests of FLARE_2_0.5, the extensometer was removed precisely at the point of yielding. As a result, the correction factor is solely based on the elastic portion of the curve and does not account for the strain hardening behaviour that occurs beyond the yielding point. Consequently, for the calculation of the ultimate strain, these two samples are excluded from the average.

Another significant observation is the lack of non-linear behaviour attributed to the composite contribution. Specifically, when considering the residual stresses during deformation, it is expected that the composite layers will experience a reduction in their stiffness at approximately 0.2% strain, resulting in a change in slope for the stress-strain curve of the fibre metal laminate. This could be explained by the presence of the aluminium layers, which can prevent this non-linearity from occurring, which also occurs at the very beginning of the curve and may therefore be invisible.

The tensile properties of the fibre metal laminates are presented in Table 6.2 and would be compared to the MVF method predictions in the following.

Laminate	**Elastic modulus [GPa]**	**Yield strength [MPa]**	**Ultimate strength [MPa]**	**Ultimate strain [%]**
FLARE_2_0.4	38.9 (2.57)	234 (6.65)	375 (4.28)	2.95 (0.07)
FLARE_2_0.5	44.1 (2.12)	243 (13.2)	367 (3.36)	2.83 (0.58)

Table 6.2: Tensile properties of FLARE. *Standard deviations in brackets.*

6.3 Comparison with the prediction using the MVF

Using the properties of aluminium as shown in Table 5.1 and those of the composite determined through tensile testing (refer to Table 6.1), the previously introduced metal volume fraction method can be employed to make predictions about certain tensile properties of the FML samples.

The results for the elastic modulus are depicted and compared to the experimental data in Figure 6.10. In terms of the composite contribution, both the elastic modulus (orange curve) and the "inelastic modulus" (blue curve) were considered.

It is observed that the prediction based on the second stiffness of the flax fibre reinforced epoxy yields more reliable results. This observation aligns with the fact that the stress-strain curve of the fibre metal laminate exhibits only one stiffness, and that the second stiffness of the composite predominantly captures the composite behaviour. However, it also means that care must be taken not to jump to conclusions that flax-based composites have high stiffness and that the same will be true of FLARE.

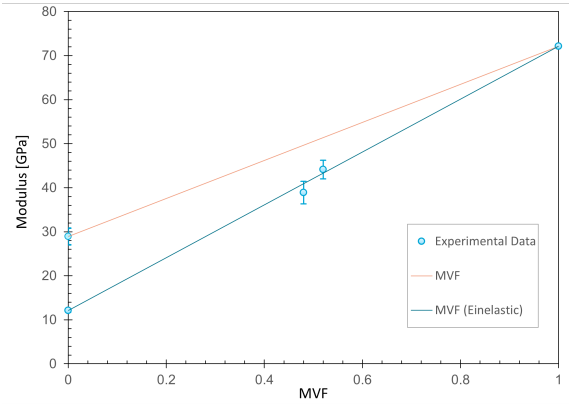

Figure 6.10: MVF method for elastic modulus of FML.

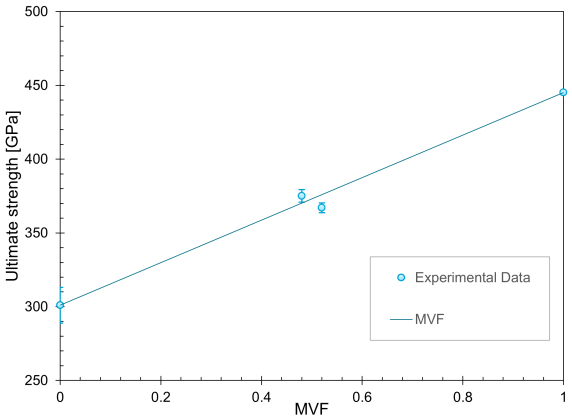

Figure 6.11: MVF method for ultimate strength of FML.

The MVF prediction for the ultimate strength is depicted in Figure 6.11, showing a notable alignment with the experimental data. However, it is evident that the strength of FLARE_2_0.5 samples is unexpectedly lower than that of FLARE_2_0.4 samples. This discrepancy can be attributed to the lower fibre volume content and higher porosity, which impact the resistance properties of the FML.

Conclusion

Concluding this chapter, the validity of the MVF method was confirmed in predicting the tensile ultimate strength of FLARE. However, a discrepancy of around 20% was noted in the case of elastic modulus prediction. This disparity can be attributed to the inherent nonlinear behaviour of flax fibre reinforced epoxy, necessitating characterisation through not

only Young's modulus but also an "inelastic modulus" that represents the majority of its behaviour. Interestingly, this non-linearity is not observed in the case of the fibre metal laminate.

Consequently, by selecting the appropriate "inelastic modulus" for the composite within the MVF method, a more precise forecast of FLARE's elastic modulus is achieved.

It is crucial to acknowledge that caution must be taken when extrapolating this conclusion, given that only one specific type of sample has been thoroughly characterised and further investigation is needed to better understand this phenomenon.

Chapter 7

Vibration damping behaviour

Existing literature suggests that incorporating flax fibres in composites offers a significant advantage: improved damping behaviour. However, the question arises as to what extent this benefit holds true for Fibre Metal Laminates (FMLs). Investigating the evolution of these intrinsic fibre properties in such a hybrid material becomes therefore crucial in designing an optimal structure that fulfils the requirements of the intended application. Thus, in the following, the vibration damping behaviour of flax fibre reinforced epoxy, FLARE and their glass fibre counterparts is evaluated.

Two distinct methods were investigated for the evaluation of damping characteristics: Dynamic Mechanical Analysis (DMA) and Vibration Beam Testing (VBT). The main difference between these two approaches lies in the amplitude of deformation applied to the sample. DMA involves subjecting the sample to small deformations, resulting in the measurement of a so-called "material" damping ratio. In contrast, VBT, specifically the free vibration decay method, employs large deformations, leading to the assessment of the "structural" damping. Notably, the literature study reveals that varying deformation amplitudes in composites result in different friction mechanisms, leading to those distinct damping behaviours. Another difference exists in the additional damping introduced by the test set-up, which will be elaborated on in the following.

Finally, this chapter showcases the results obtained from both types of tests in comparison to predictions derived using various types of rules of mixture. Additionally, it includes the comparison between the two testing methods employed in the study.

7.1 Dynamic Mechanical Analysis: "material" damping

7.1.1 Experimental methodology

Dynamic Mechanical Analysis (DMA) was conducted in accordance with the ASTM standards D5023-15, using the RSA-G2 Solid Analyzer by TA instruments. This method involves subjecting the sample to oscillatory deformation, while measuring the material's response across a range of time, temperature, or frequency. By comparing the stress and strain responses, the

viscoelastic behaviour of the material can be characterised. In this study, particular attention was given to the dissipation of energy under cyclic loading, which is represented by the tangent of the phase shift between stress and strain ($tan(\delta)$). This parameter is of significant interest as it characterises the material's damping behaviour.

A three-point bending configuration is employed in the experimental setup, chosen as it offers the desired and optimal mode of deformation for measuring medium to high modulus material. Furthermore, this clamping system ensures the purest deformation mode, effectively eliminating any clamping effects that can affect the damping behaviour. Figure 7.1 illustrates the experimental test setup.

The composite and FML samples were cut using respectively water jet cutting and the shear guillotine. To ensure consistent deformation while adhering to the machine's force limit, the geometry of each sample was adjusted accordingly. Their dimensions are shown in Table 7.1.

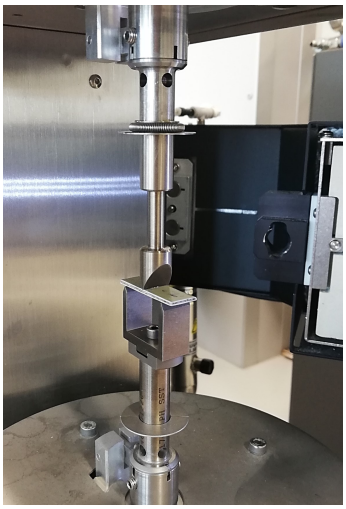

Figure 7.1: Three-point bending DMA set-up.

Specimen	Length [mm]	Span length [mm]	Width [mm]
Composite	35	25	10
FLARE_2_0.4	35	25	11.5
FLARE_2_0.5	45	40	11.5
FML_5	50	40	10

Table 7.1: DMA samples dimensions.

Finally, in order to measure the loss factor at a specific frequency for both the FML and composite samples, oscillatory time sweeps were conducted at room temperature, with a frequency of 1Hz and a deformation of 0.01%. This particular strain amplitude was chosen as it ensures that the samples are within the linear viscoelastic region, which was identified through dynamic strain sweeps.

Various configurations were tested to assess the influence of both the metallic layer via its thickness and therefore its volume fraction, and the fibre orientation within the composite layer. Particular focus was given to the symmetrical cross-ply configuration for FML, as according to the literature review, it is the most promising option for achieving both impact resistance and vibration damping. A comprehensive summary of all sample types is presented in the test matrix Figure 7.2. For each sample, the measurement is repeated two times, including remounting the sample.

	Fibre		Metal thickness			Fibre orientation				
DMA	Flax	E-Glass	0.3	0.4	0.5	$[0°]_2$	$[0°/90°]_s$	$[90°/0°]_s$	$[+/-45°]_s$	Nb of samples
Test 1	x						x			3
Test 2	x							x		2
Test 3	x								x	2
Test 4	x		x				x			3
Test 5	x		x					x		2
Test 6	x		x						x	2
Test 7	x			x		x				2
Test 8	x			x			x			3
Test 9	x				x	x				2
Test 10	x				x		x			3
Test 11		x					x			3
Test 12		x						x		2
Test 13		x							x	2
Test 14		x	x				x			3
Test 15		x	x					x		2
Test 16		x	x						x	2
										33

Figure 7.2: Test matrix for DMA.

7.1.2 DMA results

As previously indicated, the loss factor for each sample was plotted against time, and an example is shown in Figure 7.3 for the FLARE_5_0.3 samples. The loss factor shows an initial decrease before stabilising at its final value.

The outcomes for various fibre orientations, fibre types, and the presence or not of a metallic layer are depicted in the form of a bar chart in Figure 7.4. As anticipated, FFRE exhibits superior damping behaviour compared to its glass fibre counterpart, particularly evident in the $[0°/90°]_s$ layup, with a damping coefficient on average twice as high. However, this difference becomes less pronounced when considering FLARE and GLARE samples, which exhibit almost the same loss factor. Moreover, a significant decrease of almost 80% in the loss factor is observed when comparing FFRE to FLARE, with the latter even exhibiting a lower loss factor than GFRE in the case of layups $[90°/0°]_s$ and $[\pm 45°]_s$.

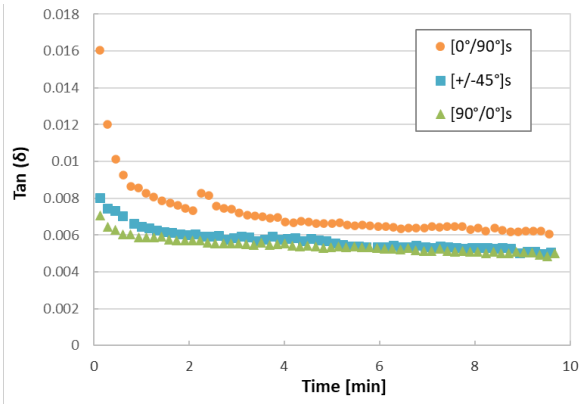

Figure 7.3: DMA results for FLARE_5_0.3 samples.

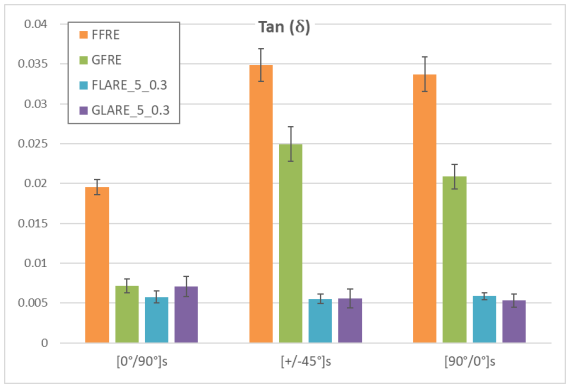

Figure 7.4: Comparison of the loss factor for different samples.

Regarding the influence of the fibre orientation, it appears that the $[\pm 45°]_s$ configuration exhibits the best damping behaviour for the composite samples. This can be attributed to the fact that the metal component is considerably stiffer than the composite, thereby dominating the overall deformation and restricting the contribution of other layers in vibration absorption.

All this suggests that the damping behaviour of an FML is likely to be predominantly influenced by the metal component rather than the composite itself, as the fibre type and orientation seem to have less significance in shaping the damping behaviour of the FML.

7.1.3 Comparison with predictive tools

Subsequently, the experimental results for each configuration were compared to predictions made using various types of rules of mixture (or MVF method), incorporating either volume fractions or weight fractions. The comparisons for the $[0°/90°]_s$ configuration are depicted in Figure 7.5. For the aluminium, the loss factor is derived from the damping coefficient 0.0012 given in the literature [73].

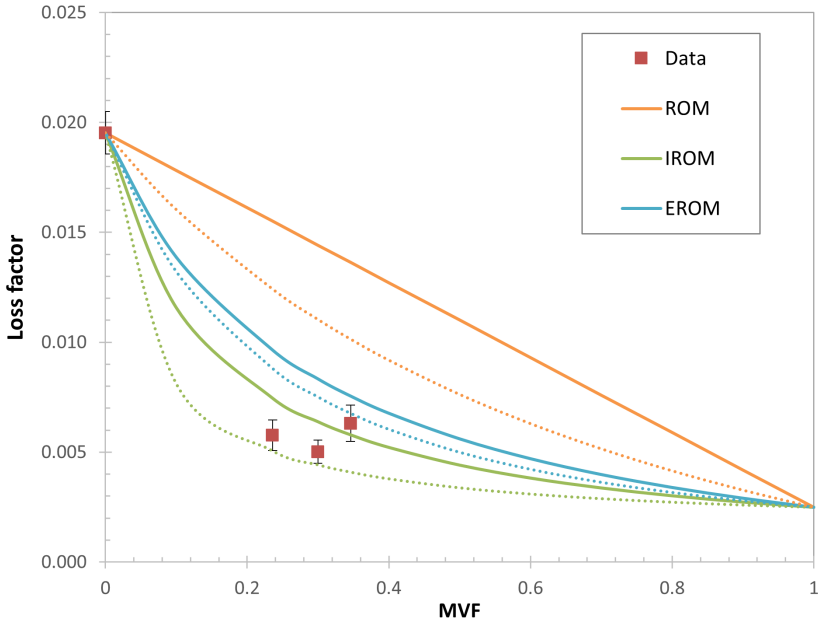

Figure 7.5: Comparison between experimental data and different predictive rules, using volume fractions (solid line) or weight fractions (dashed line), for the $[0°/90°]_s$ configuration.

From the graphs, it is evident that the simple metal volume fraction method or rule of mixture (ROM), as presented in Equation 2.2, does not provide a satisfactory approximation of the loss factor. In fact, it gives a prediction two and a half times higher on average than the experimental values, reduced to twice as much if the weight fractions are considered. Furthermore, the rule of mixture based on an energy approach (EROM), occasionally referenced in the literature [74–76], was also compared to the experimental results. It is given by the following equation:

$$\xi_{FML} = MVF\frac{E_{Al}}{E_{FML}}\xi_{Al} + (1 - MVF)\frac{E_{FFRE}}{E_{FML}}\xi_{FFRE} \tag{7.1}$$

where E represents the Young's modulus of the material and ξ its loss factor.

However, it is the inverse rule of mixture (IROM), specifically the one utilising the weight fraction of metal, which is the most accurate for all the configurations tested. Its equation, using the weight fraction of metal (MWF), is as follows:

$$\frac{1}{\xi_{FML}} = \frac{MWF}{\xi_{Al}} + \frac{(1 - MWF)}{\xi_{FFRE}} \tag{7.2}$$

The inverse rule of mixture, used for loading perpendicular to the stacking sequence direction, is analogous to the case of an electrical circuit in series. And, in this case, the laminate can be considered as a set of mass-spring-damper systems mounted one after the other to dampen vibrations. It therefore makes sense to use it to predict the damping coefficient of such hybrid material. In addition, using the weight fraction instead of the volume fraction leads to a better approximation as it illustrates the mass of the system, and emphasises the contribution of the metal, which is dominant in the damping behaviour. Nevertheless, the prediction underestimates the loss factor. By calculating the average relative deviation between the first two experimental data points and the curve shown in Figure 7.5, an underestimate of around 12% is obtained. In fact, that method does not take into account the energy that might be dissipated at the interface between the composite and metallic layers, which may explain the discrepancy between theory and experiment. This estimate does not include the third data point due to its discrepancy, as elaborated upon in the following explanation.

Another noteworthy observation from the graph is that the loss factor of FLARE_5_0.5 samples is higher than that of FLARE_5_0.4 samples. This disparity can be attributed to variations in manufacturing quality, particularly the difference in void content. Indeed, as the samples are relatively small, the measurement is very localised and it is possible that singularities, such as voids, are more present within the FLARE_5_0.5 samples even if several have been tested. Hence, it is acknowledged that the experimental data should be juxtaposed with the void content, and it is anticipated that the outcomes obtained in this study might exhibit an overestimation when contrasted with those of a theoretical void-free sample.

7.2 Vibration Beam Tests: "structural" damping

7.2.1 Experimental methodology

To evaluate the structural damping behaviour, free vibration beam tests (VBT) were conducted following the ASTM standards E756-05.

Test set-up

The experimental set-up for the free vibration beam tests involves two transducers: one transducer applies the excitation signal to the beam, while another transducer measures the beam's response. For this specific study, an automatic impulse hammer was chosen to generate the excitation force, and a PSV-500 laser scanning vibrometer by Polytec was employed to record the velocity at multiple locations on the beam. The selection of these transducers

offers several advantages. The impulse hammer ensures consistent input signal generation, contributing to the repeatability of the measurements. On the other hand, the laser vibrometer, being a non-contacting transducer, avoids introducing any additional damping during the measurement process, ensuring precise and unaltered data collection.

Figure 7.6 illustrates the entire experimental test set-up, which is positioned on an optical table to isolate it from external vibrations. The rectangular samples are clamped on one side while their tip is left free to move.

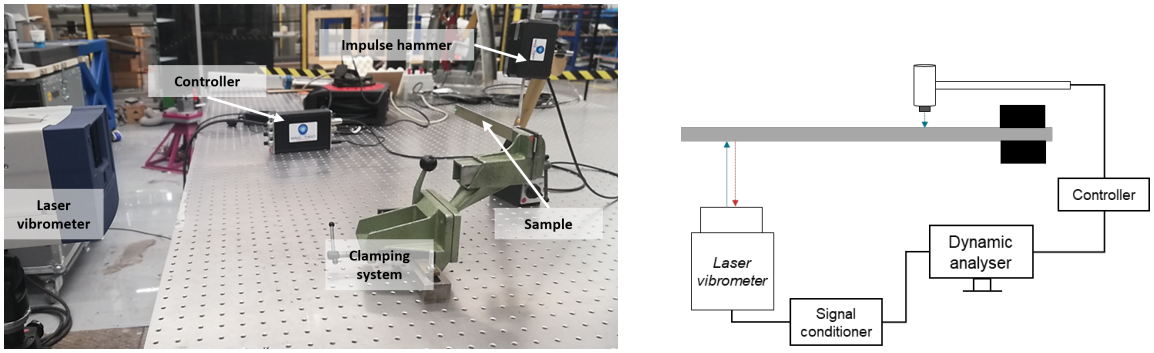

(a) VBT experimental set-up. **(b)** Diagram of the set-up.

Figure 7.6: Vibration Beam Test set-up.

To generate a suitable input signal, the impulse hammer is positioned in close proximity to the fixture and at a reasonable distance from the beam. The amplitude and impulse duration are carefully adjusted to ensure the production of a sharp and unsaturated signal, enabling accurate measurements during the free vibration beam tests. The choice of these parameters depends in particular on the rigidity of the cantilever beam, which may have a tendency to bounce off the tip of the hammer.

After each impulse impact, the laser vibrometer measures the velocity of the beam at a specific location. To achieve this, it utilises the Doppler effect, which involves assessing the frequency shift of laser light that is reflected back and detected by an interferometer. With this data, the transfer function can be determined using the Fourier transforms of the input and output signals. This function is referred to as the frequency response function and serves the purpose of identifying resonant frequencies, damping, and mode shapes of a physical structure.

Moreover, in this study, to reconstruct the entire deflection profile of the cantilever beam, a grid of multiple measurement points was defined on the specimen and scanned by the laser. That grid depends on the free length of the specimen and one measuring point needs to be located at the impact location as shown in Figure 7.7. At each point, the frequency response function is averaged over ten consecutive measurements.

Sample geometry

All the samples were cut into rectangular shapes, with one dimension (length) being significantly larger than the other two. In addition, since the aim was to compare the damping

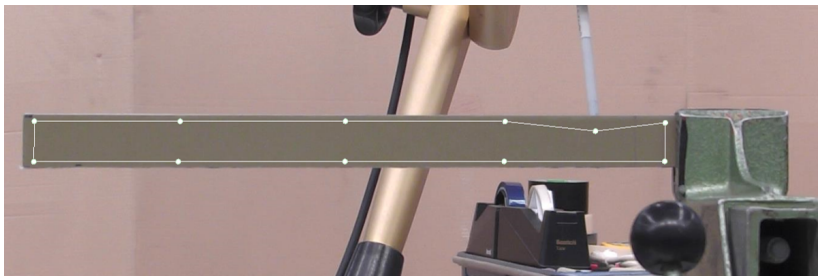

Figure 7.7: Grid of measurement points used to reconstruct the vibration behaviour of the beam.

behaviour of materials having different stiffnesses, the dimensions of each sample were adapted to match their eigenfrequencies and provide a more reliable comparison of the damping for the different eigenmodes. Using the Euler-Bernoulli beam theory, the natural frequencies for each mode of bending vibration of a cantilever beam can be expressed as follows:

$$f_n = C_n \sqrt{\frac{Et^2}{12\rho L^4}} \tag{7.3}$$

where E is the elastic modulus, t the thickness of the beam, ρ the density of the material, L the free length, f_n the nth resonance frequency and C_n a coefficient for the nth mode related to the boundary conditions [77].

Consequently, by adjusting the free length, it becomes possible to compensate for changes in other parameters that influence the natural frequencies and are related to the characteristics of the material. Finally, the free length of the samples varies from 170mm for the most flexible samples to 250mm for the stiffest, with the width always set at 20mm.

The test matrix (Figure 7.8) provides a summary of all the specimens that were tested.

	Fibre		Metal thickness			Fibre orientation				
VBT	Flax	E-Glass	0.3	0.4	0.5	$[0°]_2$	$[0°/90°]_s$	$[90°/0°]_s$	$[+/-45°]_s$	Nb of samples
Test 1	x					x				1
Test 2	x						x			2
Test 3	x							x		2
Test 4	x								x	2
Test 5	x		x				x			2
Test 6	x		x						x	2
Test 7	x			x		x				1
Test 8	x			x			x			2
Test 9	x			x				x		2
Test 10	x				x	x				1
Test 11	x				x		x			4**
Test 12	x				x			x		2
Test 13	x				x				x	2
Test 14		x					x			2
Test 15		x						x		2
Test 16		x							x	2
Test 17		x	x				x			2
Test 18		x	x					x		2
Test 19		x	x						x	2
										30

Figure 7.8: Test matrix for VBT. **Samples from two different plates.*

Post-processing of the data collected

After collecting the Frequency Response Function (FRF) at each measurement point, the data are subjected to post-processing using the Simcenter Testlab Modal Analysis software. In fact, the FRF of the overall structure, being an average of all FRFs, may contain noise or other random variations that hinder the identification of vibration modes. To address this, a modal curve fitting is performed to extract a meaningful set of modes and their associated modal parameters. This process allows for a more accurate and reliable characterisation of the structural dynamic behaviour.

In essence, the goal is to determine the most suitable mathematical modal model that accurately describes the measured FRF data. This model involves a linear superposition of fitted polynomial functions, each representing a single mode of vibration. The number of polynomials used corresponds to the potential modes that need to be identified within the specified frequency range.

Finally, as illustrated in Figure 7.9, the analysis provides the mode shape corresponding to each natural frequency, enabling the association of the calculated loss factor with a specific mode of vibration.

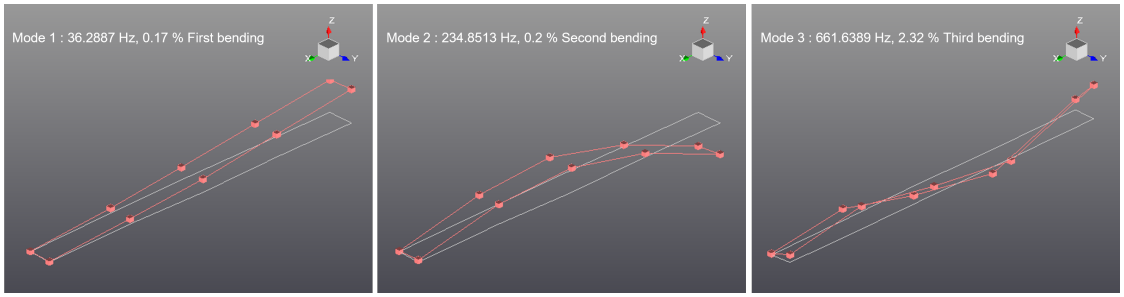

Figure 7.9: Typical mode shapes, in particular the first three bending modes, obtained by modal analysis.

Additionally, it is important to note that the loss factor calculated on the raw data is determined using the half-power bandwidth method on one FRF, whereas the loss factor calculated on the modal analysis is obtained with the mathematical model by considering multiple FRFs. Consequently, the former method could incorporate errors linked to noise, and the latter could potentially be affected by inaccurate determination of vibration modes during modal analysis.

7.2.2 VBT results

In the following, unless specifically mentioned otherwise, the values used are those obtained from the modal analysis and represent an average across all specimens of the same type.

In Figure 7.10, the impact of the fibre type on the loss factor value is illustrated for two distinct configurations. As anticipated, the flax fibre reinforced epoxy sample exhibits significantly higher damping capabilities, with a loss factor 2 to 3 times greater compared to its glass fibre counterpart. Nevertheless, the introduction of 3mm thick aluminium layers eliminates this disparity, suggesting that in the case of FMLs, the damping behaviour is dominated by the metal component, as observed in the DMA.

Regarding the impact of fibre orientation, a clearer perspective is provided in Figure 7.11 for both composite and FML samples. Notably, the $[\pm 45°]_s$ configuration demonstrates the highest damping performance for both FFRE and GFRE, whereas the unidirectional orientation shows the lowest damping. More precisely, there is a relative difference of 28% between the two configurations for the FFRE. This phenomenon can be ascribed to the in-plane shear strain energy of composites, which reaches its maximum value for this particular fibre orientation. However, for FLARE and GLARE, the correlation between loss factor and fibre angle seems less obvious, or even non-existent. This could be attributed to a relatively smaller change in stiffness due to the presence of the aluminium layers, which ultimately reinforces the conclusion that the damping behaviour is primarily influenced by the metal components.

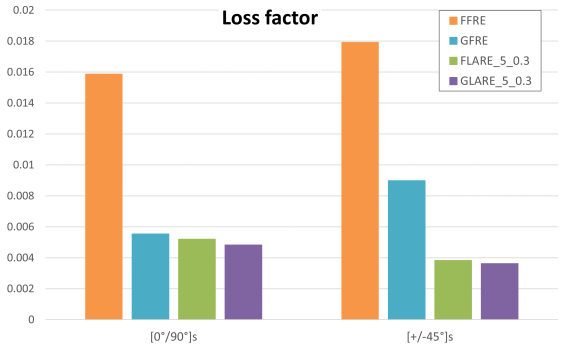

Figure 7.10: Comparison of loss factor for 1st bending mode.

Figure 7.11: Influence of fibre orientation on the loss factor for 1st bending mode.

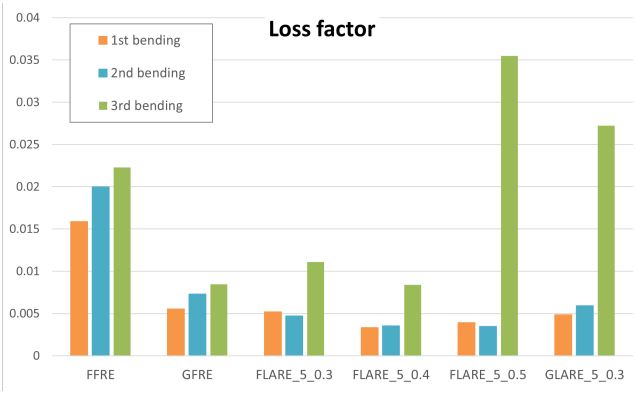

Figure 7.12: Impact of the mode of vibration on the loss factor for the $[0°/90°]_s$ samples.

Unlike DMA, VBT offers the advantage of accessing the damping behaviour for multiple modes of vibration. In Figure 7.12, a comparison of the loss factor for the 1st, 2nd, and 3rd bending modes of the $[0°/90°]_s$ configuration is presented. For the composite, the loss factor increases gradually with higher modes of vibration, although this trend is less pronounced for the FMLs. However, it is important to note that for all the specimens, the loss factor measured is consistently higher for the 3rd mode, even reaching a value almost 6 times higher than for the other vibration modes in the case of FLARE_5_0.5. Generally, the damping factor can vary for different modes of vibration due to the distinct energy dissipation mechanisms associated with each mode. Nonetheless, a larger error is introduced during the modal analysis for the

third mode of the FML samples, as it can be seen in Figure 7.9, the peak associated with it combines both a bending and a torsion mode. Since the torsion mode is typically associated with more damping, the value of the loss factor for the 3rd bending mode is overestimated and may not be considered reliable in the present case.

7.2.3 Comparison with predictive tools

Finally, a comparison between experimental data and predictions based on different rules of mixture has been performed. The results for the 1st bending mode of the $[0°/90°]_s$ configuration are displayed in Figure 7.13. The graph presents both the directly measured damping factor from the averaged Frequency Response Function (FRF) and the damping factor extracted from the modal analysis. Similarly to DMA, the same three predictive rules are presented in the context of VBT, utilising either the metal volume fraction or metal weight fractions. The damping coefficient of 0.0012 has been considered for aluminium.

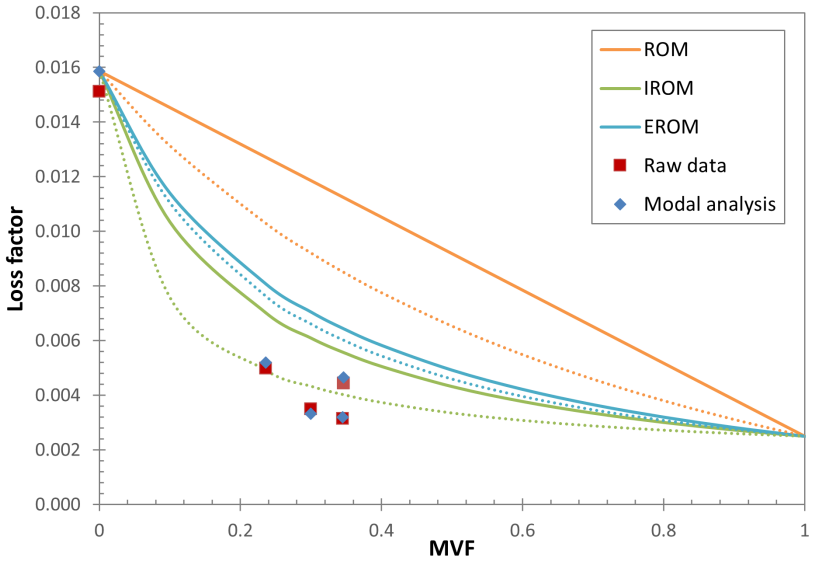

Figure 7.13: Comparison between experimental data and different predictive rules, using volume fractions (solid line) or weight fractions (dashed line), for the $[0°/90°]_s$ samples in 1st bending mode.

Consistently, the inverse rule of mixture using the metal weight fraction provides the best approximation, slightly overestimating the results with an average relative difference of 17%. The convex curvature of the predictive curve distinctly reflects the dominance of aluminium in the vibration damping behaviour.

Moreover, the raw data and modal analysis for the loss factor show a high degree of similarity, which suggests a well-isolated first bending mode in the Frequency Response Function (FRF) with minimal noise interference. In the case of FLARE_5_0.5, specimens from two different plates were tested, and the data from each plate are presented separately. A notable discrepancy of 31% between these two data points can be observed. The higher loss factor for the samples from plate number 5 can be attributed to a higher void content in those specimens. Indeed, a higher void content is linked to a lower stiffness, resulting in an improved ability to

deform and, consequently, a higher capacity to dissipate energy. Additionally, voids introduce an additional source of internal friction, making them overall beneficial for damping.

The findings for the second bending mode and the other configurations lead to similar conclusions and are presented in Appendix A.1. However, when considering the 3rd mode of vibration, the combination of bending and torsion causes an overestimation of the loss factor, and consequently, the predictions using the inverse rule of mixture appear to be less accurate.

7.3 Comparison between DMA and VBT

Based on the results obtained for damping using DMA and VBT, a comparison between the two measurement methods can be conducted. For this purpose, the loss factor for the various tested configurations is presented against the specific Young's modulus in Figure 7.14 for DMA and Figure 7.15 for the 2nd bending mode of VBT (same modal shape as with DMA).

In both cases, the visual representations show that the flax fibre reinforced epoxy samples exhibit the best damping capabilities, while the difference in loss factor is marginal for all the FML samples. Specifically, these findings align with the common trend where materials with higher strength and stiffness generally demonstrate lower damping capabilities.

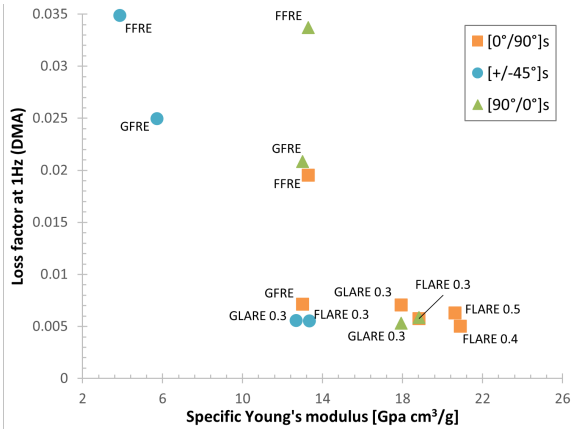

Figure 7.14: Loss factor determined by DMA against specific Young's modulus.

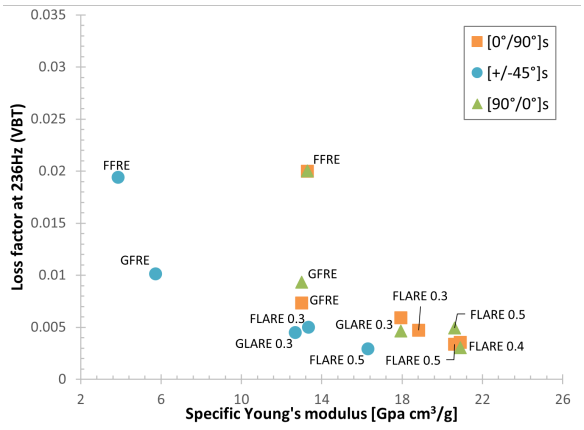

Figure 7.15: Loss factor determined by VBT against specific Young's modulus.

Interestingly, the loss factors measured during the vibration beam test are consistently lower than those measured by DMA. This result aligns with the findings of Duc et al. [11], who provided an explanation for this discrepancy. They attributed it to the different energy dissipation modes that occur for small and larger deformations within the composite, as elucidated in the literature review. Furthermore, the difference in loss factors is more pronounced for the composite samples compared to the FMLs, which corresponds to the fact that in FMLs, the damping behaviour is predominantly governed by the metal layer and, as a result, is less affected by changes in the dissipative friction mechanisms. The vibration frequency also plays a role more time for the sample to dissipate energy at low frequency.

Lastly, it is important to bear in mind that the test setups are different, particularly in terms of boundary conditions. The clamping of the beam in VBT may introduce an additional

source of damping compared to DMA which is considered clamp-free. Nevertheless, since both tests are conducted at relatively low frequencies and small amplitudes, any additional damping resulting from air friction can be disregarded and treated as negligible.

Conclusion

To summarise this chapter, it has been observed that the introduction of metallic layers leads to a significant reduction in damping properties. By going from no aluminium to a MVF of 0.24, the loss factor is reduced by around 70%, while by going from a MVF of 0.24 to 0.35, the loss factor of the FML is reduced by only 20%. In addition, it is interesting to note that the orientation of the fibres in the laminate had no influence on the damping characteristics, unlike the behaviour observed in the composite alone. Thus, the damping behaviour of FLARE is dominated by the metal.

With regard to loss factor prediction, the classic metal volume method proved inadequate, with a divergence of 65%. In fact, this approach does not capture the additive effect of the damping abilities of each layer in a manner similar to a series circuit. Moreover, the use of volume fractions does not allow the influence of the density of each constituent material on the overall damping behaviour to be transcribed. That is why, an approach based on the inverse rule of mixture and weight fractions provided more accurate predictions. Nonetheless, a slight deviation was still noticeable. Therefore, it could be insightful to delve into the influence of the fixed parameters employed in the predictive model, specifically the value of the aluminium loss factor (ξ_{Al}=0.0024), which was not determined through the same measurement methods but rather sourced from the literature. Figure 7.16 shows the influence of an increase or decrease of a certain percentage of the initial value.

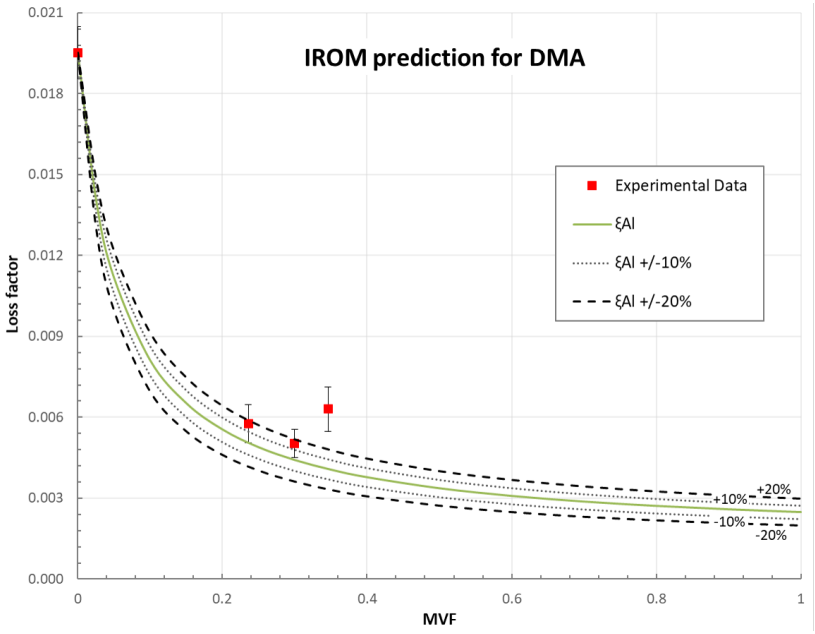

Figure 7.16: Study of sensitivity of the loss factor prediction to the ξ_{Al} parameter. Analysis presented in the case of IROM with weight fractions for DMA results.

No indication of the accuracy of ξ_{Al} is given in the literature, but it was observed that for both DMA and VBT, the experimental data fall within the range defined by $\xi_{Al} \pm 20\%$. Moreover, the graph shows that the general behaviour remains unchanged despite a variation in the input parameter. However, the predictions show deviations almost equivalent to the variations in the aluminium input value. For example, with a 10% change in the aluminium loss factor, a variation in the prediction of almost 9% is observed for a MVF of 0.3. This observation is consistent with the notion that damping behaviour is primarily influenced by the metal component. Therefore, a more accurate determination of the aluminium loss factor is essential.

Furthermore, the DMA and VBT methods lead to the same conclusions regarding trends in the loss factor. However, there exists a disparity in the values obtained between the two methods, which can be attributed to distinct dissipative mechanisms at play.

Finally, it was observed that the damping behaviour of FLARE is dominated by the metal component, resulting in a relatively modest damping effect, despite the composite material demonstrating good intrinsic damping capabilities. However, if the predictive curve is extrapolated for low values of MVF (less than 0.1 like FLARE_5_0.1) the damping factor reaches values at least equal to half that of its constitutive composite.

Chapter 8

Impact resistance of FLARE

Now that the damping behaviour of flax fibre metal laminates is better understood, the focus will shift to investigating their impact resistance in detail, as it should represent another significant advantage of this hybrid material. Based on the literature review, it has been established that composites, and particularly natural fibre reinforced composites, generally exhibit a low impact resistance, which limits their use in certain applications. Therefore, incorporating metallic layers appears to be a coherent solution to enhance the impact behaviour of composites. Better still, the impact resistance of FMLs has been found to surpass that of pure metals, although this was not one of the main motivations behind the development of GLARE.

Thus, in an effort to enhance the understanding and predictability of the impact behaviour of Fibre Metal Laminates, analytical models have been previously developed for conventional FMLs. Of particular interest is the model proposed by Morinière [13], which has shown promising results and could serve as the basis for the predictive model in the case of FLARE. Therefore, this chapter presents a detailed explanation of the implementation of this model with the necessary modifications in a generic code.

In order to validate the applicability of this numerical model to FLARE, this chapter also includes a presentation of the low-velocity impact tests that have been conducted. Low-velocity impact involves impacts occurring at velocities below 10m/s, such as tool dropping or ground equipment collisions, that are commonly encountered in real-world environments. Finally, the experimental results are compared to the predictions, and the impact performance of FLARE is evaluated in relation to other materials.

8.1 Low velocity impact analytical model

The low-velocity impact model employed in this study draws from Morinière's research [13] mentioned in the literature review. Using a quasi-static approach, the predictive model undertakes a gradual failure analysis by combining Classical Laminate Theory with the strain hardening behaviour of the metal. This analytical process is integrated into an energy-balance framework that elucidates how the dissipated energy emerges from the plate's deformation and the diverse failure modes.

To delve deeper, this model hinges on a structural energy balance analysis, where the kinetic energy of the projectile is responsible of the plate's deformation. By using plate theory and CLT to evaluate the deformation characteristics of the laminate, it becomes possible to quantify the energy dissipation resulting from this deformation and to deduce the resulting contact force. Finally, a complete energy analysis can be used to determine the total energy dissipated during the impact event. Additionally, a simplified mass-spring system model, as described by Hoo Fatt et al. [78], can be employed to elucidate the dynamics of the impact.

The following sections describe the key steps in the analysis, which were implemented in Python code to obtain the predictive results.

Test conditions and material definition

The initial stage involves characterising the governing components of the impact behaviour, primarily the projectile and the plate.

The target plate's configuration is outlined through parameters such as stacking sequence, ply orientation, the thickness of the aluminium layer, and dimensions of the plate. Material properties for each constituent are sourced from Morinière et al. [20] for aluminium, Table 6.1 for flax fibre reinforced epoxy and Table 8.1 for its E-glass fibre counterpart. The projectile is described by its impacting mass m, geometry, and initial velocity taken from the test results.

ρ $[g/cm^3]$	1.86	Density at $23°C$
α_L $[1/°C]$	6.10 10^{-6}	Longitudinal coefficient of thermal expansion
α_T $[1/°C]$	26.2 10^{-6}	Transversal coefficient of thermal expansion
E_1 [GPa]	37.9	Longitudinal tensile Young's modulus
E_2 [GPa]	8.5	Transverse tensile Young's modulus
σ_1^{ult} [MPa]	1080	Ultimate longitudinal strength
σ_2^{ult} [MPa]	39	Ultimate transversal strength
τ_{12}^{ult} [MPa]	89	Ultimate shear strength
μ [-]	0.28	Poisson ratio

Table 8.1: E-glass fibre reinforced epoxy properties with $V_f = 0.5$. *Adapted from [22].*

Since the materials exhibit sensitivity to strain rate, the model takes into account the influence of the strain rate that can be approximated, in the case of low velocity impact, by dividing the impact velocity by half of the average plate dimensions. Notably, elevated strain rates contribute to a rise in both the tensile strengths of composite and the yield strength of the aluminium. For the glass fibre composite, the strain rate of $100s^{-1}$ leads to a 10% increase in strength [20], while for the flax fibre composite, a strain rate of $80s^{-1}$ leads to an approximately 17% increase [79]. And, the yield strength of thin aluminium sheets is increased to 375MPa for a strain rate of $100s^{-1}$.

Furthermore, it is essential to establish the contact interaction between the plate and the indenter. While the indenter has a conical shape, the model assumes a simplified scenario where the contact area is treated as a flat surface. To be more precise, the contact surface

is considered as circular with a radius equivalent to the tangency radius of the indenter, as defined below:

$$R_t = A\sqrt{\frac{R^2}{A^2 + F^2}} \tag{8.1}$$

where R is the radius of the spherical part of the indenter nose, and the lengths A and F are shown in Figure 8.1.

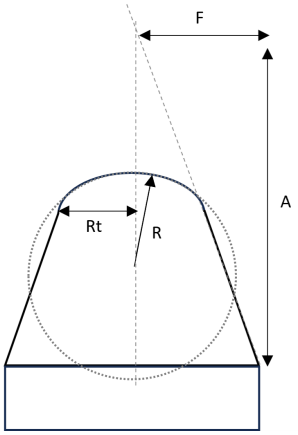

Figure 8.1: Definition of the radius of tangency.

Contrary to previous work, the contact radius is assumed to be equal to the tangency radius throughout the impact. This approach is justified by the fact that altering the contact radius during the failure sequence has minimal impact on the results and leads to increased computational time.

Plate deformation under impact

In order to replicate the effect of the impactor during an impact event, it is crucial to establish an accurate deflection profile for the plate. This profile must adhere to the boundary conditions of a completely clamped plate and is explicitly formulated for an impact taking place precisely at the middle of the plate. Moreover, in the present case, a large deflection of the plate is expected so that the in-plane deformations can be neglected in the formulation.

By assuming that the flexural profile of a FML is a combination of the one of the metallic layers and the one of the composite, the deflection profile of the neutral axis of the laminate can be derived from the work of Morinière et al. [20] as follows:

$$w(x,y) = \begin{cases} \Delta & (1) \\ MVF.\frac{\Delta}{(1-\frac{2R_t}{a})^2(1-\frac{2R_t}{b})^2}\left(1-\frac{2x}{a}\right)^2\left(1-\frac{2y}{b}\right)^2 ... & (2) \\ ... + (1-MVF).\frac{\Delta}{(1-(\frac{2R_t}{a})^2)(1-(\frac{2R_t}{b})^2)}\left(1-(\frac{2x}{a})^2\right)\left(1-(\frac{2y}{b})^2\right) & \end{cases} \tag{8.2}$$

$$(1) \quad 0 \leqslant x \leqslant R_t, \quad 0 \leqslant y \leqslant R_t$$

$$(2) \quad R_t < x \leqslant \frac{a}{2}, \quad R_t < y \leqslant \frac{b}{2}$$

where Δ is the maximum displacement at the plate centre, a the plate length and b its width.

Stress analysis: Classic Laminate Theory

From this deflection profile, the Von Kármán strains, which describe the large deflection of thin plates, can be derived by following the Kirchhoff hypothesis for displacement fields. The Classical Laminate Theory is then used to calculate the stresses in each layer of the laminate and carry out the failure analysis. In addition, the initial curing stresses resulting from the manufacturing process are taken into account.

The Von Mises and Tsai-Hill failure criteria are used to assess the failure of metallic and composite layers, respectively. When a layer fails, its elastic properties are instantaneously degraded, and the stresses of the failed layer are redistributed among the unaffected layers based on their corresponding stiffness properties.

To take account of the strain-hardening behaviour of the metal layers, modifications are made to the CLT as elucidated in the literature review. The Ramberg-Osgood relationship is used to correct the Young's modulus of aluminium once it has reached its yield strength. However, compared with previous work, a lower limit has been set for the modulus at 650MPa, in line with the stress-strain curve of aluminium [3].

Energy calculation and impact response

The energy calculation is performed to deduce the impact behaviour of the FML. The strain energy is integrated across the laminate's thickness and can be partitioned into membrane energy, denoted as U_m, bending energy as U_b, and the energy associated with membrane-bending coupling, designated as U_c. These quantities are determined using the ABD matrix of the laminate [80]. The formulations of these relationships are derived from Morinière's research [13] and are presented as follows for a quarter of the plate:

$$
\begin{aligned}
U_m = &\int_{R_t}^{\frac{a}{2}} \int_{R_t}^{\frac{b}{2}} \left\{ \frac{1}{8} A_{11} \left(\frac{\partial w}{\partial x} \right)^4 + \frac{1}{4} A_{12} \left(\frac{\partial w}{\partial x} \right)^2 \left(\frac{\partial w}{\partial y} \right)^2 + \frac{1}{8} A_{22} \left(\frac{\partial w}{\partial y} \right)^4 + \dots \right. \\
&\left. \dots \frac{1}{2} \left[A_{16} \left(\frac{\partial w}{\partial x} \right)^2 + A_{26} \left(\frac{\partial w}{\partial y} \right)^2 \right] \frac{\partial w}{\partial x} \frac{\partial w}{\partial y} + \frac{1}{2} A_{66} \left(\frac{\partial w}{\partial x} \frac{\partial w}{\partial y} \right)^2 \right\} dxdy \\
U_c = &- \int_{R_t}^{\frac{a}{2}} \int_{R_t}^{\frac{b}{2}} \left\{ \frac{1}{4} B_{11} \left(\frac{\partial w}{\partial x} \right)^2 \frac{\partial^2 w}{\partial x^2} + \frac{1}{2} B_{12} \left[\left(\frac{\partial w}{\partial y} \right)^2 \frac{\partial^2 w}{\partial x^2} + \left(\frac{\partial w}{\partial x} \right)^2 \frac{\partial^2 w}{\partial y^2} \right] + \dots \right. \\
&\dots \frac{1}{4} B_{22} \left(\frac{\partial w}{\partial y} \right)^2 \frac{\partial^2 w}{\partial y^2} + B_{16} \left[\frac{\partial^2 w}{\partial x^2} \frac{\partial w}{\partial x} \frac{\partial w}{\partial y} + \left(\frac{\partial w}{\partial x} \right)^2 \frac{\partial^2 w}{\partial x \partial y} \right] + \dots \\
&\left. \dots B_{26} \left[\frac{\partial^2 w}{\partial y^2} \frac{\partial w}{\partial x} \frac{\partial w}{\partial y} + \left(\frac{\partial w}{\partial y} \right)^2 \frac{\partial^2 w}{\partial x \partial y} \right] + 2 B_{66} \frac{\partial^2 w}{\partial x \partial y} \frac{\partial w}{\partial x} \frac{\partial w}{\partial y} \right\} dxdy \\
U_b = &\int_{R_t}^{\frac{a}{2}} \int_{R_t}^{\frac{b}{2}} \left[\frac{1}{2} D_{11} \left(\frac{\partial^2 w}{\partial x^2} \right)^2 + D_{12} \frac{\partial^2 w}{\partial x^2} \frac{\partial^2 w}{\partial y^2} + \frac{1}{2} D_{22} \left(\frac{\partial^2 w}{\partial y^2} \right)^2 + \dots \right. \\
&\left. \dots 2 \left(D_{16} \frac{\partial^2 w}{\partial x^2} + D_{26} \frac{\partial^2 w}{\partial y^2} \right) \frac{\partial^2 w}{\partial x \partial y} + 2 D_{66} \left(\frac{\partial^2 w}{\partial x \partial y} \right)^2 \right] dxdy
\end{aligned}
\tag{8.3}
$$

Then minimising the total potential energy with respect to the maximum deflection it becomes possible to compute the contact load during each failure event:

$$F_i = 4\frac{U_{mi}}{\Delta_i} + 3\frac{U_{ci}}{\Delta_i} + 2\frac{U_{bi}}{\Delta_i} \tag{8.4}$$

Besides accounting for strain energy, the energy dissipated due to delamination is also taken into consideration. Specifically, during low-velocity impact, various failure modes lead to energy dissipation, with delamination emerging as the primary mode during a perforating low-velocity impact [13].

Under the assumption of a simplified concentrated force scenario, the propagation of a single central delamination in mode II occurs when the force resulting from the plate deformation surpasses a critical threshold force [20]:

$$F_{del} = \sqrt{\frac{8\pi^2 E_{lam} t_{lam}^3 G_{IIc}}{9(1-\nu_{lam}^2)}} \tag{8.5}$$

where E_{lam}, t_{lam} and ν_{lam} represent the plate stiffness, thickness, and Poisson's ratio. A mode II interlaminar fracture toughness value of 0.44N/mm is adopted for both E-glass and flax fibre reinforced epoxy composites [66, 81]. Subsequently, the associated delamination energy is calculated as follows:

$$E_{del} = \frac{2\pi E_{lam} t_{lam}^2 G_{IIc}^2}{9(1-\nu_{lam}^2)\tau_{12}^{ult}} \tag{8.6}$$

Finally, the energy absorbed during the impact is the sum of energy dissipated in each event through plate deformation and delamination. From it, the impact velocity V_0 can be determined using the kinetic energy, while the reduction in velocity during the impact can be determined for the impact response curves as follows:

$$\frac{1}{2}mV_{i+1}^2 = \frac{1}{2}mV_i^2 - E_{abs_i} \tag{8.7}$$

Note: In the present case, the calculation of the time response is omitted, as it is not required for the initial comparison with the experimental findings.

8.2 Experimental methodology

To evaluate the impact resistance of FLARE, single low-velocity impact tests were conducted at room temperature for each configuration presented in the following test matrix Figure 8.2. The test method and parameters are adopted from the work of Morinière [13], allowing for a direct comparison between the impact behaviour of FLARE and a conventional FML.

For each type of sample, an Up-and-Down method was employed to determine the impact energy threshold at which the impactor penetrates the samples. In other words, for a fixed impactor weight, the drop height is adjusted step by step such that the sample is perforated

	Fibre		Metal thickness			
Impact	Flax	E-Glass	0.3	0.4	0.5	Nb of samples
Test 1	x		x			7
Test 2	x			x		7
Test 3	x				x	7
Test 4		x	x			3
						27

Figure 8.2: Impact test matrix.

but not fully penetrated. To provide more precision, partial perforation is defined as the material being slightly punctured, and full perforation occurs when fracture propagates through the entire plate thickness. On the other hand, penetration occurs when the projectile goes through the material thickness.

Subsequently, the test is considered valid if it is conducted at an impact energy that results in full perforation, which is indicated by the presence of a visible crack along the diameter of the contact area on the aluminium rear side.

Test set-up

The tests were conducted using an in-house instrumented drop-weight test set-up, as shown in Figure 8.3. The impactor, equipped with a specific indenter nose, is dropped from the desired height using an impact carriage guided by two rails. Upon reaching the dampener, the impactor is released from the carriage, allowing it to impact the sample.

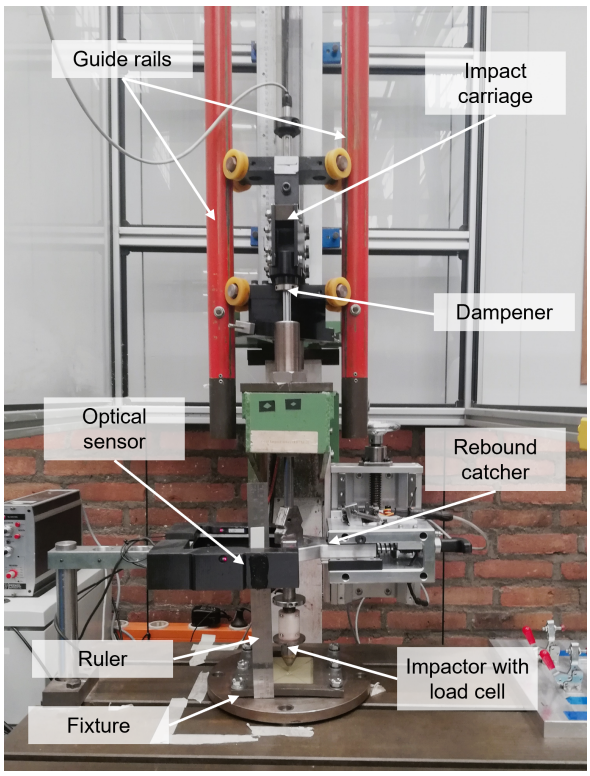

Figure 8.3: In-house instrumented drop-weight tower.

This setup effectively prevents excessive swinging during the fall, ensuring as much as possible a controlled and stable impact event. In addition to that, an optical sensor is utilised to trigger data recording and the rebound catcher prevents the occurrence of multiple impacts by capturing the impactor after the first impact.

The load cell positioned on top of the indenter is responsible for measuring the contact force $F(t)$ between the indenter and the sample throughout the impact. In addition, to measure the velocity of the impactor both before and after impact, a high-speed camera is employed (not visible in Figure 8.3).

Finally, the rectangular specimens are clamped using two frames with an aperture of 125 by 75mm as depicted in Figure 8.4. They are fastened in place by applying a torque of 40Nm on each bolt to ensure good clamping during testing. Regarding the impactor nose geometry, a conical shape steel indenter with a radius of 4.75mm, similar to the one used by Morinière, was employed. The impactor, with a total mass of 1.70 kg, hits the sample at its centre.

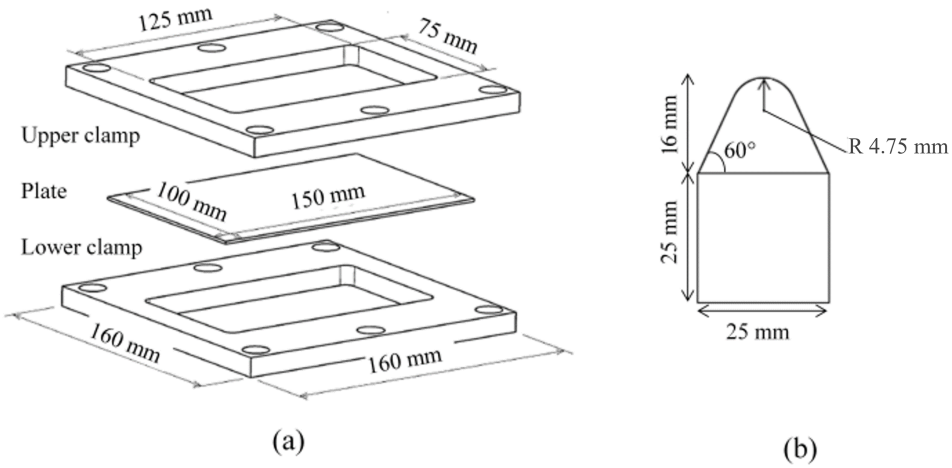

Figure 8.4: a) Fixture geometry. b) Impactor nose dimensions [13].

Post-processing

Unfortunately, the force signal recorded by the transducer contains additional repetitive sinusoidal noise, which must be subtracted from the data. To achieve this, prior to each impact test, the force is recorded by the force transducer as a reference signal. Then, after performing a time shift, the reference signal is subtracted from the recorded impact data.

Subsequently, this force signal can be numerically integrated to derive the velocity $V(t)$, displacement $D(t)$, and absorbed energy $E(t)$ using the following equations:

$$V(t) = V_0 + gt - \frac{1}{m}\int_0^t F(\tau)d\tau \tag{8.8}$$

$$D(t) = V_0 t + \frac{1}{2}gt^2 - \frac{1}{m}\int_0^t (\int_0^t F(\tau)d\tau)d\tau \tag{8.9}$$

$$E(t) = \frac{1}{2}m(V_0^2 - V(t)^2) \tag{8.10}$$

where, V_0 is the initial impactor velocity, g the gravitational acceleration and m the total mass of the impactor.

Moreover, a moving average was applied during the analysis to minimise scatter in the force data and highlight significant variations.

8.3 Low-velocity impact test results

The experimental results from the low-velocity impact tests for the FLARE_5_0.3 specimens, shown as force-distance curves, are depicted in Figure 8.5. Corresponding graphs were obtained for FLARE_5_0.4 and FLARE_5_0.5 samples and are presented in Appendix A.2.

The graph reveals the presence of multiple distinguished force peaks, which can be a characteristic feature of the impact response of structures with complex deformation behaviour. Primarily, two force peaks are observed. When the impactor comes into contact with the material, the sample undergoes both elastic and plastic deformations, resulting in energy dissipation through strain energy. As the impactor penetrates deeper into the material, inducing further deformation, the initiation of delamination occurs, followed by ply failure. Consequently, the first load peak might be attributed to the material's ability to absorb energy through delamination, or alternatively, through other energy dissipation mechanisms such as fibre or matrix failure within a composite ply. The second force peak corresponds to the primary failure of the aluminium layers.

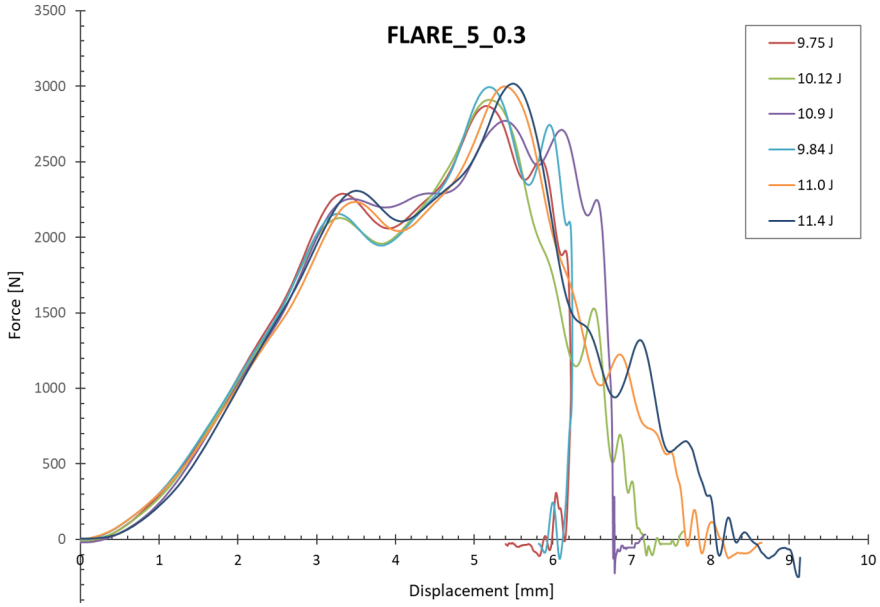

Figure 8.5: Force-displacement curves for FLARE_5_0.3 samples.

However, as the metal volume fraction increases, the prominence of the first force peak diminishes. This phenomenon might be attributed to the influence of the metallic layers, which limit the extent of delamination and delay composite failures by taking a substantial portion of the applied load.

Moreover, a significant discrepancy in the maximum displacement can be observed among specimens of the same type. This can be attributed to the inherent variability in the impact tests conducted using the in-house instrumented impact tower. Despite using the same drop height and impactor mass, the impact energy is not consistently uniform from one test to another, leading to varying results in the maximum displacement observed.

In Figure 8.6, a comprehensive comparison of the impact response for all the samples is provided. As anticipated, the impact energy required to cause full perforation increases with the metal volume fraction. This observation might suggest that the impact behaviour of FLARE is dominated by the aluminium. However, as the thickness of the aluminium layer increases, so does the overall thickness of the laminate. And this increase in thickness has a significant effect on the impact behaviour of FLARE.

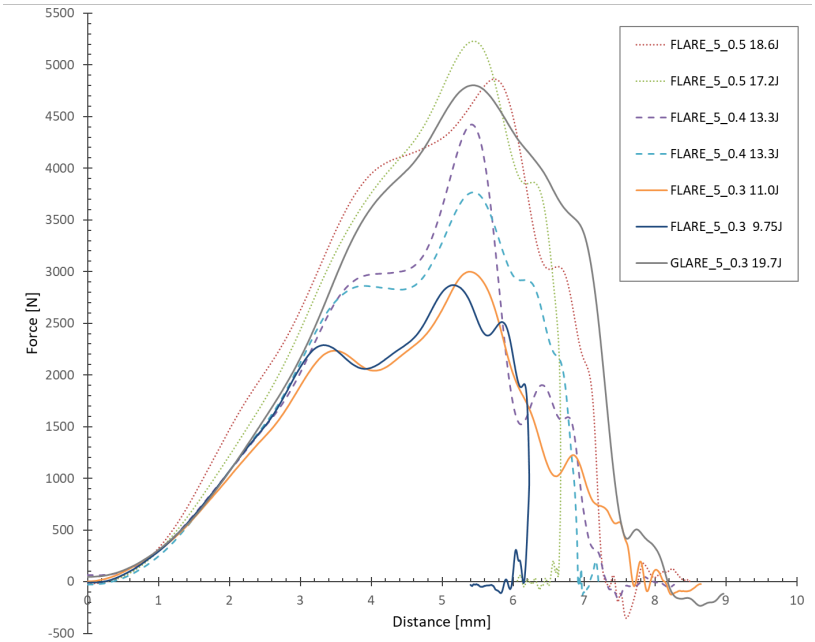

Figure 8.6: Comparison of the force-displacement curves of different type of samples.

When comparing FLARE_5_0.3 with its glass fibre counterpart, it becomes evident that the type of fibre has a significant impact on the maximum impact force. In fact, the maximum impact force of GLARE_5_0.3 is comparable to that of FLARE with thicker aluminium layers. This observation highlights the crucial role played by the type of fibre in the impact behaviour of the material. However, it is essential to qualify the conclusion that the impact behaviour of FML is influenced by fibres. In fact, the samples are not directly comparable, mainly because of the variations in void contents, which has an influence on the material's response to impact.

Finally, for the same type of fibres, an increase in the MVF favours the absorption of more impact energy. Test data indicates that FLARE_5_0.5 absorbed 74% more impact energy compared to FLARE_5_0.3. Additionally, for the identical aluminium thickness, FLARE absorbed 42% less impact energy than GLARE. Consequently, even though the failure of the

plate is precipitated by the failure of the last fibre layer, the aluminium plays a prominent role in energy absorption.

Regarding impact-induced damage, Figure 8.7 illustrates the characteristic damage pattern observed on both the front and back aluminium layers. The front aluminium layer exhibits a crack along the periphery of the impact site, while the back aluminium layer displays a crack extending across the diameter of the impacted region. This pattern closely resembles the damage observed by Morinière [13] in the case of GLARE samples.

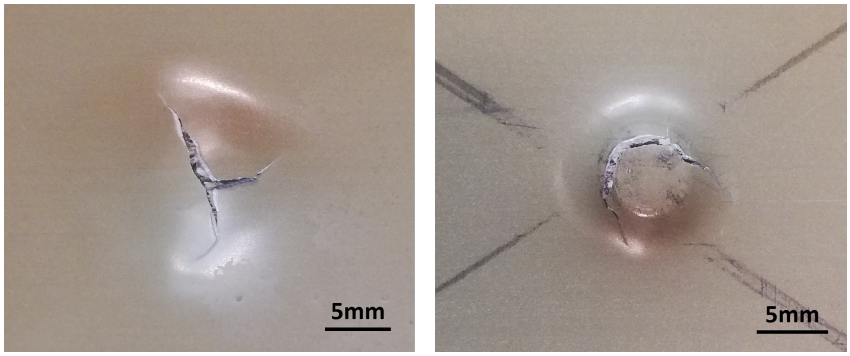

Figure 8.7: Impact damage in FLARE_5_0.5. *Left*: rear side. *Right*: front side.

To be more specific, two distinct types of damage were observed on the rear side. The damage either manifests as a crack running perpendicular to the outer fibre direction (for FLARE_5_0.5 and some of FLARE_5_0.4) or as a crack following the rolling direction of the aluminium layer (observed in FLARE_5_0.4 and FLARE_5_0.3), which is parallel to the outer fibre direction. According to Vlot [36] they are respectively characteristic of a fibre-dominated and an aluminium-dominated impact behaviour. This suggests that depending on the aluminium thickness (or MVF), both failure modes can occur in FLARE. A similar phenomenon was observed in GLARE, which exhibits varying failure modes depending on the behaviour of the glass fibres and layup of the laminate [35, 36].

8.4 Comparison with the analytical model

In Table 8.2, the values obtained from the analytical model and the averaged experimental results are presented. However, it is worth noting that for GLARE_5_0.3, only one sample was considered valid for the analysis. The other two samples experienced only minor punctures, indicating that the impact energy was insufficient to classify these tests as perforation impacts.

Moreover, in the case of the experimental results, the absorbed energy is determined by calculating the difference between the kinetic energy before impact, based on the impact velocity, and the kinetic energy after impact, which corresponds to the rebound velocity. On the other hand, for the model results, the absorbed energy is computed as the sum of the energy dissipated by strain energy and delamination.

	FLARE_5_0.3		**FLARE_5_0.4**		**FLARE_5_0.5**		**GLARE_5_0.3**	
	Model	**Test**	**Model**	**Test**	**Model**	**Test**	**Model**	**Test**
Fmax [kN]	5.74 (+96.1%)	2.93 (*0.10*)	6.67 (+59.7%)	4.18 (*0.36*)	7.38 (+54.3%)	4.78 (*0.31*)	6.26 (+30.3%)	4.80
Δmax [mm]	7.15 (+1.69%)	7.03 (*0.75*)	8.30 (+9.59%)	7.57 (*1.02*)	7.85 (+0.28%)	7.83 (*1.33*)	8.62 (+4.82%)	8.22
V_0 **[m/s]**	2.92 (-17.0%)	3.52 (*0.11*)	3.74 (-5.36%)	3.95 (*0.10*)	3.71 (-19.4%)	4.60 (*0.30*)	3.83 (-20.6%)	4.82
Eabs [J]	9.41 (-2.18%)	9.62 (*1.15*)	11.87 (-7.34%)	12.81 (*0.81*)	11.71 (-30.2%)	16.77 (*3.12*)	12.49 (-24.0%)	16.44

Table 8.2: Analysis and test results for the different specimens.

Overall, the analysis yields results that align with the trends observed in the test results, albeit with sometimes significant margin of error. Notably, the predicted maximum force for FLARE tends to be higher, even displaying a margin of error as substantial as 96%. The predicted maximum deflection falls more within the range of the test results for all the samples. Finally, the analytical model consistently underestimates the absorbed energy and thus the impact velocity.

In addition to its predictive capacity for material performance, the analytical model provides a comprehensive impact response along with the corresponding sequence of failures, as shown in Figure 8.8.

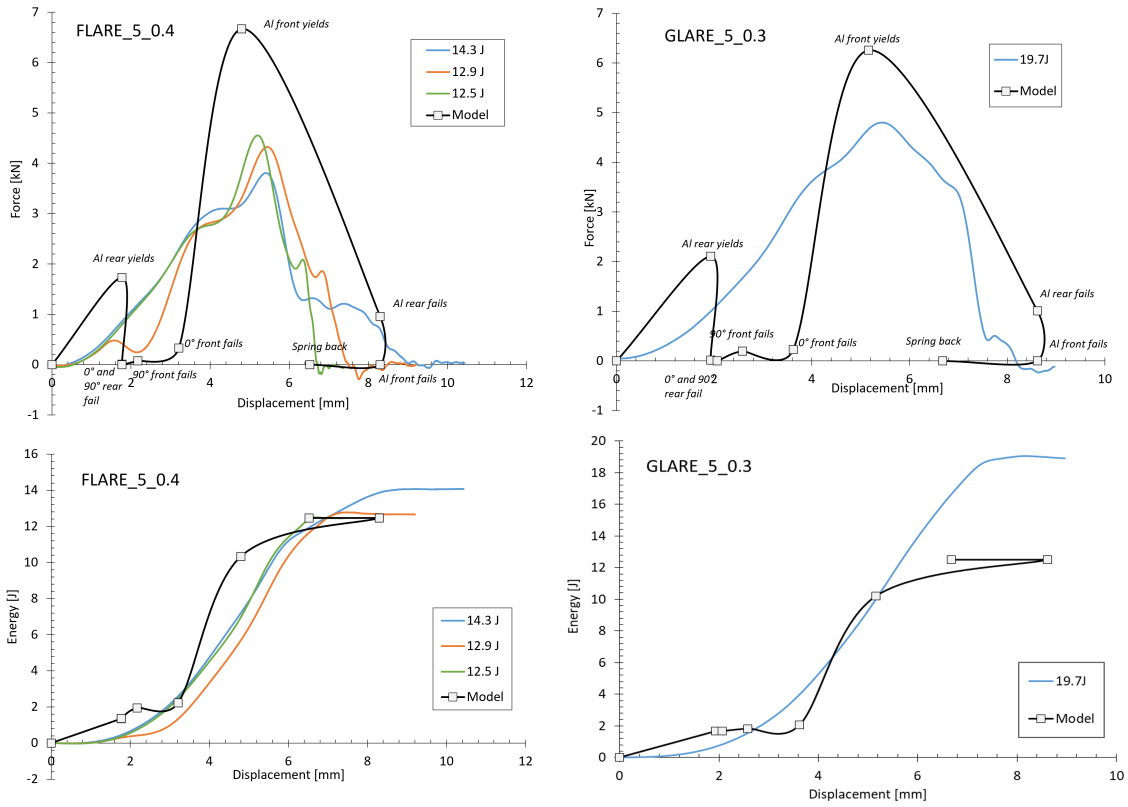

Figure 8.8: Impact response of FLARE_5_0.4 and GLARE_5_0.3.

Apart from the aforementioned overestimations and underestimations, the force-displacement model curves exhibit a pronounced initial force peak, which corresponds to the failure of the first composite ply for the FLARE samples. In the analytical model, the failure criteria assume the rupture of an entire ply, an occurrence unlikely to happen in reality. Likewise, the proposition that a failed layer at the impact site will no longer support load corresponds to an unrealistic situation. These assumptions could account for the presence of the peak load that is not captured during testing [20].

In the model, the final layer failure occurs at the same force as the preceding failure event, attributed to a catastrophic failure. Additionally, the laminate's spring back is accounted for in the model, whereas it does not appear to be captured by the test results.

Regarding the energy-displacement curves, it is clear that the predicted total absorbed energy is lower than the actual value, even reaching a relative difference of almost 55%. This could be due to an underestimation of the absorbed energy associated with delamination and/or the omission of the energy dissipated by other failure modes such as fibre breakage and petaling in the energy calculation.

Finally, the unsatisfactory outcomes derived from the generic model discussed in the preceding section underscore the chosen deflection profile in Equation 8.2 may not accurately depict the deformation of the FML during low-velocity impact. Indeed, the model was initially developed for relatively thin laminates, but the current FMLs exhibit increased thickness, potentially rendering the developed model inapplicable. Particularly, the transverse shear deformations can no longer be neglected. Thus, the utilisation of First- or Higher-order Shear Deformation Theory becomes essential for the computation of stresses, and the failure criteria must be adapted.

Conclusion

In conclusion, this chapter provides insights into the impact behaviour of FLARE, revealing similarities with GLARE (E-glass fibre reinforced) but with slightly reduced resistance.

It was observed that an increase in metal volume fraction leads to higher impact energy needed for perforation. The choice of fibre type also plays a crucial role in impact behaviour, as weaker fibres precipitate the failure of the FML. Hence, the impact resistance of FLARE arises from the interaction between the composite and metal components, defying a straightforward dominance. Nevertheless, in terms of the primary mechanism driving energy absorption, the deformation and failure of the aluminium layer seem to be predominant.

With regard to the prediction using the quasi-static analytical model, a similar dynamic for the impact curves was observed, but with a significant divergence in the final impact properties compared with the experimental, sometimes reaching 60%. This issue can be attributed to the limited applicability of the model to laminates with moderate thickness, where the influence of transverse shear stresses becomes significant. Furthermore, the model does not capture the non-linear behaviour of the flax fibre composite and relies on an unrealistic sudden and complete rupture assumption, which does not align well with actual behaviour. Finally, only strain energy and delamination have been taken into account for the calculation of the

impact energy dissipation, although fibre fracture and petaling also make some contribution. Nevertheless, the model can still serve its purpose for making relative comparisons, like assessing the impact of changes in metal volume fraction, providing an initial conceptual understanding.

Chapter 9

Discussion

After conducting this study on the impact and damping characteristics of FLARE, a better understanding has been gained of how the synergy between the metal and composite components operates within this hybrid material.

The presence of metallic layers significantly enhances both the tensile properties and impact resistance of flax fibre reinforced epoxy. However, this improvement comes at the cost of considerably diminishing the vibration damping potential of this composite, as the damping behaviour of FLARE is predominantly governed by the metal layers. Additionally, it is inaccurate to presume that substituting glass fibres with flax fibres, having similar specific properties according to the literature, within an FML will guarantee the retention of identical mechanical properties. Indeed, as elucidated earlier, the nonlinear behaviour of flax fibres cannot be disregarded when evaluating the tensile behaviour of FLARE. This is particularly evident in the fact that the high Young's modulus is not sustained beyond a strain of 0.2%, and therefore cannot summarise the capabilities of the flax fibre composite. In addition, even though the impact resistance might appear to be predominantly influenced by the metal, weaker fibres can lead to a decrease in the overall impact resistance of FML.

Therefore, a design approach, divergent from the one conceived for GLARE, must be embraced to optimise the synergistic benefits of the flax fibre composite-metal combination. For instance, considering more extreme metal volume fraction values with exceedingly thin metal layers or focusing on applications where potential limitations can be overcome through strategic structural design might offer a viable approach.

Subsequently, building upon the insights derived from the experimental investigations and the developed predictive models, potential strategies for harnessing the advantages of the fibre metal laminate concept are presented in the following. In particular, potential concrete applications will be showcased.

9.1 FLARE with low metal volume fraction

As emphasised in this study, flax fibre reinforced epoxy is an environmentally friendly composite material that holds great promise across a wide range of applications, spanning from

aesthetic to structural purposes. Besides to its favourable specific mechanical properties, this material distinguishes itself through its functional attributes, notably its capacity for vibration and acoustic damping. However, its most significant advantage lies in its minimal environmental impact, characterised by its biodegradability and low embodied energy [82]. In a global context where reducing the carbon footprint of transportation, construction, and other equipment is imperative, flax fibre composites emerge as a compelling material option.

Regrettably, several factors curtail its broad applicability, including inherent flammability, susceptibility to moisture absorption, and restricted resistance to chemicals and UV radiation. To address this issue, various surface treatments and coatings are being used, often involving chemical processes that might not align with environmentally friendly practices. Furthermore, in certain applications demanding properties like electromagnetic shielding, thermal conductivity, or electrical conductivity, the flax fibre composite cannot be directly employed.

This is where the concept of Fibre Metal Laminates comes into play. Indeed, unlike GLARE, where the emphasis is on the use of metal for its mechanical properties, the metal can be seen here as both a protective and functional layer combined to the composite. At the cutting edge of coatings technology, an FML with a minimal metal volume fraction can offer significant advantages.

Consider the case of a unidirectional FML composed of the same aluminium and composite materials investigated in this study, with a metal volume fraction of 0.05 and a $[Al/(0°)_n/Al]$ layup. Based on the validated predictive tools and the material properties estimated during this work, some of its specific properties are given in Table 9.1.

Elastic modulus $[GPa.cm^3/g]$	24.3
Second modulus $[GPa.cm^3/g]$	11.8
Ultimate tensile strength $[MPa.cm^3/g]$	240.8
Loss factor (DMA) $[cm^3/g]$	0.015
Loss factor (VBT) $[cm^3/g]$	0.011
Impact resistance	Equivalent to FFRE alone

Table 9.1: Estimated specific properties for FLARE 2/1 with MVF=0.05.

The impact resistance cannot be precisely quantified using the analytical model presented in this study due to its limitations with thicker laminates. Indeed, for a FML with such a low metal volume fraction, achieving the required thickness for the model would entail aluminium layers of less than 0.1mm thickness, which is not compatible with the desired sheet-like structure. Therefore, it is presumed that the inclusion of very thin layers of aluminium does not substantially enhance the impact resistance of the composite under low-velocity impacts. Nonetheless, these layers are likely to contribute to an improved resistance against erosion.

To position this type of FML in relation with other materials, Figure 9.1 shows a comparison between flax fibre reinforced epoxy, glass fibre reinforced epoxy, 2024-T3 aluminium, and the FLARE component designed above.

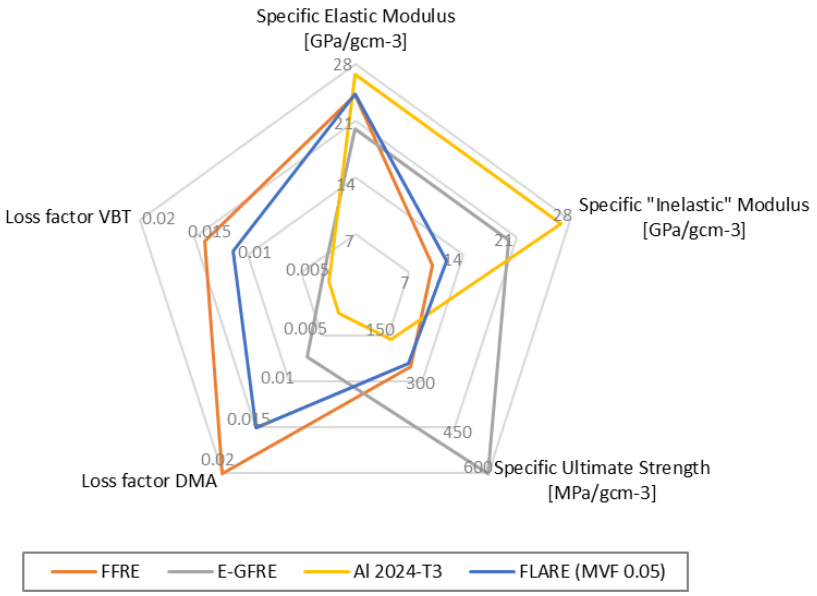

Figure 9.1: Comparison of the properties of different material.

The main advantages of using such a FLARE configuration are its good stiffness, which matches that of various other materials on a specific basis (owing to its low density), and its effective damping properties. However, it also poses a challenge concerning its strength. And presently, a trade-off must be made between impact resistance and damping capabilities. But it is important to note that the data used in this analysis are derived from a sample that might not represent the highest manufacturing quality. Thus, enhancing the manufacturing process, which could result in better fibre volume fraction or reduced void content, could offer a potential avenue for addressing these drawbacks.

In consideration of these findings, certain applications requiring especially damping, can be envisaged for FLARE with thin metal layers. Some examples are:

- **Body car panels**: The current material used for exterior body car panels are mostly glass fibre composite or aluminium alloys. These materials must meet specific criteria such as stiffness, vibration damping, and sound absorption to enhance passenger comfort [83]. Consequently, the incorporation of FLARE with its thin metal layers emerges as a promising prospect. Notably, the metal layers not only enhance composite durability through protection but also offer essential lightning strike protection to establish a Faraday cage, safeguarding users. The use of such a material will not only improve the car's fuel efficiency by reducing its weight but will also reduce its ecological footprint. Metal laminates based on natural fibres have already been studied for car front hood [48]. However, for other panels such as doors, crashworthiness still needs to be perfected before this type of FLARE can be used, for example by incorporating balsa core to create a sandwich structure.

- **Boat hull and floorboards**: The prevalent material for ship hulls is carbon steel protected from corrosion in different ways [84]. Vessel hulls and floors must have good bending properties and good damping capacities, while at the same time being as light as possible in order

to reduce the vessel's fuel consumption. Flax fibre reinforced epoxy seems to meet all the criteria. However, natural fibre composites tend to have a high water absorption rate, which leads to a rapid decrease in their mechanical performance. In addition, they are not immune to the physical and chemical degradation that occurs in underwater applications. Protective gel-coat is a short term solution, because it wears out quickly, leaving the composite surface exposed to the environment [85]. Much more reliable external protection is therefore essential for such applications. Thus, the addition of thin metallic layers to create FLARE might be an optimal solution.

Ultimately, the selection of the metallic layers allows for further tailoring of the fibre metal laminate to align with the specific application requirements. For instance, stainless steel can be a practical choice to enhance cost-effectiveness. Alternatively, aluminium and its alloys are extensively employed due to their advantageous characteristics such as low density, good corrosion resistance, high specific tensile strength, and efficient electrical and thermal conductivity. Moreover, for scenarios necessitating high temperature resistance, titanium, which is also corrosion-resistant and bio-compatible, can be a viable option. Similarly, magnesium, acclaimed for its exceptional low density, could prove an interesting alternative to aluminium alloys.

9.2 FLARE designed for wind turbine blades

An alternative avenue for utilising fibre metal laminates is to target applications where damping holds a less critical role or can be strategically incorporated through intelligent structural design, rather than solely relying on material properties. This approach opens up the potential to emphasise attributes like enhanced impact resistance and increased strength, while concurrently addressing environmental considerations.

An illustrative case for the application potential of FLARE lies within wind turbine blades, particularly those designed for offshore environments.

The materials of choice for turbine blades are synthetic glass fibre composites, because of their high strength-to-weight and stiffness-to-weight ratios, their fatigue performance, and their ability to be manufactured in complex shapes. However, these synthetic materials are not easily biodegradable and make the blades difficult to recycle. In fact, the fibre reinforced polymer blades of wind turbines, which are designed to have a lifespan of just 20 to 25 years, are most often landfilled [14]. Other end-of-life options are being developed, such as incineration or grinding for use as aggregate in concrete, but they do not appear to be commercially exploited on a large scale. However, the disposal of blades in landfill sites has become a major concern. Current estimates indicate that approximately 10 tonnes of composite materials are required for every megawatt of wind turbine power generation. Taking into account the current range of wind turbines, from 2 to 8 MW for offshore installations, projections indicate that there could be 43 million tonnes of blade waste to manage by 2050 [86]. The adoption of bio-based composites as an alternative to the current synthetic materials in wind turbine blades could provide a viable solution to address this issue.

The cross section of a wind turbine blade is shown in Figure 9.2. The main constituent is E-glass fibre reinforced epoxy with different fibre orientations, sometimes sandwiched with a core material (balsa or foam). In addition, a gel coat is applied to the top to act as a barrier against environmental factors such as UV rays, humidity, salt or atmospheric pollutants [87]. It also helps to reduce erosion due to rain or airborne particles, preventing degradation and extending the life of the blade.

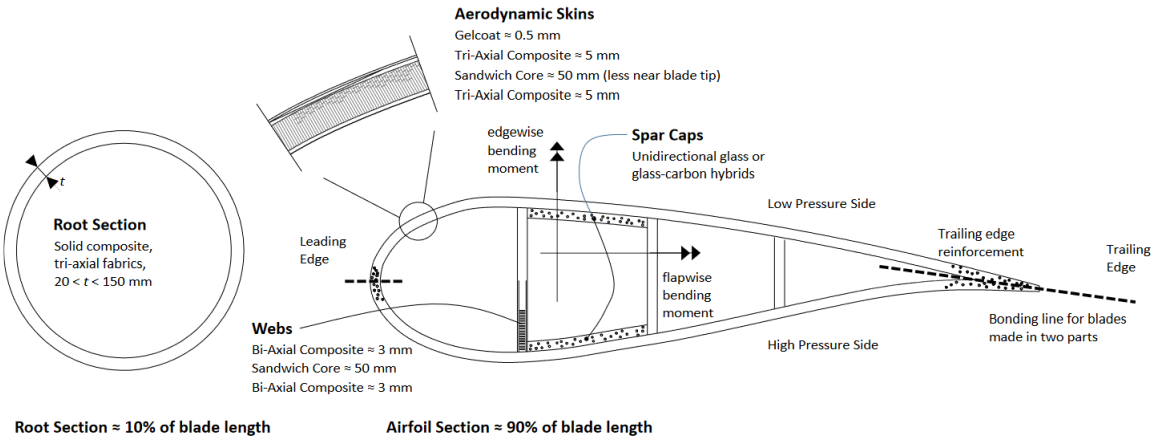

Figure 9.2: Cross-section of a wind turbine blade [14].

The structural configuration is meticulously engineered to endure wind-induced loads that primarily generate bending stresses, torsion, and buckling. Consequently, from a materials standpoint, the stiffness-to-weight ratio assumes paramount significance, as elevated flexural stiffness effectively safeguards the turbine blade against excessive bending and potential contact with the tower [56]. Furthermore, given the turbine's intended operational lifespan, the high-cycle fatigue performance of composites is a critical consideration.

Hence, flax fibre reinforced epoxy (FFRE) emerges as a promising alternative to replace the traditional glass fibre composite in this context. Yet, it is important to acknowledge that FFRE's stiffness encounters a reduction beyond a certain critical strain threshold. Furthermore, wind turbine blades are prone to physical impacts and surface erosion, both of which can detrimentally affect the composite's integrity. Moreover, this concern is particularly pertinent for offshore installations where water ingress can compromise the performance of the natural fibre composite.

Therefore, the adoption of the FML concept appears to offer a viable solution. The incorporation of metallic layers within the structure in a 2/1 configuration could effectively enhance its bending stiffness while also serving as a robust safeguard for the composite, eliminating the necessity for a gel-coat. Furthermore, given the susceptibility of wind turbines to lightning strikes, the metallic layer could also serve as an effective lightning strike protection mechanism.

In the current scenario, the metallic layers can be designed with a relatively substantial thickness, primarily to enhance impact resistance. In contrast to the earlier mentioned applications, the necessity for vibration damping does not necessitate a material-based solution. Instead, it can be accomplished by strategically distributing the mass and stiffness of the

structure, reducing resonant frequencies and thus minimising the magnification of vibrations. Another viable approach could be to use FLARE as the outer skin of a sandwich structure, possibly with a foam core, a structure already found in wind turbine blades with GFRE.

A comparison between certain properties of E-glass fibre reinforced composite and FLARE is presented in Table 9.2 for the case of the tri-axial composite ($[\pm 45°/0°]_{4s}$) with a total thickness of about $5mm$. For FLARE the aluminium alloy 2024-T3 is considered.

Material	Stiffness [GPa]	Strength [MPa]	Density [g/cm^3]	Cost [€/m^2]
E-GFRE	19.7	337	1.85	31.6
FFRE	12.2	124.3	1.2	15.7
FLARE (MVF=0.2)	24.2	195.4	1.52	18.8
FLARE (MVF=0.5)	42.3	302.2	1.99	31.2

Table 9.2: Comparison of different materials for the tri-axial composite configuration.

It is evident that FLARE exhibits comparable, if not superior, stiffness to GFRE. However, achieving comparable strength necessitates a substantial addition of metal, consequently raising the material's density. Regarding the cost evaluation, the pricing used was 2.3€/kg for AL 2024-T3 [88], 1.03€/kg for flax fibre, 2.3€/kg for glass fibre [17,89], and 6€/kg for epoxy [18]. The cost analysis indicates that FLARE holds its own against E-GFRE in terms of competitiveness, suggesting that further research into the design of wind turbine blades using this hybrid material could yield profitable outcomes.

Hence, incorporating natural fibre into wind turbine blade design remains a complex endeavour, as the material must possess a sufficiently elevated strength-to-weight ratio. Nevertheless, the FML concept is an avenue that deserves to be explored with a view to reducing the ecological impact of an energy supply method that claims to be "green".

9.3 Other potential applications for FLARE

9.3.1 Shipping containers

In the year 2022, international freight transportation was responsible for approximately 2% of the total global energy-related CO2 emissions, as reported by the International Energy Agency[1]. Most of this freight is moved using intermodal containers that can be seamlessly transferred between trucks, trains, or ships. These containers are predominantly constructed from CorTen steel (A242 HSLA), which is a high-strength low-alloy steel specifically engineered to withstand weathering [90]. Their design comprises several key elements, including a frame structure that imparts stacking strength to the container, a floor panel, and corrugated roof and side panels. The corrugation of the sheet metal serves to improve structural strength and rigidity, making the container well-suited to resist compression and buckling.

Typically, a standard 40-foot container of standard height has a tare weight of 3.8 tons, and millions of such containers are transported globally each year. Consequently, reducing

[1] https://www.iea.org/energy-system/transport/international-shipping

the weight of these shipping containers presents a compelling opportunity to decrease fuel or energy consumption during transportation and, in turn, reduce greenhouse gas emissions [90]. Efforts to lighten these containers have focused on replacing roof and side panels with aluminium. However, the adoption of the FML concept holds the promise of achieving further weight reduction while simultaneously meeting essential mechanical requirements, as well as addressing concerns such as corrosion resistance and weathering resistance. In addition, the use of natural fibres in FML, such as flax, reduces embodied-energy and provides thermal insulation, which is particularly advantageous for storing goods in optimum conditions. The metal layer can be recycled by burning composite layers of flax fibres, whose calorific value can be exploited.

The 2mm thick corrugated steel panels can be substituted with either aluminium panels made from Al 5052 alloy, designed for marine applications, or FLARE panels using either of these metals in a 2/1 configuration. A comparative analysis of the specific elastic modulus and tensile strength of these various materials is depicted in Figure 9.3. For the FMLs, a metal volume fraction of 0.4 was taken into account, striking a balance between density and mechanical properties. Two configurations were considered: one featuring a unidirectional composite $[0°]_4$, and the other incorporating a cross-ply configuration $[0°/90°]s$.

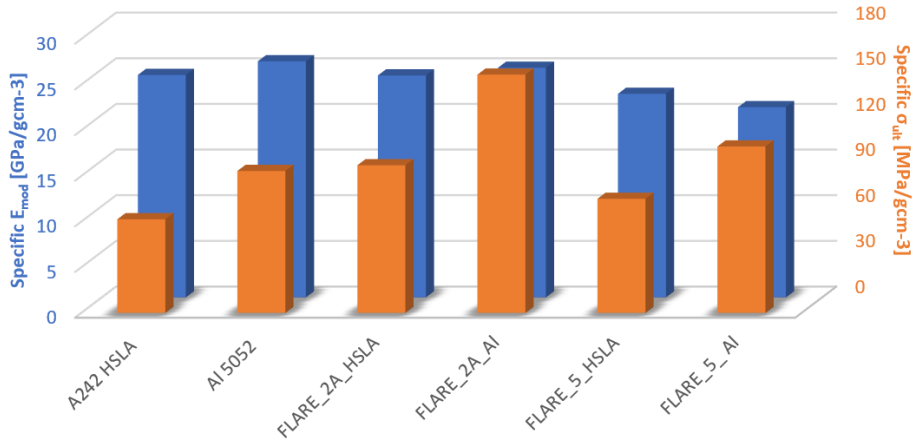

Figure 9.3: Specific properties of the different materials considered for the roof and side panels of containers.

The graph shows that FLARE_2A is competitive with traditional steel in terms of specific stiffness, and even surpasses it in terms of specific tensile strength. The cross-ply configuration reduces mechanical performance, but can be very useful for improving impact properties and vibration damping. Finally, FLARE made of steel sheets may have a lower properties-to-weight ratio compared to its aluminium counterpart but it remains a viable option, especially in terms of cost-effectiveness.

However, it should be noted that shipping container panels are only subjected to tensile loads during the lifting and handling phases. They are mainly exposed to compressive loads due to the stacking of several containers. It is therefore essential to carry out a buckling analysis to ensure their structural integrity. Nevertheless, it is mainly the frame structure that addresses the buckling problem, so it is most likely possible to use FLARE for these "non-structural" panels.

Hence, the application of the FML concept with natural fibre composites holds great promise in reducing the carbon footprint associated with shipping containers and related transportation systems.

9.3.2 Whipple shield

As space exploration continues to advance, the menace posed by space debris and meteoroids cannot be underestimated due to the ever-present danger of hyper-velocity impacts. To address this problem, the "Whipple shield" was developed as a lightweight protective solution. Unlike traditional monolithic metallic shields, the Whipple shield adopts a distinctive design, featuring a thin sacrificial outer bumper positioned at a distance from the spacecraft's primary wall, as illustrated Figure 9.4a). The function of this external bumper is to ensure that incoming projectiles fragment and disperse on impact, thereby attenuating their kinetic energy. There are several variants of the Whipple metal shield, such as the stuffed shield where layers of high-resistance fabric are placed in the middle, or the Multi-shock shield which features multiple bumpers strategically aligned to enhance protection against impacts [91].

Frequently, the outer bumper material of choice is aluminium alloys like Al 6061-T6 due to their advantageous combination of low density, high strength, and favourable deformation characteristics. Alternatively, hard and brittle ceramics can also serve this purpose [92]. In essence, the paramount criteria for this selection encompass the imperative need for lightweight properties, energy absorption capabilities, sufficient strength, and compatibility with the demanding space environment.

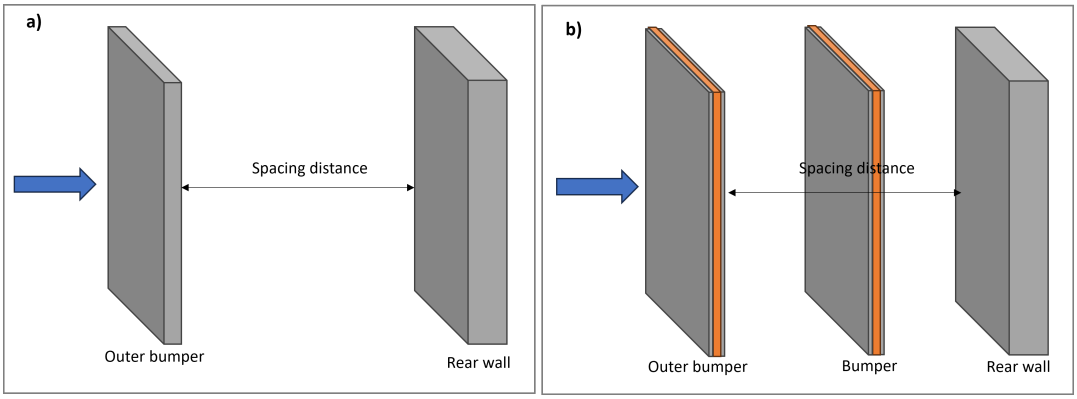

Figure 9.4: a) Metallic Whipple Shield classic configuration. b) Triple-wall Whipple Shield with FLARE bumpers.

To further reduce the weight of this protective shield, one approach could be to consider FLARE panels as bumper layers within a triple-wall configuration, as depicted in Figure 9.4b). Indeed, in low-velocity impact tests, FLARE demonstrated promising energy absorption capabilities, with potential for further enhancement through adjustments in the layup. However, in order to confirm this positive trend for hyper-velocity impacts, additional experimental investigations are warranted.

Furthermore, it is worth noting that flax fibres offer several advantages, including vibration damping and low thermal expansion, making them highly suitable for space applications. Finally, they contribute to a reduced environmental footprint in space manufacturing.

Chapter 10

Conclusions and Recommendations

10.1 Conclusions

The Fibre Metal Laminate concept was originally used to create synergy between the impact resistance of metals and excellent fatigue and corrosion resistance of synthetic fibre reinforced polymers. One of these leading hybrid materials is glass fibre reinforced aluminium, primarily engineered for aerospace purposes. However, with the rising concerns about climate change, and the issues of recycling glass fibre composites, a new generation of FMLs with a reduced carbon footprint is worth considering. In particular, flax fibre reinforced metal laminates (FLARE) may have real potential by combining the good impact behaviour of metals with the excellent vibration damping of bio-based composites, making it possible to obtain low embodied energy metal laminates that are easily recyclable.

Therefore, the primary objective of this study was to conduct experimental investigations into the impact and damping characteristics of FLARE, an area that lacks prior research. In addition, in order to make good use of the knowledge acquired on FMLs, this project aimed to validate and, if needed, modify existing predictive analytical models tailored to conventional FMLs, ensuring their applicability to FLARE.

To achieve these objectives, several research sub-questions were answered:

1. To what degree does FLARE maintain the advantageous vibration damping properties inherent in flax fibre composites?

Flax fibre reinforced epoxy (FFRE) is known for its high damping capabilities due to the unique hierarchical structure of these fibres. It is therefore legitimate to ask how this advantage evolves when metal layers are added to the composite. The experimental investigations conducted on FLARE samples using dynamic mechanical analysis and beam vibration testing have yielded a significant finding: **the vibration damping capability of FLARE is primarily governed by the metal component**. Notably, the loss factor demonstrates a pronounced decrease as the metal volume fraction (MVF) is raised, tapering off toward the level associated with pure metal.

Therefore, FLARE does not uphold the vibration absorption capacity characteristic of its composite constituent, exhibiting a similarity to conventional FMLs in this aspect. Nevertheless, there is a potential avenue for optimisation: by deliberately reducing the metal volume fraction to lower levels than conventionally employed, FLARE could emerge as a favourable option for applications that demand efficient vibration damping.

2. How does FLARE behave under a low velocity impact?

The low velocity impact tests conducted indicate a resemblance between the impact responses of FLARE and conventional FMLs like GLARE, but with a lower impact resistance for FLARE. In fact, the composite layers play a relatively minor role in absorbing impact energy but help to distribute the impact force throughout the laminate. It is the significant deformation of the metal layers, which leads to overall deformation before failure, that enables a substantial part of the impact energy to be absorbed. The metal therefore plays a predominant role in the impact response, but it is the failure of the fibres that precipitates the one of the laminates. Consequently, **the impact resistance of an FML depends on both of its components** and can be fibre or metal dominated depending on the layup.

3. What predictive tools developed for conventional FMLs are applicable for natural fibre metal laminate?

Throughout the course of this work, a range of predictive tools were examined and evaluated. The most promising among these are summarised in the following table, with their limitations and constraints.

Parameter to predict	**Predictive tool used**	**Better accuracy with...**	**Limitations**
Ultimate strength	MVF method		
Elastic modulus	MVF method	"Inelastic modulus" for FFRE contribution	
Damping coefficient	Inverse rule of mixture	Weight fractions	
Low velocity impact	Quasi-static analytical model		Not well suited to moderately thick laminates. FFRE behaviour assumed to be linear with "inelastic modulus". Complete and sudden ply failure assumed.

Ultimately, through the integration of all the gathered insights, it becomes evident that the vibration damping ability and impact resistance of the material are unfortunately moving in divergent directions. However, by contributing to the knowledge of the behaviour of natural fibre metal laminates, this study has also highlighted other ways of using the FML concept. More specifically, this work suggests that FMLs can pave the way for expanding the use of bio-based materials in structural and multi-functional contexts, taking advantage of synergistic effects.

10.2 Recommendations

Drawing from the findings and conclusions outlined in this project, several suggestions for prospective research can be proposed.

Manufacturing process

To validate the advantages of integrating flax fibre composites with metallic layers, it is advisable to use a manufacturing process involving prepreg techniques. This approach is expected to yield improved fibre volume content and reduced voids, thereby enhancing the overall mechanical properties of the FML. In addition, it might be more beneficial to focus on out-of-autoclave manufacturing methods in order to make FLARE a cost-effective product and bring it into widespread use.

Exploring alternative metals and incorporating a bio-based matrix presents another avenue for improving the properties of FLARE and enhancing its recyclability. Notably, using the predictive tools validated in this study can help to make an initial selection between the possible options.

Mechanical behaviour of FLARE

As highlighted in this report, the non-linear behaviour of flax fibre composites is not reflected in the tensile behaviour of FLARE. It would therefore be interesting to investigate this phenomenon further, aiming to ascertain whether the composite's contribution to FLARE's stiffness is indeed solely attributed to its "inelastic modulus". Specifically, conducting load–unload test with incremental steps could provide insights into the stiffness evolution of the FML and determine what happens to the non-linear behaviour of the composite.

In addition to its quasi-static mechanical behaviour, it would be pertinent to investigate the fatigue performance of FLARE, particularly if it is to be used in structures subjected to fatigue loading. An in-depth comparison with E-GLARE and E-GFRE, in various configurations, could provide valuable information.

Damping behaviour of FLARE

Regarding the damping characteristics of natural fibre metal laminates, it is recommended to conduct additional experimental studies to enhance the accuracy of the predictive guideline proposed in this research. This would mean encompassing a wider spectrum of metal volume fraction values for a more detailed analysis.

In addition, investigating how variations in specimen geometry (especially thickness) for a constant MVF affect the damping behaviour of the FLARE, as well as examining other FML configurations (such as 3/2), could provide valuable information to establish further design guidelines.

Impact behaviour

Concerning the impact response of FLARE, it is suggested to conduct quasi-static indentation tests coupled with acoustic emission monitoring and scanning electron microscope analysis.

This approach would offer deeper insights into the sequence of failure mechanisms and contribute to a more comprehensive understanding of the material's behaviour.

Further investigation of the influence of stacking sequence (fibre orientation) and metal thickness, with fixed MVF, will enhance the comprehension of FLARE's performance under impact. This exploration can also yield additional design recommendations.

Finally, the quasi-static analytical model necessitates further enhancements, particularly in terms of accommodating thick and moderately thick laminates. This would involve the incorporation of First- or High-order Shear Deformation Theory to deduce strain from the plate's deflection profile. Furthermore, there is room for incorporating more realistic stiffness degradation rules. Additionally, the model should be expanded to encompass alternative modes of energy dissipation, such as fibre failure or petaling, in order to provide a more comprehensive representation of real-world scenarios.

To conclude, the study of natural fibre metal laminates, and especially FLARE, requires further research. This will be essential for a better understanding of the synergy effects inherent in these hybrid materials, enabling their potential integration into structural applications to reduce the environmental impact.

References

[1] E. C. Botelho, R. A. Silva, L. C. Pardini, and M. C. Rezende, "A review on the development and properties of continuous fiber/epoxy/aluminum hybrid composites for aircraft structures," *Materials Research*, vol. 9, pp. 247–256, 9 2006.

[2] A. Vlot and J. W. Gunnink, eds., *Fibre Metal Laminates*. Springer Netherlands, 2001.

[3] P. Soltani, M. Keikhosravy, R. H. Oskouei, and C. Soutis, "Studying the tensile behaviour of GLARE laminates: A finite element modelling approach," *Applied Composite Materials*, vol. 18, pp. 271–282, 8 2011.

[4] H. Kuan, W. Cantwell, M. A. Hazizan, and C. Santulli, "The fracture properties of environmental-friendly fiber metal laminates," *Journal of Reinforced Plastics and Composites*, vol. 30, pp. 499–508, 3 2011.

[5] C. Santulli, H. T. Kuan, F. Sarasini, I. D. Rosa, and W. Cantwell, "Damage characterisation on PP-hemp/aluminium fibre–metal laminates using acoustic emission," *Journal of Composite Materials*, vol. 47, pp. 2265–2274, 8 2013.

[6] L. Yan, N. Chouw, and K. Jayaraman, "Flax fibre and its composites – A review," *Composites Part B: Engineering*, vol. 56, pp. 296–317, 1 2014.

[7] A. Lefeuvre, A. Bourmaud, C. Morvan, and C. Baley, "Elementary flax fibre tensile properties: Correlation between stress–strain behaviour and fibre composition," *Industrial Crops and Products*, vol. 52, pp. 762–769, 1 2014.

[8] A. L. Duigou, P. Davies, and C. Baley, "Environmental Impact Analysis of the Production of Flax Fibres to be Used as Composite Material Reinforcement," *Journal of Biobased Materials and Bioenergy*, vol. 5, pp. 153–165, 2011.

[9] M. Assarar, D. Scida, A. E. Mahi, C. Poilâne, and R. Ayad, "Influence of water ageing on mechanical properties and damage events of two reinforced composite materials: Flax–fibres and glass–fibres," *Materials & Design*, vol. 32, pp. 788–795, 2 2011.

[10] F. Bensadoun, D. Depuydt, J. Baets, I. Verpoest, and A. W. van Vuure, "Low velocity impact properties of flax composites," *Composite Structures*, vol. 176, pp. 933–944, 9 2017.

[11] F. Duc, P. Bourban, and J. Månson, "Damping Performance of Flax Fibre Composites," 2014.

[12] T. H. Panzera, T. Jeannin, X. Gabrion, V. Placet, C. Remillat, I. Farrow, and F. Scarpa, "Static, fatigue and impact behaviour of an autoclaved flax fibre reinforced composite for aerospace engineering," *Composites Part B: Engineering*, vol. 197, p. 108049, 9 2020.

[13] F. D. Morinière, "Low-velocity impact on fibre-metal laminates," 2014.

[14] R. Gentry, L. Bank, J. F. Chen, F. Arias, and T. Al-Haddad, "Adaptive Reuse of FRP Composite Wind Turbine Blades for Civil Infrastructure Construction," 2018.

[15] J. Homan, "Fatigue initiation in fibre metal laminates," *International Journal of Fatigue*, vol. 28, pp. 366–374, 4 2006.

[16] H. L. Bos, "The potential of flax fibres as reinforcement for composite materials," 2004.

[17] Z. Mahboob, I. E. Sawi, R. Zdero, Z. Fawaz, and H. Bougherara, "Tensile and compressive damaged response in Flax fibre reinforced epoxy composites," *Composites Part A: Applied Science and Manufacturing*, vol. 92, pp. 118–133, 1 2017.

[18] P. Mallick, *Fiber-Reinforced Composites*. CRC Press, 11 2007.

[19] T. J. D. Vries, "Blunt and sharp notch behaviour of Glare laminates," 2001.

[20] F. D. Morinière, R. C. Alderliesten, and R. Benedictus, "Low-velocity impact energy partition in GLARE," *Mechanics of Materials*, vol. 66, pp. 59–68, 2013.

[21] P. Iaccarino, A. Langella, and G. Caprino, "A simplified model to predict the tensile and shear stress-strain behaviour of fibreglass/aluminium laminates," *Composite Science and Tehcnology*, vol. 9, pp. 1784–1793, 2007.

[22] D. M. Isaac and I. Ori, *Engineering mechanics of composite materials*. Oxford University Press., second ed., 2006.

[23] E. Kandare, S. Yoo, V. Chevali, and A. Khatibi, "On the notch sensitivity of flax fibre metal laminates under static and fatigue loading," *Fatigue & Fracture of Engineering Materials & Structures*, vol. 41, pp. 1691–1705, 8 2018.

[24] C. H. Song, K. Giasin, A. Saifullah, and A. Barouni, "Investigation of the Contact Interface between Natural Fibre Metal Laminates under Tension Using Finite Element Analysis (FEA)," *Polymers*, vol. 14, p. 4650, 11 2022.

[25] S. Krishnakumar, "Fiber Metal Laminates — The Synthesis of Metals and Composites," *Materials and Manufacturing Processes*, vol. 9, pp. 295–354, 3 1994.

[26] L. B. Vogelesang and A. Vlot, "Development of fibre metal laminates for advanced aerospace structures," *Journal of Materials Processing Technology*, vol. 103, pp. 1–5, 6 2000.

[27] G. H. Roebroeks, "Fibre-metal laminates: Recent developments and applications," *International Journal of Fatigue*, vol. 16, pp. 33–42, 1 1994.

[28] H. F. Wu, L. L. Wu, W. J. Slagter, and J. L. Verolme, "Use of rule of mixtures and metal volume fraction for mechanical property predictions of fibre-reinforced aluminium laminates," *Journal of Materials Science*, vol. 29, pp. 4583–4591, 9 1994.

[29] R. C. Alderliesten and R. Benedictus, "Fiber/Metal Composite Technology for Future Primary Aircraft Structures," *Journal of Aircraft*, vol. 45, pp. 1182–1189, 7 2008.

[30] R. Alderliesten, *Fatigue and Fracture of Fibre Metal Laminates*, vol. 236. Springer International Publishing, 2017.

[31] T. Sinmazçelik, E. Avcu, M. Özgür Bora, and O. Çoban, "A review: Fibre metal laminates, background, bonding types and applied test methods," *Materials & Design*, vol. 32, pp. 3671–3685, 8 2011.

[32] A. Salve, R. Kulkarni, and A. Mache, "A Review: Fiber Metal Laminates (FML's) -Manufacturing, Test methods and Numerical modeling," *International Journal of Engineering Technology and Sciences*, vol. 6, 2016.

[33] E. Kroon, G. Roebroeks, and J. W. Gunnink, "Report TD-R-02-007: Influence of general quality on Glare material performance," *Fibre Metal Laminates Centre of Competence*, 2002.

[34] M. Kawai, M. Morishita, S. Tomura, and K. Takumida, "Inelastic behavior and strength of fiber-metal hybrid composite: Glare," *International Journal of Mechanical Sciences*, vol. 40, pp. 183–198, 2 1998.

[35] M. Sadighi, R. C. Alderliesten, and R. Benedictus, "Impact resistance of fiber-metal laminates: A review," *International Journal of Impact Engineering*, vol. 49, pp. 77–90, 11 2012.

[36] A. Vlot, "Impact properties of Fibre Metal Laminates," *Composites Engineering*, vol. 3, pp. 911–927, 1 1993.

[37] T. Li Piani, J. Weerheijm, F. Moriniere, J. Hoogland, I. Schipperen, G. Roebroeks, and R. Alderliesten, "An Application of the Energy Partition Method on the Blast response of Composite panels," *Heron*, vol. 65, p. 24, 11 2021.

[38] M. Chandrasekar, M. R. Ishak, M. S. Salit, Z. Leman, M. Jawaid, and J. Naveen, "Mechanical properties of a novel fibre metal laminate reinforced with the carbon, flax, and sugar palm fibres," *BioResources*, vol. 13, pp. 5725–5739, 6 2018.

[39] N. L. Feng, K. Subramaniam, and N. M. Ishak, *An Overview of the Natural/Synthetic Fibre-Reinforced Metal-Composite Sandwich Structures for Potential Applications in Aerospace Sectors*, pp. 177–194. Springer International Publishing, 2022.

[40] M. Chandrasekar, M. Ishak, S. Sapuan, Z. Leman, and M. Jawaid, *Tensile and flexural properties of the hybrid flax/carbon based fibre metal laminate.* 2016.

[41] I. Mohammed, A. R. A. Talib, M. T. H. Sultan, M. Jawaid, A. H. Ariffin, and S. Saadon, "Mechanical Properties of Fibre-Metal Laminates Made of Natural/Synthetic Fibre Composites," *BioResources*, vol. 13, 1 2018.

[42] M. Vasumathi and V. Murali, "Effect of Alternate Metals for use in Natural Fibre Reinforced Fibre Metal Laminates under Bending, Impact and Axial Loadings," *Procedia Engineering*, vol. 64, pp. 562–570, 2013.

[43] S. D. Malingam, L. F. Ng, K. H. Chan, K. Subramaniam, M. Z. Selamat, and K. A. Zakaria, "The static and dynamic mechanical properties of kenaf/glass fibre reinforced hybrid composites," *Materials Research Express*, vol. 5, p. 095304, 8 2018.

[44] N. L. Feng, S. DharMalingam, K. A. Zakaria, and M. Z. Selamat, "Investigation on the fatigue life characteristic of kenaf/glass woven-ply reinforced metal sandwich materials," *Journal of Sandwich Structures & Materials*, vol. 21, pp. 2440–2455, 10 2019.

[45] M. A. A. El-Baky, A. E. Alshorbagy, A. M. Alsaeedy, and M. Megahed, "Fabrication of Cost Effective Fiber Metal Laminates Based on Jute and Glass Fabrics for Enhanced Mechanical Properties," *Journal of Natural Fibers*, vol. 19, pp. 303–318, 1 2022.

[46] L. M. G. Vieira, J. C. dos Santos, T. H. Panzera, J. C. C. Rubio, and F. Scarpa, "Novel fibre metal laminate sandwich composite structure with sisal woven core," *Industrial Crops and Products*, vol. 99, pp. 189–195, 5 2017.

[47] L. M. G. Vieira, Y. Dobah, J. C. dos Santos, T. H. Panzera, J. C. C. Rubio, and F. Scarpa, "Impact Properties of Novel Natural Fibre Metal Laminated Composite Materials," *Applied Sciences*, vol. 12, p. 1869, 2 2022.

[48] N. M. Ishak, S. D. Malingam, M. R. Mansor, N. Razali, Z. Mustafa, and A. F. A. Ghani, "Investigation of natural fibre metal laminate as car front hood," *Materials Research Express*, vol. 8, p. 025303, 2 2021.

[49] D. Sivakumar, L. F. Ng, and M. Z. Selamat, "Investigation on Fatigue Life Behaviour of Sustainable Bio-Based Fibre Metal Laminate," *Journal of Mechanical Engineering*, pp. 123–140, 2017.

[50] D. Sivakumar, L. Ng, N. Zalani, M. Selamat, A. A. Ghani, and S. Fadzullah, "Influence of kenaf fabric on the tensile performance of environmentally sustainable fibre metal laminates," *Alexandria Engineering Journal*, vol. 57, pp. 4003–4008, 12 2018.

[51] Z. Qu, X. Pan, X. Hu, Y. Guo, and Y. Shen, "Evaluation of Nano-Mechanical Behavior on Flax Fiber Metal Laminates Using an Atomic Force Microscope," *Materials*, vol. 12, p. 3363, 10 2019.

[52] K. R. Ramakrishnan, M. Kanerva, E. Sarlin, and M. Hokka, "Impact damage resistance of novel adhesively bonded natural fibre composite – Steel hybrid laminates," *International Journal of Lightweight Materials and Manufacture*, vol. 5, pp. 29–43, 3 2022.

[53] Z. Zhang, S. Cai, Y. Li, Z. Wang, Y. Long, T. Yu, and Y. Shen, "High performances of plant fiber reinforced composites—A new insight from hierarchical microstructures," *Composites Science and Technology*, vol. 194, p. 108151, 7 2020.

[54] J. M. van Hazendonk, J. C. van der Putten, J. T. Keurentjes, and A. Prins, "A simple experimental method for the measurement of the surface tension of cellulosic fibres and its relation with chemical composition," *Colloids and Surfaces A: Physicochemical and Engineering Aspects*, vol. 81, pp. 251–261, 12 1993.

[55] S. Liang, P. Gning, and L. Guillaumat, "A comparative study of fatigue behaviour of flax/epoxy and glass/epoxy composites," *Composites Science and Technology*, vol. 72, pp. 535–543, 3 2012.

[56] D. U. Shah, P. J. Schubel, and M. J. Clifford, "Can flax replace E-glass in structural composites? A small wind turbine blade case study," *Composites Part B: Engineering*, vol. 52, pp. 172–181, 2013.

[57] I. V. de Weyenberg, J. Ivens, A. D. Coster, B. Kino, E. Baetens, and I. Verpoest, "Influence of processing and chemical treatment of flax fibres on their composites," *Composites Science and Technology*, vol. 63, pp. 1241–1246, 7 2003.

[58] V. Tojaga, A. Prapavesis, J. Faleskog, T. C. Gasser, A. W. van Vuure, and S. Östlund, "Continuum damage micromechanics description of the compressive failure mechanisms in sustainable biocomposites and experimental validation," *Journal of the Mechanics and Physics of Solids*, vol. 171, p. 105138, 2 2023.

[59] J. Baets, D. Plastria, J. Ivens, and I. Verpoest, "Determination of the optimal flax fibre preparation for use in unidirectional flax–epoxy composites," *Journal of Reinforced Plastics and Composites*, vol. 33, pp. 493–502, 3 2014.

[60] G. Coroller, A. Lefeuvre, A. L. Duigou, A. Bourmaud, G. Ausias, T. Gaudry, and C. Baley, "Effect of flax fibres individualisation on tensile failure of flax/epoxy unidirectional composite," *Composites Part A: Applied Science and Manufacturing*, vol. 51, pp. 62–70, 8 2013.

[61] F. Duc, P.-E. Bourban, and J.-A. E. Månson, "Dynamic mechanical properties of epoxy/flax fibre composites," *Journal of Reinforced Plastics and Composites*, vol. 33, pp. 1625–1633, 9 2014.

[62] K. Oksman, "High Quality Flax Fibre Composites Manufactured by the Resin Transfer Moulding Process," *Journal of Reinforced Plastics and Composites*, vol. 20, pp. 621–627, 5 2001.

[63] C. Poilâne, A. Vivet, L. Momayez, B. B. Doudou, M. Ayachi, and J. Chen, "Propriétés mécaniques de préimprégnés lin/époxyde = Mechanical properties of flax/epoxy industrial prepregs," *JNC 16 Toulouse*, 2009.

[64] I. V. de Weyenberg, T. C. Truong, B. Vangrimde, and I. Verpoest, "Improving the properties of UD flax fibre reinforced composites by applying an alkaline fibre treatment," *Composites Part A: Applied Science and Manufacturing*, vol. 37, pp. 1368–1376, 9 2006.

[65] J. George, J. Ivens, and I. Verpoest, "Mechanical properties of flax fibre reinforced epoxy composites," *Die Angewandte Makromolekulare Chemie*, vol. 272, pp. 41–45, 1999.

[66] R. Panciroli and O. Giannini, "Comparing the impact resistance of flax/epoxy and glass/epoxy composites through experiments and numerical simulations," *Composite Structures*, vol. 264, p. 113750, 5 2021.

[67] P. Wambua, B. Vangrimde, S. Lomov, and I. Verpoest, "The response of natural fibre composites to ballistic impact by fragment simulating projectiles," *Composite Structures*, vol. 77, pp. 232–240, 1 2007.

[68] Y. Li, S. Cai, and X. Huang, "Multi-scaled enhancement of damping property for carbon fiber reinforced composites," *Composites Science and Technology*, vol. 143, pp. 89–97, 5 2017.

[69] F. Duc, P. E. Bourban, C. J. Plummer, and J. A. Månson, "Damping of thermoset and thermoplastic flax fibre composites," *Composites Part A: Applied Science and Manufacturing*, vol. 64, pp. 115–123, 9 2014.

[70] G. Rajkumar, M. Krishna, H. Narasimhamurthy, Y. Keshavamurthy, and J. Nataraj, "Investigation of Tensile and Bending Behavior of Aluminum based Hybrid Fiber Metal Laminates," *Procedia Materials Science*, vol. 5, pp. 60–68, 2014.

[71] S. Dariushi, S. Farahmandnia, and A. M. Rezadoust, "An experimental investigation on infusion time and strength of fiber metal laminates made by vacuum infusion process," *Proceedings of the Institution of Mechanical Engineers, Part L: Journal of Materials: Design and Applications*, vol. 235, pp. 1800–1808, 8 2021.

[72] V. Brügemann, G. Roebroeks, and J. W. Gunnink, "Report TD-R-03-005: Test Procedures for Fibre Metal Laminates," *Fibre Metal Laminates Centre of Competence*, 2003.

[73] E. C. Botelho, L. C. Pardini, and M. C. Rezende, "Hygrothermal effects on damping behavior of metal/glass fiber/epoxy hybrid composites," *Materials Science and Engineering: A*, vol. 399, pp. 190–198, 6 2005.

[74] J. M. Berthelot and Y. Sefrani, "Longitudinal and transverse damping of unidirectional fibre composites," *Composite Structures*, vol. 79, pp. 423–431, 7 2007.

[75] M. J. L. Guen, R. H. Newman, A. Fernyhough, G. W. Emms, and M. P. Staiger, "The damping-modulus relationship in flax-carbon fibre hybrid composites," *Composites Part B: Engineering*, vol. 89, pp. 27–33, 3 2016.

[76] J. Vantomme, "A parametric study of material damping in fibre-reinforced plastics," 1995.

[77] ASTM Standard E756-05, "Standard Test Method for Measuring Vibration-Damping Properties of Materials," *ASTM International*, 2017.

[78] M. S. H. Fatt, C. Lin, D. M. Revilock, and D. A. Hopkins, "Ballistic impact of GLARE™ fiber-metal laminates," *Composite Structures*, vol. 61, pp. 73–88, 2003.

[79] W. Wang, X. Zhang, N. Chouw, Z. Li, and Y. Shi, "Strain rate effect on the dynamic tensile behaviour of flax fibre reinforced polymer," *Composite Structures*, vol. 200, pp. 135–143, 9 2018.

[80] C. Kassapoglou, *Design and analysis of composite structures: With applications to aerospace structures.* John Wiley & Sons, Ltd, second ed., 2010.

[81] Y. Saadati, J. F. Chatelain, G. Lebrun, Y. Beauchamp, P. Bocher, and N. Vanderesse, "A study of the interlaminar fracture toughness of unidirectional flax/epoxy composites," *Journal of Composites Science*, vol. 4, 2020.

[82] L. Pil, F. Bensadoun, J. Pariset, and I. Verpoest, "Why are designers fascinated by flax and hemp fibre composites?," *Composites Part A: Applied Science and Manufacturing*, vol. 83, pp. 193–205, 4 2016.

[83] M. A. Fentahun and M. A. Savaş, "Materials Used in Automotive Manufacture and Material Selection Using Ashby Charts," *International Journal of Materials Engineering*, vol. 8, pp. 40–54, 2018.

[84] N. M. N. et al., "A Review on Mechanical Performance of Hybrid Natural Fiber Polymer Composites for Structural Applications," *Polymers 2021, Vol. 13, Page 2170*, vol. 13, p. 2170, 6 2021.

[85] E. Poodts, D. Ghelli, T. Brugo, R. Panciroli, and G. Minak, "Experimental characterization of a fiber metal laminate for underwater applications," *Composite Structures*, vol. 129, p. 36, 10 2015.

[86] P. Liu and C. Y. Barlow, "Wind turbine blade waste in 2050," *Waste Management*, vol. 62, pp. 229–240, 4 2017.

[87] B. K. Storm, "Surface protection and coatings for wind turbine rotor blades," 2013.

[88] K. Simoiu, "Development of a Low-Cost Fiber Metal Laminate With a Focus on Low-Velocity Impacts," 2016.

[89] D. U. Shah, "Developing plant fibre composites for structural applications by optimising composite parameters: a critical review," *Journal of Materials Science*, vol. 48, pp. 6083–6107, 9 2013.

[90] C. A. Buchanan, M. Charara, J. L. Sullivan, G. M. Lewis, and G. A. Keoleian, "Lightweighting shipping containers: Life cycle impacts on multimodal freight transportation," *Transportation Research Part D: Transport and Environment*, vol. 62, pp. 418–432, 7 2018.

[91] S. Ryan and E. Christiansen, "Micrometeoroid and Orbital Debris (MMOD) Shield Ballistic Limit Analysis Program," 2010.

[92] A. Pai, R. Divakaran, S. Anand, and S. B. Shenoy, "Advances in the Whipple Shield Design and Development: A Brief Review," *Journal of Dynamic Behavior of Materials*, vol. 8, pp. 20–38, 3 2022.

Appendix A

Additional results

A.1 Vibration Beam Test additional results

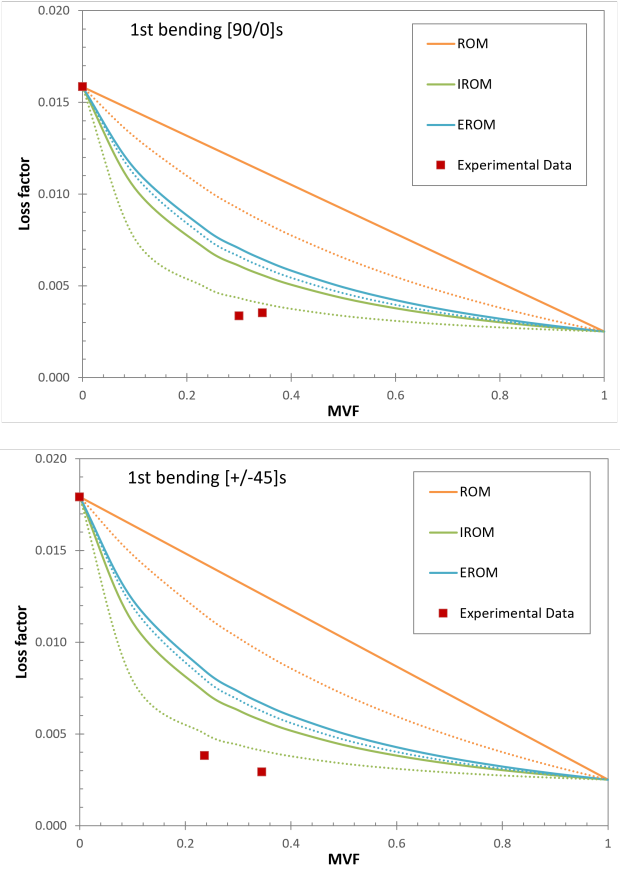

Figure A.1: Comparison between experimental data and different predictive rules, using volume fractions (solid line) or weight fractions (dashed line), for samples in 1st bending mode.

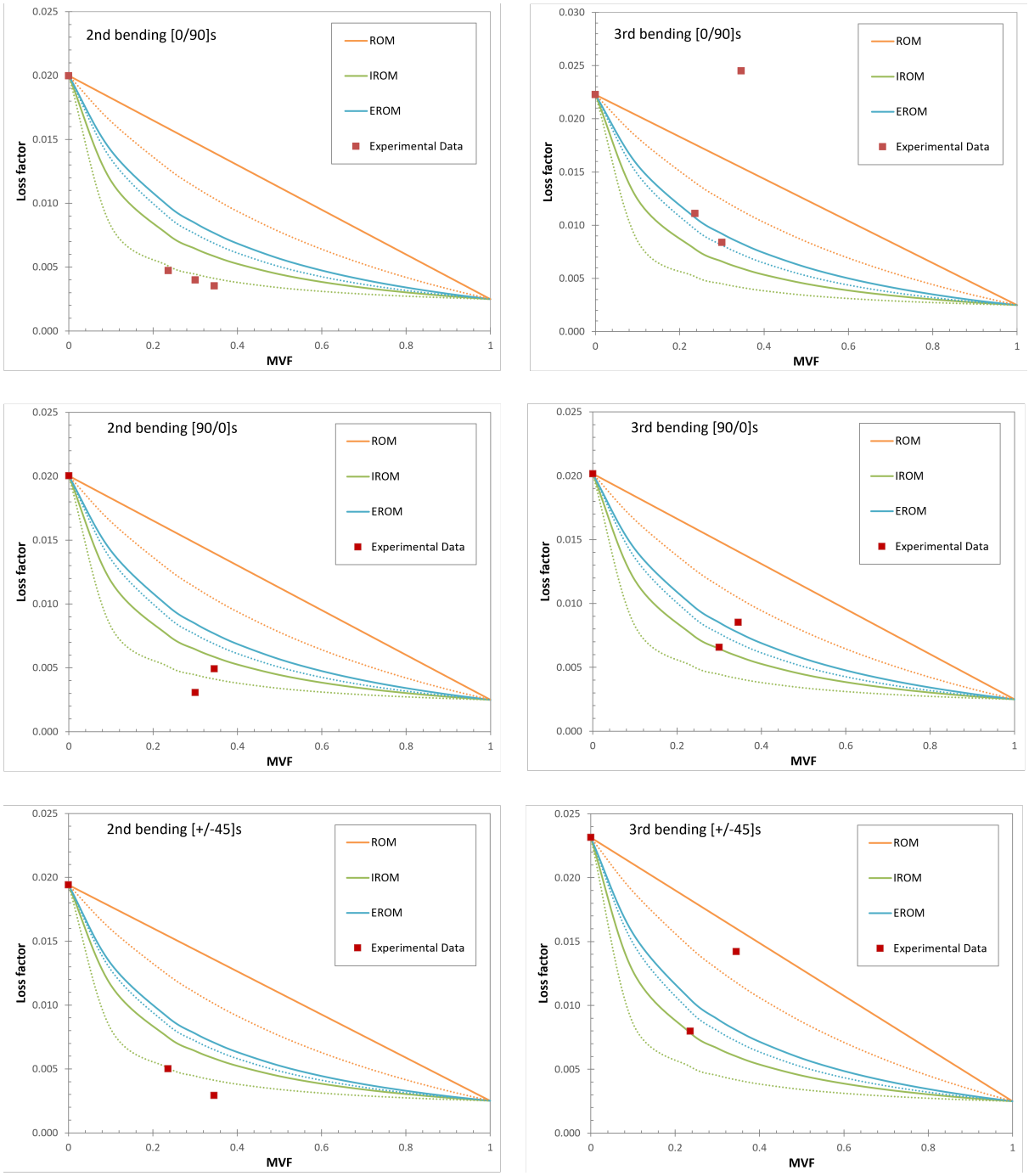

Figure A.2: Comparison between experimental data and different predictive rules, using volume fractions (solid line) or weight fractions (dashed line), for samples in 2nd and 3rd bending modes.

A.2 Low-velocity additional results

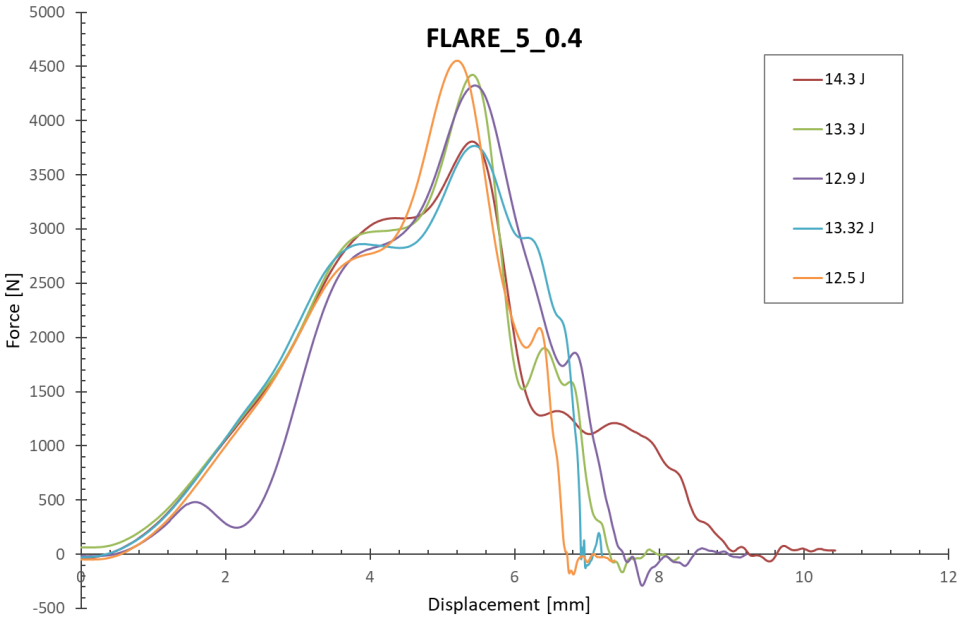

Figure A.3: Force-displacement curves for FLARE_5_0.4 samples.

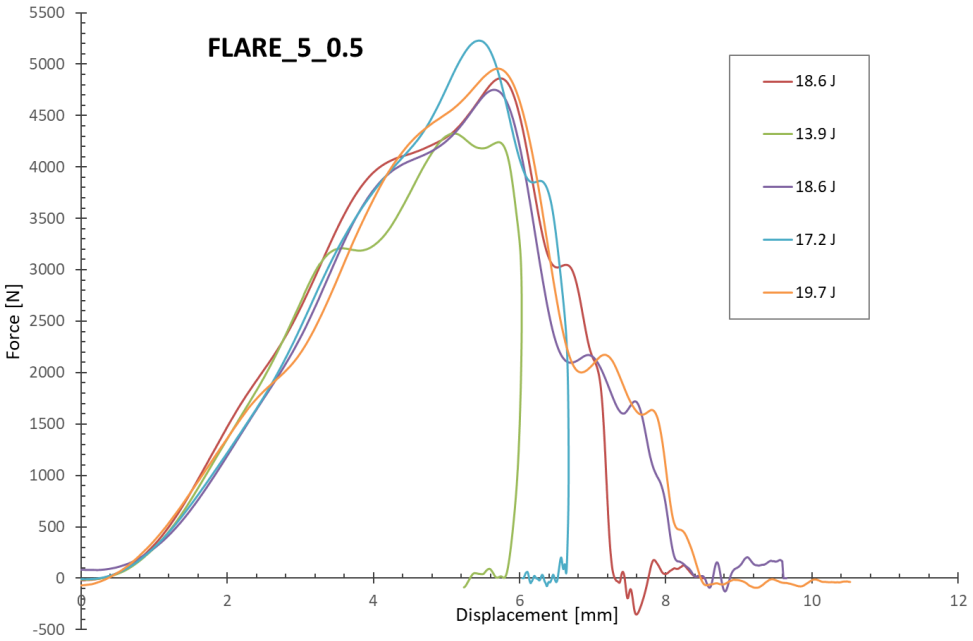

Figure A.4: Force-displacement curves for FLARE_5_0.5 samples.